



2011

COMPUTATIONAL ANALYSES OF THE UPTAKE AND DISTRIBUTION OF CARBON MONOXIDE (CO) IN HUMAN SUBJECTS

Kinnera Chada

University of Kentucky, kinnerarey@gmail.com

Recommended Citation

Chada, Kinnera, "COMPUTATIONAL ANALYSES OF THE UPTAKE AND DISTRIBUTION OF CARBON MONOXIDE (CO) IN HUMAN SUBJECTS" (2011). *University of Kentucky Doctoral Dissertations*. 224.
http://uknowledge.uky.edu/gradschool_diss/224

This Dissertation is brought to you for free and open access by the Graduate School at UKnowledge. It has been accepted for inclusion in University of Kentucky Doctoral Dissertations by an authorized administrator of UKnowledge. For more information, please contact UKnowledge@lsv.uky.edu.

ABSTRACT OF DISSERTATION

Kinnera Chada

The Graduate School

University of Kentucky

2011

COMPUTATIONAL ANALYSES OF THE UPTAKE AND DISTRIBUTION OF
CARBON MONOXIDE (CO) IN HUMAN SUBJECTS

ABSTRACT OF DISSERTATION

A dissertation submitted in partial fulfillment of the
requirements for the degree of Doctor of Philosophy in the
College of Engineering at the University of Kentucky

By
Kinnera Chada
Lexington, Kentucky

Director: Dr. Eugene N Bruce, Professor of Biomedical Engineering
Lexington, Kentucky

2011

Copyright © Kinnera Chada 2011

ABSTRACT OF DISSERTATION

COMPUTATIONAL ANALYSES OF THE UPTAKE AND DISTRIBUTION OF CARBON MONOXIDE (CO) IN HUMAN SUBJECTS

Carbon monoxide (CO) is an odorless, colorless, tasteless gas that binds to hemoglobin with high affinity. This property underlies the use of low doses of *CO* to determine hemoglobin mass (M_{Hb}) in the fields of clinical and sports medicine. However, hemoglobin bound to *CO* is unable to transport oxygen and exposure to high *CO* concentrations is a significant environmental and occupational health concern. These contrasting aspects of *CO*—clinically useful in low doses but potentially lethal in higher doses—mandates a need for a quantitative understanding of the temporal profiles of the uptake and distribution of *CO* in the human body. In this dissertation I have (i) used a mathematical model to analyze *CO*-rebreathing techniques used to estimate total hemoglobin mass and proposed a *CO*-rebreathing procedure to estimate hemoglobin mass with low errors, (ii) enhanced and validated a multicompartment model to estimate O_2 , *CO* and CO_2 tensions, bicarbonate levels, pH levels, blood carboxyhemoglobin (*HbCO*) levels, and carboxymyoglobin (*MbCO*) levels in all the vascular (arterial, mixed venous and vascular subcompartments of the tissues) and tissue (brain, heart and skeletal muscle) compartments of the model in normoxia, hypoxia, *CO* hypoxia, hyperoxia, isocapnic hyperoxia and hyperbaric oxygen, and (iii) used this developed mathematical model to propose a treatment to improve O_2 delivery and *CO* removal by comparing O_2 and *CO* levels during different treatment protocols administered for otherwise-healthy *CO*-poisoned subjects.

KEYWORDS: Mathematical model, CO Rebreathing methods, CO poisoning, Normobaric oxygen, Hyperbaric oxygen.

Kinnera Chada

Student's Signature

06-02-2011

Date

COMPUTATIONAL ANALYSES OF THE UPTAKE AND DISTRIBUTION OF
CARBON MONOXIDE (CO) IN HUMAN SUBJECTS

By

Kinnera Chada

Eugene N Bruce

Director of Dissertation

Abhijit R. Patwardhan

Director of Graduate Studies

06-02-2011

Date

RULES FOR THE USE OF DISSERTATIONS

Unpublished dissertation submitted for the Doctor's degree and deposited in the University of Kentucky Library are as a rule open for inspection, but are to be used only with due regard to the rights of the authors. Bibliographical references may be noted, but quotations or summaries of parts may be published only with the permission of the author, and with the usual scholarly acknowledgments.

Extensive copying or publication of the dissertation in whole or in part also requires the consent of the Dean of the Graduate School of the University of Kentucky.

A library that borrows this dissertation for use by its patrons is expected to secure the signature of each user.

Name

Date

DISSERTATION

Kinnera Chada

The Graduate School
University of Kentucky
2011

COMPUTATIONAL ANALYSES OF THE UPTAKE AND DISTRIBUTION OF
CARBON MONOXIDE (CO) IN HUMAN SUBJECTS

DISSERTATION

A dissertation submitted in partial fulfillment of the
requirements for the degree of Doctor of Philosophy in the
College of Engineering at the University of Kentucky

By
Kinnera Chada
Lexington, Kentucky

Director: Dr. Eugene N Bruce, Professor of Biomedical Engineering
Lexington, Kentucky

2011

Copyright © Kinnera Chada 2011

ACKNOWLEDGEMENTS

The following dissertation, while an individual work, benefited from the insights and direction of several people. First, my Dissertation Chair, Dr. Eugene N. Bruce, provided constant support, timely guidance and evaluations at every stage of the dissertation process. I would like to thank Dr. Margaret Bruce for helping me with performing literature searches for model development and validation. Next, I wish to thank the complete Dissertation Committee, respectively: Dr. Abhijit R. Patwardhan, Dr. Michael B. Reid, and Dr. Hainsworth Y. Shin. Each individual provided valuable insights that challenged my thinking and substantially improved the quality of this dissertation. I would like to thank the external examiner, Dr. Dexter F. Speck for his time and valuable comments. I would like to acknowledge all the researchers and finding agencies that have provided me with data and financial support for completing this project.

I thank Dr. Vernon Benignus (US EPA, Research Triangle Park), Garvican et al. (2010) (Australian Institute of Sport, Canberra, Australia) and Dr. Lindell K. Weaver and his group (LDS Hospital, Salt Lake City, Utah) for providing both data published in their papers and unpublished measurements of parameter values from their subjects.

I received equally important support and assistance from my family. My husband, parents, aunts, uncles, siblings, grand parents, Dr. Bruce and Peggy have continuously supported and encouraged me for completing the dissertation process in a timely manner. I thank my uncle for the additional financial support. I would specially like to thank my mother and my husband for taking care of me and my daughter during the dissertation process. I thank all of them for truly believing in my abilities and for their encouragement to pursue my goals.

TABLE OF CONTENTS

Acknowledgements.....	iii
List of Tables	vi
List of Figures.....	vii
Chapter 1: Introduction.....	1
First specific aim.....	4
Second specific aim	4
Third specific aim.....	5
Chapter 2: Computational Analyses of Carbonmonoxide (<i>CO</i>) Rebreathing Methods to Estimate Hemoglobin Mass in Humans.....	6
Introduction.....	7
Methods.....	11
Results.....	21
Discussion.....	33
Conclusions.....	44
Summary.....	45
Chapter 3: Enhanced Mathematical Model.....	69
Introduction.....	70
Methods.....	71
Results.....	86
Discussion.....	92
Conclusions.....	97
Summary.....	97
Chapter 4: Computational analyses of treatments after carbon monoxide (<i>CO</i>) poisoning in human.....	112
Introduction.....	113

Methods.....	116
Results.....	122
Discussion.....	127
Conclusions.....	133
Summary.....	133
Chapter 5 Conclusion and Future work	144
Conclusions.....	145
Future work.....	150
References.....	153
Vita.....	163

LIST OF TABLES

Table 2.1: Symbols and their definitions	46
Table 2.2: Estimation of hemoglobin mass ($^M \hat{M}_{Hb}$, $^E \hat{M}_{Hb}$)	47
Table 2.3: Mean values with standard deviations of various variables and mean errors in calculation of $^M \hat{M}_{Hb}$ for protocol B and protocol P simulations	48
Table 2.4: Mean values with standard deviations of estimated V_{COMb} and errors in calculation of $^E \hat{M}_{Hb}$ for simulations of protocol B and protocol P	49
Table 2.5: Mean values with standard deviations of errors in $^E \hat{M}_{Hb}$ from Benignus's subjects for protocol B, protocol P and protocol N simulations	50
Table 3.1: Parameters and their default values	99
Table 3.2: Experimental data for brain tissue and blood oxygen tensions	100
Table 3.3: Slopes for the V_E - $P_A CO_2$ curves from my model and experiments.....	101
Table 4.1: Questions related to CO poisoning treatments	136
Table 4.2: Subject specific parameters	137
Table 4.3: Symbols and Definitions.....	138
Table 4.4: %HbCO levels at the end of CO exposure	139
Table 4.5: O ₂ delivery and CO removal during 6 hr NBO ₂ treatment.....	140
Table 4.6 A: O ₂ delivery and CO removal during different treatments for subject, S115.....	141
Table 4.6 B: O ₂ delivery and CO removal during different treatments for subject, S118.....	142
Table 4.6 C: O ₂ delivery and CO removal during different treatments for subject, S119.....	143

LIST OF FIGURES

Figure 2.1 Determination of T_{mix} in protocol B and protocol P.....	51
Figure 2.2: Uptake kinetics of CO in protocol B and protocol P.....	52
Figure 2.3: Comparison of model predicted % $HbCO$ with experimental data.....	53
Figure 2.4: Comparison of model predicted % $HbCO$ with experimental data from three blood sites for Schmidt and Prommer method	54
Figure 2.5: Mean % error in estimated Hb mass using exact data from the model	55
Figure 2.6: CO flux from blood to muscle tissues in the commonly used rebreathing methods	56
Figure 2.7: Comparison of model calculated V_{COMb} with Prommer and Schmidt's estimated V_{COMb}	57
Figure 2.8: Errors in estimation of M_{Hb}	58
Figure 2.9: Comparison of model calculated V_{COMb} with Prommer and Schmidt's estimated V_{COMb}	59
Figure 2.10: Comparison of model calculated V_{CO} exhaled with Prommer and Schmidt's estimated V_{CO} exhaled in protocol B.....	60
Figure 2.11: Effects of varying durations of CO rebreathing in 100% O_2 and the ambient conditions before or after CO rebreathing on errors in estimation of H_{mass}	61
Figure 2.12: Uptake kinetics of CO in protocol N for one typical subject. The % $HbCO$ levels in different vascular compartments of the model	62
Figure 2.13: Proposed regression equations to estimate V_{COMb} for calculation of M_{Hb}	63
Figure 2.14: Comparison of errors from different blood sites for protocols B , P and N.....	64
Figure 2.15: Effects of T_{sample} on estimation of M_{Hb} in protocol N	65
Figure 2.16: Model fit of a healthy, recreationally-active female human subject from experiment.....	66
Figure 2.17: Effects of T_{mix} on estimation of M_{Hb} in protocol B.....	67
Figure 2.18: Effects of T_{mix} on estimation of M_{Hb} in protocol P	68
Figure 3.1: Architecture of modified model	102
Figure 3.2: Prediction of changes in cardiac output with increasing % $HbCO$ levels.....	103
Figure 3.3: Prediction of changes in brain blood flow with increasing % $HbCO$ levels.....	104

Figure 3.4: Validation of brain tissue and blood gas (O_2 , CO_2) tensions	105
Figure 3.5: Comparison of arterial and mixed venous blood gases and pH with experimental data	106
Figure 3.6: Comparison of model predicted arterial O_2 saturations and ventilatory response with experimentally measured data at various levels of hypoxia	107
Figure 3.7: Comparison of model predicted ventilatory response with experimentally measured data at various levels of inspired oxygen fractions.....	108
Figure 3.8: Comparison of model predicted ventilatory response and model predicted arterial PCO_2 changes with experimentally measured data	109
Figure 3.9: Comparison of changes in ventilation with changes in alveolar PCO_2 (P_ACO_2) after breathing increasing inspired concentrations of CO_2	110
Figure 3.10: Model predicted oxygen saturation with experimentally measured values for different conditions	111
Figure 4.1: Poikilocapnic normobaric oxygen (NBO_2) vs. Isocapnic normobaric oxygen (NBO_2).	143

Chapter 1: INTRODUCTION

Inhalation of **carbon monoxide (CO)** interrupts the efficient mechanism of hemoglobin (Hb) molecule to transport oxygen. O_2 is stored in the lungs as a gas and in the blood. In the blood it is present in two (Vander et al., 2004) forms: (1) dissolved in plasma (normally 1.5% or 3 ml in 1 liter blood) and (2) reversibly combined with hemoglobin (normally 98.5% or 197 ml in 1 liter blood). Each hemoglobin molecule can bind to four oxygen molecules forming fully-saturated oxyhemoglobin (HbO_2). Hb is present in the red blood cells and O_2 transport to the tissues occurs primarily in the HbO_2 form, as there are about 280 million Hb molecules in each red blood cell. *CO* is an odorless, colorless, tasteless gas that has a much higher binding affinity for hemoglobin and competes with O_2 for the same binding sites on Hb. Hb binds *CO* ~220 times more strongly than it binds O_2 , to form carboxyhemoglobin ($HbCO$). In the presence of *CO*, the oxygen dissociation curve shifts to the left resulting in increased affinity of Hb for O_2 . This increased affinity prevents unloading of O_2 from Hb and impairs O_2 delivery to the tissues. Thus inhalation of *CO* can decrease the oxygen-carrying capacity of hemoglobin and impair tissue oxygenation.

In addition to Hb, *CO* also binds to myoglobin (Mb). Mb is a monomeric heme protein present in the muscle tissue and each myoglobin molecule can bind to one O_2 molecule forming oxymyoglobin (MbO_2). Mb is an oxygen store and also binds to *CO* to form carboxymyoglobin ($MbCO$). *Mb* binds *CO* ~36 times more strongly than it binds O_2 . Thus, inhalation of *CO* can decrease the oxygen-storing capacity of myoglobin and impair tissue oxygenation.

Exposure to *CO* concentrations exceeding permissible exposure levels (average of 50 ppm over 8 hrs) is a significant environmental and occupational health concern (EHC, 1979; Raub et al., 1999). There are approximately 4000 deaths and over 40,000 emergency department visits resulting from *CO* exposures in the United States each year (Raub et al., 2000; Tucker and Eichold, 2005). *CO* toxicity causes mortality primarily due to the effects of severe hypoxia by attaching itself to Hb and Mb and reducing the oxygen carrying capacity of these heme proteins. Both the therapy (i. e., normobaric vs. hyperbaric oxygen) and the duration of treatment are determined by the percent of

%HbCO in the blood and the state of consciousness of the patient when admitted to the hospital. Unfortunately, the %HbCO provides limited information regarding the total body burden of *CO* and the severity of the *CO* exposure because %HbCO correlates only weakly with extravascular *CO* content, and because a given %HbCO could have been achieved via an infinite variety of exposure conditions.

Although high doses of *CO* are toxic, techniques involving rebreathing relatively low concentrations of *CO* have been used with moderate success in both clinical and sports medicine to measure total hemoglobin mass, a value which provides information regarding adaptation to exercise training and various illnesses (Heinicke et al., 2001; Garvican et al., 2010; Schmidt and Prommer, 2005, 2010). As is the case with *CO* poisoning, the accuracy of *CO*-rebreathing methods is dependent on the ability to account for all the *CO* in the body, which %HbCO levels alone do not provide.

It would be difficult, and in some cases impossible, to obtain the information necessary to accurately determine the total body burden of *CO* in a patient (*CO* poisoned victim) or a study subject (hemoglobin mass determination). The total body burden of *CO* is the amount of *CO* present in the blood (%HbCO), lungs, nonmuscle tissue and muscle tissue (%MbCO). Determination of total body burden of *CO* is difficult mainly because non-invasive measurements of *MbCO* are not possible. Use of a mathematical model, however, greatly improves the ability to address this question of assessing the total body burden of *CO*. I hypothesize that “using a validated mathematical model to accurately estimate the amount of *CO* bound to myoglobin during and after *CO* inhalation will (i) allow improving the accuracy of *CO*-rebreathing methods to determine hemoglobin mass and (ii) aid in suggesting treatments ensuring fast *CO* removal from the body, after *CO* poisoning.”

Our laboratory has developed mathematical models that predict the uptake, distribution, and elimination of *CO* under a variety of exposure conditions (Bruce and Bruce, 2003,2006; Bruce et al., 2008). In my MS thesis, I enhanced the most recent model (Bruce et al., 2008) by adding a separate myocardial compartment and assessing

the effects of exercise on myocardial oxygen content in the presence of *CO* (Erupaka et al., 2010). My doctoral dissertation comprises three projects, where each project is designed to accomplish the Specific Aims listed below.

The first Specific Aim of my Doctoral dissertation was to use this enhanced model (Erupaka et al., 2010) to evaluate two commonly used *CO* rebreathing methods (Burge and Skinner, 1995; Schmidt and Prommer, 2005) to estimate hemoglobin mass (M_{Hb}) and to propose an alternative method with lower errors than the methods currently in use. The main aim of this project was to use a validated mathematical model to simulate the two commonly used *CO* rebreathing protocols (Burge and Skinner, 1995; Schmidt and Prommer, 2005) for a population of healthy subjects and then analyze the simulation results to determine any potential sources of errors in estimation of M_{Hb} . As a process of validation experimentally measured %HbCO levels (Garvican et al., 2010) from healthy human subjects during the two *CO* rebreathing protocols were compared with the model estimated %HbCO levels. Also, a new standardized *CO* rebreathing method to determine M_{Hb} with lower errors than the methods currently in use has been proposed and modifications to the existing *CO* rebreathing methods to improve estimation of M_{Hb} have been suggested. Methods to accomplish the first Specific Aim are discussed in detail in chapter 2 of this dissertation.

The second Specific Aim was to further enhance the earlier model (Erupaka et al., 2010) in order to be able to model the effects of poikilocapnic normobaric (NBO₂), isocapnic normobaric (INBO₂) and poikilocapnic hyperbaric (HBO₂) oxygen therapy on brain oxygen levels. To achieve this aim it was necessary to enhance the model by adding a separate brain tissue compartment and to include control of ventilation, cardiac output, and brain blood flow with changes in O_2 and CO_2 levels. In order to understand the role of CO_2 during isocapnic and poikilocapnic treatment protocols, mass balance equations for CO_2 were added for all the compartments in the model. The main aim of this project was to enhance my earlier model and validate it for various conditions of changing O_2 or CO_2 concentrations like hypoxia, hyperoxia,

hyperbaric oxygen, hypercapnia and hypocapnia. Methods to accomplish the second Specific Aim are discussed in detail in chapter 3 of this dissertation.

The third Specific Aim was to use this enhanced and validated model to predict PO_2 's in the brain, heart and skeletal muscle tissues, and to compare the rates of CO removal in CO -poisoned patients treated with NBO_2 , HBO_2 or $INBO_2$. The main aim of this project was to compare NBO_2 , HBO_2 and $INBO_2$ therapies, to determine the best treatment strategy to be administered, ensuring fastest CO removal and O_2 delivery after healthy subjects were exposed to varying concentrations and durations of CO poisoning. Methods to accomplish my third Specific Aim are discussed in detail in chapter 4 of this dissertation.

**Chapter 2: Computational Analyses of Carbon monoxide (CO) Rebreathing
Methods to Estimate Hemoglobin Mass in Humans**

Contents of this chapter will be submitted as a manuscript

INTRODUCTION

Determination of total hemoglobin mass (M_{Hb}) is important in the fields of clinical and sports medicine (Garvican et al., 2010; Heinicke et al., 2001; Schmidt and Prommer, 2005). Routine measurements of M_{Hb} are made to determine the effects of adaptation to exercise training, environmental stresses, illness and trauma. Radioactive methods and dilution techniques are the most popular procedures to measure M_{Hb} . Determinations of M_{Hb} from the radioactive methods are reliable but have the disadvantage of being radioactive. The radioactivity is due to injection of radioactive markers like ^{51}Cr or ^{11}CO -labeled RBC's. The dilution techniques to determine M_{Hb} are less harmful due to the usage of safe doses of carbon monoxide (CO), Evans blue dye or indocyanine green as markers. Recently Gore et al. (2005) had concluded that the determination of M_{Hb} using the CO rebreathing dilution technique has an error comparable to that of the radioactive methods and also errors lower than that obtained from other dilution techniques.

In the CO rebreathing methods, a known volume of CO (V_{CO_i}) is rebreathed in 100% O_2 . The duration of rebreathing is different for the various CO rebreathing protocols (Burge and Skinner, 1995; Garvican et al., 2010; Hutler et al., 2000, Schmidt and Prommer, 2005). However, the two commonly used CO rebreathing techniques to determine M_{Hb} were described by Burge and Skinner in 1995 and by Schmidt and Prommer in 2005. In these methods during the process of CO rebreathing, CO leaves the alveolar space and enters the vascular space via diffusion. In the vascular space, Hb binds CO to form HbCO. Depending on the CO rebreathing protocol, administered CO can leave the vascular space either by diffusion to the extravascular compartments containing heme pigments like myoglobin (Mb), cytochrome c oxidase, etc or to the lungs (from where CO is exhaled after the period of rebreathing). When equilibration of arterial and venous HbCO levels occurs, CO is assumed to be well mixed in the vascular space. In the CO rebreathing techniques, mixing time is determined as the time at which the %HbCO levels obtained from two or more blood sites (arterial, capillary or venous) are equal. Experimentally, the best one can do with current analyses of HbCO is to determine the time at which the differences between %HbCO levels is $\leq 0.1\%$. The CO rebreathing

methods are based on the principle that, after mixing of *CO* in the vascular space is complete, the M_{Hb} equals to the ratio of the volume of *CO* bound to Hb (V_{COHb}) and the maximal capacity of Hb to bind to *CO* (Equation 2.1).

$$M_{Hb} = K \cdot V_{COHb} \cdot \frac{100}{1.58 \Delta HbCO_i} \dots\dots\dots 2.1$$

where,

$K=1$ (as all values are in BTPS)

$V_{COHb} = V_{CO_i} - V_{CO \text{ Lungs}} + \text{rebreathing system at end of rebreathing } (V_{CO \text{ L+S}}) -$

$V_{CO \text{ exhaled between end of rebreathing and time of blood sampling } (V_{CO \text{ ex}}) -$

$V_{CO \text{ bound to myoglobin at } T_{\text{sample}}} (V_{COMb})$

$\Delta HbCO_i = \text{Change in \%HbCO between time } T_0 \text{ and } T_{\text{sample}} \text{ for blood compartment 'i'.$ where $i = \text{arterial (ar), capillary (cot, cm), venous (vm)}$

$T_0 = \text{Start time of the experiment}$

$T_{\text{sample}} = \text{Sampling time}$

$1.58 = \text{Hufners constant in BTPS (Gorelov, 2004)}$

A prerequisite to accurately calculate the M_{Hb} using these methods is to ensure that mixing of *CO* in the vascular space is complete ($^{true}T_{mix}$). Due to the measurement limitations of %HbCO and dependence of determinations of $^{true}T_{mix}$ on these values, M_{Hb} is calculated from blood samples taken at 1-2 min away from $^{true}T_{mix}$. This time is referred to as sampling time, T_{sample} . Optimal values for $^{true}T_{mix}$ or T_{sample} to calculate M_{Hb} are often debatable in the *CO* rebreathing methods (Gore et al., 2006, Schmidt and Prommer, 2005). Depending on the *CO* rebreathing method applied, estimated values of the $^{true}T_{mix}$ (referred as T_{mix} in the text) range from 2-12 minutes (Burge and Skinner, 1995; Garvican et al., 2010; Schmidt and Prommer, 2005). Duration of *CO* rebreathing, volume of *CO* administered, site of blood sampling and variability among subjects may be some of the factors contributing to a wide range of T_{mix} values obtained from various *CO* rebreathing methods (Burge and Skinner, 1995; Garvican et al., 2010; Gore et al., 2006; Schmidt and Prommer, 2005). Also the %HbCO values at T_{sample} are influenced by the site of sampling and diffusion of *CO* from vascular space to extravascular tissues or to the lungs (Garvican et al., 2010). In a given subject for a *CO* rebreathing method,

sampling for %HbCO from different blood sites (arterial, capillary, venous) before complete mixing of CO in the vascular space results in different estimates of M_{Hb} (Garvican et al., 2010). Thus the reliability and accuracy of M_{Hb} estimation is dependent on the blood sites sampled for %HbCO measurements (Equation 2.1) and determination of T_{mix} .

Another prerequisite for accurate estimation of M_{Hb} from CO rebreathing methods is to be able to account for the entire volume of CO at T_{sample} that has been administered at the start of the experiment (T_0). Thus the estimation of M_{Hb} is dependent on the calculation of the volume of CO bound to hemoglobin, V_{COHb} and %HbCO (Equation 2.1). However, the calculation of V_{COHb} is dependent on the measurements of (i) the volume of CO in the lungs and the rebreathing system at the end of rebreathing ($V_{CO L+S}$), (ii) the volume of CO exhaled from the end of rebreathing to T_{sample} ($V_{CO ex}$), and (iii) the volume of CO bound to Mb at T_{sample} (V_{COMb}). Thus, any errors in determination of $V_{CO L+S}$, $V_{CO ex}$, or V_{COMb} may lead to either an overestimation or underestimation of total hemoglobin mass, M_{Hb} (Garvican et al., 2010; Steiner and Wehrlin, 2010).

Prior to 2007, estimation of M_{Hb} from CO rebreathing methods assumed no loss or minimal loss of CO (1% of V_{CO_i}) to Mb (Burge and Skinner, 1995; Hutler et al., 2000; Gore et al., 2006; Schmidt and Prommer, 2005). In 2003, Bruce and Bruce used their multicompartiment model to simulate a CO rebreathing method (Burge and Skinner, 1995) and concluded that Mb in the muscle tissue is a reservoir for binding CO . Inspired by the findings of this model, recently Prommer and Schmidt (2007) have derived a formula to estimate V_{COMb} and concluded that ~2% of V_{CO_i} is bound to Mb. This formula was derived on the assumption that there is constant flux of CO from blood to the tissues containing Mb. The errors introduced in determination of M_{Hb} due to using this formula are not known. In the recent CO rebreathing experiments (Garvican et al., 2010; Steiner and Wehrlin, 2010), using Prommer and Schmidt's formula (2007) to determine V_{COMb} resulted in higher estimates of M_{Hb} from Burge and Skinner's method (1995) when compared to Schmidt and Prommer's method (2005). The inability to account for the loss

of CO from Hb to Mb present in muscle tissues will lead to an overestimation of total M_{Hb} .

The existing CO rebreathing methods result in different estimates of M_{Hb} for a given subject (Garvican et al., 2010; Steiner and Wehrlin, 2010), thus questioning the reliability and accuracy of these methods to determine M_{Hb} . Differences in the estimates of M_{Hb} from these methods makes it difficult to compare results from different studies which measure M_{Hb} to determine the effects of adaptation to exercise training, altitude and other blood related illnesses. In order to evaluate a CO rebreathing method which estimates M_{Hb} with low errors, it would be better to compare the estimates of M_{Hb} with a known value of M_{Hb} (\hat{M}_{Hb}). The commonly used CO rebreathing methods make various assumptions in calculating $V_{CO} L+S$ (Burge and Skinner, 1995), $V_{CO} ex$ (Schmidt and Prommer, 2005), or V_{COMb} (Prommer and Schmidt, 2007). Errors in determination of $V_{CO}L+S$, $V_{CO} ex$, or V_{COMb} due to these assumptions may lead to either an overestimation or underestimation of total hemoglobin mass, or, possibly, to compensating errors (Equation 2.1). Also, it is important to know if the differences in M_{Hb} from different CO rebreathing methods are due to the variations in these methods to estimate M_{Hb} or due to errors in the underlying concepts of CO dilution techniques to determine M_{Hb} .

Thus the main aim of this study is to use a validated mathematical model to simulate the two commonly used CO rebreathing protocols (Burge and Skinner, 1995; Schmidt and Prommer, 2005) for a group of healthy subjects and then analyze the simulation results to determine any potential sources of errors in estimation of M_{Hb} (\hat{M}_{Hb}). As a process of validation experimentally measured %HbCO levels (Garvican et al., 2010) in nine healthy human subjects from three different blood compartments (arterial, capillary and venous), during the two CO rebreathing protocols were compared with the model estimated %HbCO levels. In addition the model estimated M_{Hb} was compared to the experimentally determined M_{Hb} . Also, a new CO rebreathing method to determine \hat{M}_{Hb} with low errors, independent of the site of sampling has been proposed and modifications to the existing CO rebreathing methods to improve estimation of M_{Hb} have been suggested. In addition the blood sampling site and the values for T_{mix} and

T_{sample} , to obtain low errors in \hat{M}_{Hb} independent of the *CO* rebreathing method used to estimate M_{Hb} have been determined.

METHODS

Model description

The mathematical model used in this study has been described in detail previously (Erupaka et al., 2010). This validated model was capable of predicting time varying %HbCO levels, carboxymyoglobin (%MbCO) levels and O_2 tensions in various tissue and blood compartments for a variety of *CO* exposures (Erupaka et al., 2010). The major features of this model are the expansion of a standard single lumped compartment representation of skeletal muscle tissues into two tissue subcompartments interacting with three vascular subcompartments (Bruce et al., 2008) and an addition of a cardiac compartment (Erupaka et al., 2010) with an architecture similar to that of the skeletal muscle. This model (Erupaka et al., 2010) was shown to reproduce experimental data from transient *CO* exposure (Benignus et al., 1994) and one of the *CO* rebreathing method (Burge and Skinner, 1995). The %HbCO predicted by the model for arterial (%HbCO_{ar}) and skeletal muscle venous (%HbCO_{vm}) blood compartments were in agreement with the experimentally measured arterial and venous %HbCO values (Bruce and Bruce, 2008; Erupaka et al., 2010). %HbCO_{vm} is the %HbCO of the blood exiting from the third vascular subcompartment of skeletal muscle tissue. In addition to arterial and antecubital venous blood sites, the two common sites of measurement for capillary blood samples in *CO* rebreathing protocols are finger tips or ear lobe. In the current model, a blood site equivalent of measurements made from pre-warmed finger tip is assumed to be the %HbCO in blood entering the second vascular subcompartment of skeletal muscle tissue (%HbCO_{cm}). As fingers contain Mb, this blood site is assumed to surround the skeletal muscle subcompartment of the model. A model equivalent of %HbCO measurements made from the ear lobe is assumed to be that from the venous vascular compartment of the nonmuscle tissue (%HbCO_{cot}).

To determine \hat{M}_{Hb} from the model, equations 2.2-2.4 were added to the model (See Table 2.1-2.2 for details). For Garvican's data set, M_{Hb} was also estimated using

equation 2.1a in equation 2.1. In the model, V_{COMb} is calculated from the tissue volumes and MbCO concentrations of skeletal and cardiac muscle subcompartments (Equation 2.2). V_{COex} and $V_{CO L+S}$ are calculated using equations 2.3-2.4. V_{CO} exhaled calculated in the model would be the equivalent of collecting the expired CO over a specified duration of time in an experiment, e.g., $V_{CO ex}$ is the volume of exhaled CO collected from the end of rebreathing to T_{sample} . $V_{CO L+S}$ calculated in the model would be the equivalent of measuring volume of CO in the lungs and rebreathing system at a specific time, depending on the CO rebreathing method e.g., $V_{CO L+S}$ at T_{sample} or $V_{CO L+S}$ at the end of rebreathing.

$$V_{COHb} = \sum Vb_i \cdot [HbCO]_i \dots\dots\dots 2.1a$$

where,

Vb_i and $[HbCO]_i$ are the blood volume and concentration of Hb bound to CO in vascular compartment 'i'. $i =$ arterial (ar), three vascular subcompartments of skeletal muscle (bm_1, bm_2, bm_3), three vascular subcompartments of cardiac muscle (bc_1, bc_2, bc_3), other tissue venous blood compartment (vot) and mixed venous blood compartment (mx).

$$V_{COMb} = \left\{ \begin{array}{l} V_{m1} \cdot MbCO_{m1} + V_{m2} \cdot MbCO_{m2} \\ + V_{cm1} \cdot MbCO_{cm1} + V_{cm2} \cdot MbCO_{cm2} \end{array} \right\} \dots\dots\dots 2.2$$

where,

V_{m1} and V_{m2} are tissue volumes of skeletal muscle subcompartments. V_{cm1} and V_{cm2} are tissue volumes of cardiac muscle subcompartments. $MbCO_{m1}$ and $MbCO_{m2}$ are MbCO concentrations in skeletal muscle subcompartments at T_{sample} . $MbCO_{cm1}$ and $MbCO_{cm2}$ are MbCO concentrations in cardiac muscle subcompartments at T_{sample} .

$$V_{CO ex} = \int_{T_{end \text{ of rebreathing}}}^{T_{sample}} \dot{V}_A \cdot C_A CO(t) dt \dots\dots\dots 2.3$$

where,

\dot{V}_A = Measured alveolar ventilation

$C_A CO(t)$ = Alveolar CO concentration

$V_{CO ex}$ is zero in protocol B.

$$V_{CO} L + S = (V_{RS} + V_{LV}) \cdot C_A CO_{t=T} \dots\dots\dots 2.4$$

where,

V_{RS} = Volume of rebreathing system or spirometer

V_{LV} = Lung volume = Functional residual capacity for protocol B and residual volume for protocol P

$C_A CO$ = Alveolar CO concentration at time ‘T’

T= T_{sample} for protocol B and end of rebreathing time (2 min) for protocol P.

Simulation Description

This study comprised simulations of two commonly used CO rebreathing methods on two different data sets (See section “Data sets used for simulations of CO rebreathing protocols” for details). The first data set was provided by Garvican et al. (2010) and was used for model validation. The second data set was provided by Benignus et al. (1994) and was used to analyze potential sources of errors in calculation of \hat{M}_{Hb} from the CO rebreathing methods.

To validate the model and assess its predictive power to estimate %HbCO levels and M_{Hb} in different blood compartments, I used the mathematical model to simulate the CO rebreathing experiments of Garvican et al. (2010) in nine healthy (2 female, 7 male), recreationally-active, human subjects. Each subject was individually simulated using the subject specific parameters provided by the investigators, Garvican et al. (2010). The model estimated %HbCO_{ar}, %HbCO_{cm}, and %HbCO_{vm} for each subject were compared with their respective experimentally measured %HbCO levels, for the two CO rebreathing methods described in their study (Garvican et al., 2010). If the model predicted mean ± SD values of %HbCO from all the nine subjects were within the 95% confidence limits of the experimental data, then the model was considered to be capable of reproducing the experimental data. Garvican et al. (2010) also provided us with the best estimates of M_{Hb} for each subject and these values were considered as $^A M_{Hb}$ for this data set. M_{Hb} from four different blood compartments was estimated from the model using the predicted %HbCO levels and V_{COHb} (Equation 2.1a). Errors in estimation of

M_{Hb} from the two CO rebreathing protocols at different time points were calculated by comparing the model calculated M_{Hb} and $^A M_{Hb}$. It was assumed that, irrespective of the blood site sampled obtaining errors less than 2% would imply that the model is capable of estimating the experimentally determined M_{Hb} , $^A M_{Hb}$. As Garvican's data was used to validate the model for prediction of %HbCO's and \hat{M}_{Hb} 's in various blood compartments, this data set was not used for detailed analysis of determining potential sources of errors in the CO rebreathing methods.

Data (Benignus et al., 1994) from fifteen healthy, male human subjects with known M_{Hb} , ($^A M_{Hb}$) were used to simulate the two CO rebreathing studies. $^A M_{Hb}$ for each subject was calculated as the product of blood volume (measured by $Na_2^{51}CrO_4$ dilution method) and hemoglobin concentration (measured by IL-282 CO-oximeter) provided by the investigators. To allow detailed analysis of CO rebreathing methods to estimate M_{Hb} , this study comprised simulations of the methods described by Burge and Skinner in 1995 (which I refer to as protocol B) and by Schmidt and Prommer in 2005 which was later modified by Prommer and Schmidt in 2007 (which I refer to as protocol P). The volume of CO administered for a given subject was the same in both the protocols, i.e. 1 ml of CO/Kg of body weight (BW). For protocols B and P, the model was used to determine the uptake and distribution of CO in each subject. The time varying %HbCO's from the arterial, capillary other tissue, capillary muscle and muscle venous blood compartments (symbolized by %HbCO_{ar}, %HbCO_{cot}, %HbCO_{cm}, %HbCO_{vm}) and alveolar CO concentrations ($C_A CO$) were calculated by the model for protocols B and P. The simulation results of each subject were analyzed to calculate \hat{M}_{Hb} and then compared to the $^A M_{Hb}$. In this study, \hat{M}_{Hb} was determined using (i) the exact values from the model for $V_{CO L+S}$, $V_{CO ex}$, and V_{COMb} (\hat{M}_{Hb} thus calculated will be referred as $^M \hat{M}_{Hb}$) and (ii) approximated values based on the published formulas for calculating $V_{CO L+S}$, $V_{CO ex}$, and V_{COMb} (\hat{M}_{Hb} thus calculated will be referred as $^E \hat{M}_{Hb}$). $^M \hat{M}_{Hb}$ was calculated and compared to $^A M_{Hb}$ of the subjects to ensure that any errors in calculation of \hat{M}_{Hb} are probably due to the assumptions made in the methods of calculating it in the experiments

rather than to the errors in the predicted data ($V_{CO_{Hb}}$, $V_{CO\ L+S}$, $V_{CO\ ex}$, and V_{COMb}) from the model. Also, ${}^E\hat{M}_{Hb}$ was compared to ${}^A M_{Hb}$ to determine the potential possibility of errors in estimation of M_{Hb} from the existing *CO* rebreathing methods. The major sources leading to errors in calculation of \hat{M}_{Hb} from the two *CO* rebreathing methods were determined on comparing the values of $V_{CO\ L+S}$, $V_{CO\ ex}$, and V_{COMb} used to calculate ${}^M\hat{M}_{Hb}$ and ${}^E\hat{M}_{Hb}$ (See section “*Estimation of hemoglobin mass*” for details on calculation of ${}^M\hat{M}_{Hb}$ and ${}^E\hat{M}_{Hb}$). It was assumed that if the errors obtained on comparison of ${}^A M_{Hb}$ with the \hat{M}_{Hb} calculated from the model are less than 2%, it would imply that the errors in calculation of ${}^E\hat{M}_{Hb}$ are not due to errors in the underlying concepts of *CO* rebreathing methods or due to the errors in calculation of ${}^M\hat{M}_{Hb}$. See Table 2.1 for symbols and definitions.

Simulated CO rebreathing protocols

This study comprised (i) simulations of *CO* rebreathing methods as described by Garvican et al. (2010) in healthy, recreationally-active subjects to validate the model and (ii) simulations of protocol B and protocol P in healthy subjects (Benignus et al., 1994) to allow detailed analysis of *CO* rebreathing methods to estimate M_{Hb} . ACSL™ version 11.8 was used for implementing the model and running the simulations. ACSL is a computer language designed for modelling and evaluating the performance of systems described by time-dependent, nonlinear differential equations. Simulations were performed in double precision and a 12 min stabilization period was initiated with every simulation run for the baseline simulation to reach a steady state. For the duration of rebreathing, the rebreathing system or the spirometer and the lungs form a closed circuit. To simulate rebreathing, the lung volume was augmented by the volume of the rebreathing system or spirometer and alveolar ventilation was set to zero.

To validate the model, *CO* rebreathing methods described by Garvican et al. (2010) were simulated. The *CO* rebreathing methods in their study are similar to protocols B and P described below, but with some changes in the *CO* dose administered.

To simulate protocol B, each subject rebreathed 1 ml of CO/Kg of body weight in ~99% O_2 for a duration of 40 mins. Also oxygen flow rate equal to the metabolic uptake was added to the rebreathing bag to avoid hypoxia as a result of underfilling of the bag. In this protocol the subject is on 100% O_2 prior to rebreathing. The lung volume was augmented by the volume of the rebreathing system of 3.5 L.

To simulate protocol P, each subject rebreathed 1 ml of CO /Kg of BW in ~ 99% O_2 for 2 mins. Prior to CO rebreathing, the subject is on room air. CO rebreathing was followed by 13 mins of normal breathing on room air. The lung volume was augmented by the volume of the rebreathing system of 2 L.

Estimation of hemoglobin mass (M_{Hb})

In the study conducted by Garvican et al. (2010), the investigators have provided information regarding (personal communication) the sampling time and blood site at which the best estimates of M_{Hb} were obtained in their subjects for the two CO rebreathing methods. The best estimates of M_{Hb} from their study were used as the M_{Hb} for the model simulations and were considered as $^A M_{Hb}$ to allow comparison with $^M \hat{M}_{Hb}$ or $^E \hat{M}_{Hb}$. For the Burge and Skinner method, $^A M_{Hb}$ was obtained at a T_{sample} of 12.5 min in four subjects and at 10 min in five subjects. The blood sampling site was arterial blood in 8 subjects and capillary blood in 1 subject. For the Schmidt and Prommer method $^A M_{Hb}$, was obtained at T_{sample} of 7.5 min (2 subjects), 10 min (4 subjects) and 12.5 min (3 subjects). The blood sampling site was arterial blood in 6 subjects and capillary blood in 3 subjects. For the two CO rebreathing protocols, $^M \hat{M}_{Hb}$ for these subjects was calculated using the model equations 2.1-2.4 at the T_{sample} and the blood sites specified by the investigators. Also M_{Hb} was estimated using the model predicted %HbCO levels and V_{COHb} from equation 2.1a. This calculation was done to determine lower bounds on errors produced by these methods for estimating M_{Hb} . $^E \hat{M}_{Hb}$ for all the subjects were calculated using the formulas (Equations 2.5-2.7) described by Garvican et al. (2010) at the specified T_{mix} , T_{sample} and blood site. In their study the formula to calculate V_{CO} ex was different from Equation 2.6, as alveolar ventilation (\dot{V}_A) was estimated from a regression

equation and the alveolar CO concentration (C_{ACO}) was measured at a different time point. For the two CO rebreathing methods, the values obtained for ${}^E\hat{M}_{Hb}$ and ${}^M\hat{M}_{Hb}$ were compared with ${}^A M_{Hb}$.

For all the 15 healthy, male subjects of Benignus et al. (1994), M_{Hb} for protocols B and P was estimated from %HbCO calculated by the model for four blood compartments: arterial, venous blood of nonmuscle tissue (approximation of earlobe blood), blood flowing into the capillary subcompartment of muscle tissue (approximation of arterialized fingertip capillary blood) and muscle venous blood (symbolized by subscripts ar, cot, cm and vm respectively). For a given protocol to determine the T_{mix} for each subject; the time dependent pairwise differences (Figure 2.1) between %HbCO's of arterial, capillary (cot, cm) and venous blood compartments were plotted along with a reference line at ± 0.1 . The time at which $\Delta\%HbCO$ last crosses the 0.1 reference line was considered as the T_{mix} . The criterion of 0.1 reference line to determine T_{mix} was chosen due to the 0.1% detection limit of CO oximeter to measure %HbCO. After the T_{mix} was determined in each subject for a given protocol, T_{sample} was calculated as 1.5 min from T_{mix} .

To estimate M_{Hb} from equation 2.1, the $\%\Delta HbCO$ for each of the four blood sites and the volume of CO bound to Hb (V_{COHb}) were calculated. The $\%\Delta HbCO$ value for a specific blood compartment is calculated using the model predicted %HbCO's of that blood compartment at T_0 and T_{sample} ($\%HbCO_{T_{sample}} - \%HbCO_{T_0}$). However, the V_{COHb} (Table 2.2) was calculated using (i) model equations 2.2-2.4 (${}^M V_{COHb}$) and also using (ii) the formulas published (${}^E V_{COHb}$) by the authors of protocols B and P (Schmidt and Prommer, 2005; Prommer and Schmidt, 2007; Burge and Skinner, 1995) which are described below and in Table 2.2. The authors of protocol B (Burge and Skinner, 1995) used equation 2.5 to estimate V_{CO} L+S and the authors of protocol P (Schmidt and Prommer, 2005) used equation 2.6 to estimate V_{CO} exhaled. V_{COMb} was estimated using equation 2.7 in both the protocols (Prommer and Schmidt, 2007; Garvican et al., 2010). Thus for a given protocol B or P, ${}^M\hat{M}_{Hb}$ is the M_{Hb} estimated using ${}^M V_{COHb}$ and ${}^E\hat{M}_{Hb}$ is the M_{Hb} estimated using ${}^E V_{COHb}$ (Table 2.2). For the CO rebreathing methods, I assumed

that if the errors obtained on comparison of \hat{M}_{Hb} with ${}^M\hat{M}_{Hb}$ or ${}^E\hat{M}_{Hb}$ are less than 2%, then ${}^M\hat{M}_{Hb}$ or ${}^E\hat{M}_{Hb}$ will be considered as a good estimate of M_{Hb} .

$$V_{CO} L + S = \frac{2.2}{100} \cdot V_{CO_i} \dots\dots\dots 2.5$$

where,

V_{CO_i} = Total volume of CO administered

$$V_{CO} ex = \dot{V}_A \cdot \Delta T \cdot C_A CO_{t=20} \dots\dots\dots 2.6$$

where,

\dot{V}_A = Assumed alveolar ventilation = 5L/min

$\Delta T = T_{sample} - 2$

$C_A CO$ = Alveolar CO concentration at t=20 min

$$V_{COMb} = V_{COMb_{T_{mix}-T_{sample}}} \cdot \frac{T_{sample}}{T_{sample} - T_{mix}} \dots\dots\dots 2.7$$

where,

$$V_{COMb_{T_{mix}-T_{sample}}} = \left(V_{COt} - V_{CO} L + S - V_{CO} ex \right)_{T_{sample}} - \left(\frac{\Delta HbCO_{T_{sample}}}{\Delta HbCO_{T_{mix}}} \right) \cdot \left(V_{COt} - V_{CO} L + S - V_{CO} ex \right)_{T_{mix}}$$

Data sets used for simulations of CO rebreathing protocols

Garvican et al. (2010) have compared uptake kinetics of CO in the CO rebreathing methods which were proposed by Burge and Skinner (1995), and Schmidt and Prommer (2005). This data set was used to validate my model. In this experiment (Garvican et al., 2010), the investigators have measured time varying %HbCO levels from three different blood sites (ar, cm, vm), age, body weight, height, volume of CO dose administered, and Hb concentrations in nine healthy, recreationally-active subjects. Two of their nine subjects were females. The %HbCO were taken from arterial (forearm), capillary (finger tips) and venous (forearm) blood sites at different time points of the

experiment. For the two *CO* rebreathing methods, the investigators have also provided information regarding (personal communication) the sampling time and blood site at which the best estimates of M_{Hb} were obtained in these subjects. The blood volume was calculated from experimentally determined M_{Hb} and the Hb concentrations by Garvican et al., 2010. For any given subject, these calculated blood volumes were different for the two *CO* rebreathing methods. In the simulations of this study, using the blood volume values from the Burge and Skinner method showed better agreement between the model predictions of %HbCO levels and the experimental data. Thus in the simulations, values for blood volume, M_{Hb} (\hat{M}_{Hb}) and Hb concentrations for all the subjects were used from Burge and Skinner's method. In the simulations, the rebreathing bag volume, ambient temperature and ambient pressure were set to the experimentally measured values. Total body oxygen consumption was calculated as 3.2 ml/Kg and cardiac output was estimated from the regression equation (Equation C.3 in Appendix C of Erupaka et al., 2010). Previous models from our lab were developed to simulate healthy human subjects (Bruce and Bruce, 2008; Erupaka et al., 2010). In literature it was found that the capillary density, mitochondrial content, heart rate and stroke volume at rest in untrained subjects differed statistically from the healthy endurance trained human subjects (Andersen and Henriksson, 1977; Brodal et al., 1977; Ingjer, 1979; Kalliokoski et al., 2001; Sagiv et al., 2007; Tibes et al., 1977; Zoladz et al., 2005). Other parameters at rest like muscle blood volume, muscle blood flow, cardiac output, metabolic rate or ventilation, did not differ statistically between the trained and untrained groups (Kalliokoski et al., 2001; Sagiv et al., 2007; Tibes et al., 1977). Thus to simulate *CO* rebreathing methods in healthy, recreationally-active subjects, the muscle diffusion coefficient of *CO* (D_{MCO}) and capillary density of the skeletal muscle was increased by 34% (Brodal et al., 1977; Zoladz et al., 2005). The D_{MCO} was varied in proportion to muscle mass, with a value of D_{MCO} of 0.302 ml/min/Torr/Kg of muscle mass. As the subjects are assumed to be trained, a heart rate of 51 beats/min was used (Kalliokoski et al., 2001; Sagiv et al., 2007; Tibes et al., 1977) to estimate myocardial oxygen consumption and myocardial blood flow (Erupaka et al., 2010). Values for all other parameters that were not provided by the investigators and were not significantly affected with exercise training, were those used in and referenced in my previous publication (Erupaka et al., 2010).

Benignus et al. (1994) exposed fifteen healthy, male human subjects to high concentrations of *CO* for short durations. This data set was used to analyze and determine sources of errors in the *CO* rebreathing methods to estimate M_{Hb} . Previous versions of the model were able to reproduce experimental data of arterial and venous %HbCO from all the subjects for the transient *CO* exposure simulations (Bruce and Bruce, 2003; Bruce and Bruce, 2006; Bruce et al., 2008). In this experiment (Benignus et al., 1994), measurements of age, body weight, height, blood volume, hemoglobin concentration, cardiac output, ventilation, initial %HbCO and lung diffusivity coefficient of *CO* were provided by the investigators for each subject. $^A M_{Hb}$ for each subject was calculated as the product of blood volume and hemoglobin concentration measurements. The blood volume in this study was measured by $Na_2^{51}CrO_4$ dilution method. Total body oxygen consumption was calculated as 3.2 ml/Kg. D_{MCO} was varied in proportion to muscle mass, with a value of D_{MCO} of 0.225 ml/min/Torr/Kg of muscle mass. Values for all other parameters that were not provided by the investigators have been referenced in my previous publication (Erupaka et al., 2010).

Determination of effects of T_{mix} , T_{sample} and sampling blood site on estimation of M_{Hb}

In order to determine the effects of T_{mix} on estimation of M_{Hb} , $^M \hat{M}_{Hb}$ (the M_{Hb} estimated using the exact values from the model for $V_{CO} L+S$, $V_{CO} ex$, and V_{COMb}) was calculated for each *CO* rebreathing protocol from four blood compartments (ar, cot, cm, vm) for Benignus's subjects by varying the T_{mix} . In calculations of $^M \hat{M}_{Hb}$, T_{mix} was assumed as 1, 3, 5, 7, 9, 11, 13, 15 and 38 minutes and the difference between T_{sample} and T_{mix} was always 1.5 min. For each subject, the calculated $^M \hat{M}_{Hb}$ at a different T_{sample} (based on the T_{mix} value) was compared with the known hemoglobin mass of the subject, $^A M_{Hb}$ and the error in estimation of M_{Hb} was calculated from four different blood compartments. For a given *CO* rebreathing method, the errors in calculation of M_{Hb} from different blood sites and T_{mix} were plotted for these subjects. The minimal value of T_{mix} and the blood sampling site at which low errors in estimation of M_{Hb} were obtained independent of the *CO* rebreathing method applied, was determined. In this study I also looked at the effects of changing various factors like Mb concentration, V_{CO_i} , D_{MCO} (the

muscle diffusion capacity of CO), duration of rebreathing, muscle blood flow and muscle blood volume on T_{mix} in one of the Benignus's subjects (S112, Benignus et al., 1994).

Also, to determine the effects of T_{sample} on estimation of M_{Hb} , ${}^M\hat{M}_{Hb}$ was calculated from four different blood compartments (ar, cot, cm, vm) for protocols B and P for Benignus's subjects by varying the T_{sample} relative to T_{mix} . ${}^M\hat{M}_{Hb}$ were calculated at T_{sample} 's which were 1.5, 3, 5, 7, 9 and 11 minutes from the determined T_{mix} of each subject. For a given CO rebreathing protocol, the T_{mix} for each subject was determined based on the time at which the difference between the %HbCO's from all the blood compartments was $\leq 0.1\%$. ${}^M\hat{M}_{Hb}$ at different T_{sample} 's were compared with ${}^A M_{Hb}$ and the errors in estimation of M_{Hb} from different blood sites and T_{sample} were plotted for these subjects. The blood sampling site and the minimal value of T_{sample} at which low errors in estimation of M_{Hb} were obtained independent of the CO rebreathing method applied, was determined.

RESULTS

Model behavior

The time course of %HbCO levels from all the blood sites for protocol B and protocol P for a single subject are shown in Figure 2.2. In both the protocols, arterial blood %HbCO_{ar} peaks within the first 2 minutes and then decreases. The capillary blood %HbCO rises initially and then reaches a plateau. Venous blood %HbCO_{vm} increased slowly and then reaches values similar to that of capillary blood %HbCO_{cm} in both the methods. Peak %HbCO_{ar} level is higher in protocol P than in protocol B. Mixing of CO (based on determination of T_{mix} as shown in Figure 2.1) in blood occurred by ~11 min in protocol B and by ~5 min in protocol P for the Benignus's subjects. The above described uptake kinetics of CO are qualitatively in agreement with the peak %HbCO levels and the mixing times are quantitatively in agreement with the T_{mix} values reported in experimental results of protocol B and protocol P (Burge and Skinner, 1995; Schmidt and Prommer, 2005).

Model Validation

The mathematical model was used to simulate the *CO* rebreathing experiments described by Garvican et al. (2010) in nine (2 female, 7 male) healthy, recreationally-active subjects. Each subject was individually simulated using the subject specific parameters provided by the investigators and the time varying %HbCO levels in blood were predicted by the model for the two *CO* rebreathing methods. The model is able to reproduce the experimental measurements of the time varying %HbCO levels made in three different blood compartments (%HbCO_{ar}, %HbCO_{cm}, %HbCO_{vm}) during the two commonly used *CO* rebreathing methods (Figure 2.3-2.4). On the one hand, the model predicted mean %HbCO \pm SD values from the arterial (ar), capillary (cm) and venous (vm) blood compartments at different time points are within the 95% confidence limits of the experimental data for both the *CO* rebreathing methods. On the other hand, individual comparison of model predicted %HbCO levels from all the three blood compartments (ar, cm, vm) with the experimentally measured %HbCO levels at respective time points showed a good agreement for both the *CO* rebreathing methods in 6 of the 9 subjects. However, in three of the nine subjects, the rise in %HbCO levels of the blood compartment “vm” during the initial five minutes was faster than the experimental data for both the methods (Figure 2.16). After five minutes, the model predicted %HbCO levels were similar to the experimentally measured values. In these three subjects I was able to match the model predicted %HbCO_{vm} levels with the experimental values by decreasing the muscle blood flow and increasing the blood volume of muscle vascular subcompartment 3 (V_{bm3}). In all the three subjects the muscle blood flow was decreased by 20% and the blood volume V_{bm3} was increased by 20% of the total mixed venous blood volume (Figure 2.16). However even prior to changing the values of muscle blood flow and V_{bm3} in 3 of the 9 subjects, the model predicted mean %HbCO levels from all the three blood compartments are in good agreement with the mean %HbCO levels made from the experiments of Garvican et al. (2010) for the Burge and Skinner method (Figure 2.3) and the Schmidt and Prommer method (Figure 2.4). Thus, the model is able to reproduce the experimental measurements of time varying %HbCO levels from three different blood compartments and predicts the uptake and distribution of *CO* during the commonly used *CO* rebreathing methods.

Model estimates of M_{Hb} (${}^M\hat{M}_{Hb}$) from the CO rebreathing methods

${}^M\hat{M}_{Hb}$, the M_{Hb} estimated using the exact values from the model (Equations 2.1-2.4, Table 2.2) for V_{CO} L+S, V_{CO} ex, and V_{COMb} was calculated for the data sets of Garvican et al., 2010 (9 healthy-2 female and 7 male, recreationally-active subjects) and Benignus et al., 1994 (15 healthy, male subjects).

For the two CO rebreathing methods, ${}^M\hat{M}_{Hb}$ for Garvican's subjects was calculated using the T_{sample} and the blood sites specified by the investigators. In my simulations of this study the values for the known M_{Hb} , ${}^A M_{Hb}$ for Garvican's subjects were used from the Burge and Skinner's method of the experiments of Garvican et al. (2010). ${}^M\hat{M}_{Hb}$ calculated from these subjects underestimated ${}^A M_{Hb}$ by $0.32\pm 0.8\%$ in the Burge and Skinner method and by $2.2\pm 0.49\%$ in the Schmidt and Prommer method. In the simulations of Schmidt and Prommer method, using the M_{Hb} estimated from Schmidt and Prommer method of the experiments of Garvican et al. (2010), did not change the errors obtained in calculation of ${}^M\hat{M}_{Hb}$ ($2.18\pm 0.46\%$).

In addition, Equation 2.1 was used to calculate time varying M_{Hb} using the model estimated V_{COHb} (Equation 2.1a) and %HbCO's from four different blood compartments. For the Burge and Skinner method (Figure 2.5A) irrespective of the blood site sampled, errors less than 2% in estimation of M_{Hb} occurred at ~ 16 min. Estimates of M_{Hb} were close to the actual M_{Hb} values from arterial (ar) and capillary other tissue (cot) blood sites at ~ 9 min. The estimates of M_{Hb} from all four blood sites were never equal, suggesting incomplete mixing of CO in blood. For the Prommer and Schmidt method (Figure 2.5B) irrespective of the blood site sampled, errors less than 2% in estimation of M_{Hb} occurred at ~ 7 min. Estimates of M_{Hb} were close to the actual M_{Hb} values from all the blood sites at ~ 9 min. Also, the estimates of M_{Hb} from all four blood sites were similar at ~ 9 min, suggesting complete mixing of CO in blood. These results suggest that the model is capable of calculating M_{Hb} from both the CO rebreathing methods with ~ 0 errors at the capillary and arterial sampling blood sites and sampling time of ~ 9 min.

${}^M\hat{M}_{Hb}$ for the data set of Benignus et al. (1994) was calculated for the two *CO* rebreathing protocols B and P using equations 2.1-2.4 (Table 2.2) for arterial (ar), capillary other tissue (cot), capillary muscle (cm) and muscle venous (vm) blood compartments. T_{mix} for each subject was determined based on the time at which the differences between %HbCO's from all the blood compartments was $\leq 0.1\%$ (See methods, Figure 2.1). T_{sample} was considered 1.5 min away from T_{mix} . ${}^A M_{Hb}$ for the data set of Benignus et al. (1994) was calculated for each subject as the product of blood volume (measured by $Na_2^{51}CrO_4$ dilution method) and Hb concentration reported in their study. The ${}^M\hat{M}_{Hb}$ calculated for the Benignus's subjects for both the protocols B and P are in agreement with the ${}^A M_{Hb}$ of these subjects (Table 2.3). The mean errors averaged across the subjects for ${}^M\hat{M}_{Hb}$ from the "cm" and "vm" blood sites are slightly larger (~2%) for protocol B. These errors are due to the sensitivity of M_{Hb} to variability in values of % Δ HbCO (Burge and Skinner, 1995; also see discussion), as % Δ HbCO values at T_{sample} depend on the blood sampling site.

Overall, depending on the site of sampling the values of ${}^M\hat{M}_{Hb}$ for both the *CO* rebreathing methods from the data sets of Garvican et al. (2010) and Benignus et al. (1994) are within 2% of ${}^A M_{Hb}$. This result ensures that the validated model is capable of calculating good estimates of M_{Hb} (${}^M\hat{M}_{Hb}$) for protocols B and P and that any errors in calculation of \hat{M}_{Hb} are probably due to the method of calculating \hat{M}_{Hb} from the existing *CO* rebreathing methods. This result also ensures that the errors in estimation of M_{Hb} are not due to errors in the concepts for estimating M_{Hb} from *CO* rebreathing methods.

*Experimental estimates of M_{Hb} (${}^E\hat{M}_{Hb}$) from the *CO* rebreathing methods*

${}^E\hat{M}_{Hb}$ is the estimate of M_{Hb} which is calculated using the approximated values based on the published formulas for calculating V_{CO} L+S, V_{CO} ex, and V_{COMb} . The model calculated %HbCO_{ar}, %HbCO_{cot}, %HbCO_{cm}, and %HbCO_{vm} are assumed to be

experimental equivalents of %HbCO measurements made from arteries in the forearm, ear lob, pre-warmed finger tips and veins in the forearm respectively.

For the data set of Garvican et al. (2010), ${}^E\hat{M}_{Hb}$ for the two CO rebreathing methods were calculated using the equations provided by Garvican et al. (2010) for calculating $V_{CO L+S}$, $V_{CO ex}$, and V_{COMb} at the specified T_{mix} , T_{sample} and blood site. In Garvican's subjects ${}^E\hat{M}_{Hb}$ underestimated ${}^A M_{Hb}$ by $2.2 \pm 0.9\%$ in the Burge and Skinner method and by $5.8 \pm 0.5\%$ in the Schmidt and Prommer method. As Garvican et al. (2010) did not measure alveolar ventilation (\dot{V}_A) in their subjects nor did they provide the regression equation used to estimate \dot{V}_A in their study, the \dot{V}_A estimated from the model (See section "Model parameters" for details) was used to calculate $V_{CO ex}$ to estimate ${}^E\hat{M}_{Hb}$ in the Schmidt and Prommer method. Larger errors from the Schmidt and Prommer method when compared to Burge and Skinner method suggest that the actual values for M_{Hb} for Garvican's subjects are close to the \hat{M}_{Hb} 's estimated from Burge and Skinner method. It should be noted the errors in ${}^E\hat{M}_{Hb}$ were $5.7 \pm 0.7\%$ if the estimates from Schmidt and Prommer method were considered as ${}^A M_{Hb}$. The errors from Burge and Skinner method are lower as the arterial blood sites were sampled.

For the data set of Benignus et al. (1994), ${}^E\hat{M}_{Hb}$ for the protocols B and P were calculated from all the four blood compartments (ar, cot, cm, vm) using Equations 2.1, 2.5-2.7 (Table 2.2). T_{mix} for each subject was determined based on the time at which the pairwise differences between %HbCO's from all the blood compartments was $\leq 0.1\%$ (See methods, Figure 2.1). T_{sample} was considered 1.5 min away from T_{mix} . The mean errors in ${}^E\hat{M}_{Hb}$ for protocols B and P from different blood sites are shown in Table 2.4.

${}^E\hat{M}_{Hb}$ from protocol B overestimates ${}^A M_{Hb}$ by greater than 2%. The largest error is seen at the blood sites "cm" and "vm". The major source of overestimation of ${}^A M_{Hb}$ is due to the inaccuracy in estimating V_{COMb} . ${}^E\hat{M}_{Hb}$ uses Prommer and Schmidt's formula

(Prommer and Schmidt, 2007) to calculate V_{COMb} . Estimation of V_{COMb} using Prommer and Schmidt's formula is also dependent on the site of sampling (Table 2.2, 2.4). Their formula is based on the assumption that there is constant flux of CO from blood to muscle tissue. As seen in Figure 2.6, the flux of CO from blood to muscle tissue varies with time. This assumption of constant CO flux results in the underestimation of the actual volume of CO bound to myoglobin (Figure 2.7) in protocol B. This underestimation of V_{COMb} leads to overestimation of V_{COHb} , thereby resulting in an overestimation of $^A M_{Hb}$. This underestimation of V_{COMb} is more prominently seen at blood site "vm". Accurate estimation of V_{COMb} results in $^M \hat{M}_{Hb}$ close to $^A M_{Hb}$, whereas underestimation of V_{COMb} results in $^E \hat{M}_{Hb}$ greater than $^A M_{Hb}$ (Figure 2.8).

$^E \hat{M}_{Hb}$ from protocol P results in estimates close to $^A M_{Hb}$ from blood sites "ar", "cot" and "cm". However, $^E \hat{M}_{Hb}$ from blood site "vm" is overestimated by 4.9%. The estimation of V_{COMb} is greatly dependent on the site of blood sampling as the estimated V_{COMb} depends (Equation 2.7) on the ratio of %HbCO at T_{sample} and %HbCO at T_{mix} . Since this ratio is often less than one, V_{COMb} is often overestimated (Figures 2.7, 2.9). In protocol P, V_{COMb} is overestimated from blood sites "ar", "cot" and "cm" and underestimated from site "vm" (Figure 2.9). In addition to inaccurate estimation of V_{COMb} , this protocol also underestimates the volume of CO exhaled up to T_{sample} (Figure 2.10). At the blood sites "ar", "cot" and "cm", overestimation of V_{COMb} is compensated with the underestimation of V_{CO} exhaled, thereby resulting in $^E \hat{M}_{Hb}$ close to $^A M_{Hb}$ from these blood sites. However at the blood site "vm", underestimation of both V_{COMb} and V_{CO} exhaled results in overestimation of $^A M_{Hb}$. Thus the values of $^E \hat{M}_{Hb}$ in protocol P are close to $^A M_{Hb}$ based on compensatory errors from the blood sites "ar", "cot" and "cm" (Table 2.4).

Errors $> 2\%$ in estimation of $^E \hat{M}_{Hb}$ suggest that these errors are due to inaccuracies in the methods of calculating $V_{CO L+S}$, $V_{CO ex}$, or V_{COMb} . The sources of errors in calculation of $^E \hat{M}_{Hb}$ could be due to the errors in calculations of $V_{CO L+S}$, V_{CO}

ex, or V_{COMb} . In protocol P the sources of errors could either be due to the assumptions made in $V_{CO\ ex}$ (Equation 2.6), V_{COMb} (Equation 2.7) or both, as $V_{CO\ L+S}$ in this protocol is measured and not estimated. In protocol B the sources of errors could either be due to the assumptions made in $V_{CO\ L+S}$ (Equation 2.5), V_{COMb} (Equation 2.7) or both, as $V_{CO\ ex}$ in this protocol is 0. To determine the errors in \hat{M}_{Hb} due to the errors in estimation of $V_{CO\ ex}$ and $V_{CO\ L+S}$, ${}^E\hat{M}_{Hb}$ was calculated from the blood site “vm” for the protocols P and B using the model calculated V_{COMb} (Equation 2.2) instead of using Equation 2.7 to estimate V_{COMb} . Calculating ${}^E\hat{M}_{Hb}$ from blood site “vm” using Equation 2.6 to estimate $V_{CO\ ex}$ and using the model calculated V_{COMb} (Equation 2.2), results in a maximum error of 0.8% in ${}^E\hat{M}_{Hb}$ for protocol P. Calculating ${}^E\hat{M}_{Hb}$ from blood site “vm” using Equation 2.5 to estimate $V_{CO\ L+S}$ and using the model calculated V_{COMb} (Equation 2.2), results in a maximum error of 1.2% in ${}^E\hat{M}_{Hb}$ for protocol B. These errors are smaller compared to the errors obtained in ${}^E\hat{M}_{Hb}$ using Equation 2.7 to estimate V_{COMb} (Table 2.4). Thus, detailed analysis of all the simulations suggests that the major source of error leading to inexact calculation of ${}^E\hat{M}_{Hb}$ in both the protocols is due to the inaccuracy in estimating volume of CO bound to myoglobin rather than the errors in estimation of $V_{CO\ ex}$ and $V_{CO\ L+S}$. Also, using the blood sites “ar”, “cot” or “cm” to calculate ${}^E\hat{M}_{Hb}$ results in lower errors and using blood site “vm” as a sampling site in the CO rebreathing studies may lead to larger errors in calculation of ${}^E\hat{M}_{Hb}$.

Improving CO rebreathing protocols

Protocol B offers the advantage of calculating M_{Hb} close to the actual values, if the V_{COMb} were estimated accurately. However the long duration of rebreathing and a longer T_{mix} are a disadvantage of this protocol. Protocol P has a shorter T_{mix} and rebreathing duration but the estimates of V_{COMb} and $V_{CO\ ex}$ are inaccurate. The errors in estimates of M_{Hb} from protocols B and P are also dependent on the site of blood sampling. Thus, there is a need to determine a CO rebreathing method with a shorter T_{mix} which estimates M_{Hb} without compensating errors and has lower errors irrespective of the sampling blood site. In the quest to develop such a method, the validated model was used

to estimate M_{Hb} from four different blood sites (ar, cot, cm, vm) for varying durations (2, 3.5, 5, 7.5, 10 min) of CO rebreathing in 100% O_2 (Figure 2.11). In addition, the effects of administering 100% O_2 before or after CO rebreathing versus room air breathing on estimation of M_{Hb} was also tested. Based on these simulation results, a new protocol was defined.

New Protocol: In this protocol (Figure 2.12A), 1 ml/Kg of CO in 3 L of oxygen is rebreathed for 3.5 min followed by 17 min of room air breathing. Prior to rebreathing, the subject is on 100% O_2 . This new protocol (protocol N) was simulated for the Benignus's (15 healthy male) and Garvican's (9-2 female and 7 male, healthy, recreationally-active subjects) subjects and $^E \hat{M}_{Hb}$ was determined. In 3 of the 9 Garvican's subjects, the model predicted fast uptake of CO in the blood compartment "vm" during the initial 5 minutes of two mostly used CO rebreathing methods when compared to the experimental data. The muscle blood volume of third vascular subcompartment of skeletal muscle and muscle blood flow were adjusted in these subjects to match the experimental data (Figure 2.16). To simulate protocol N in these 3 subjects, the adjusted values for muscle blood volume in the third vascular subcompartment and muscle blood flow were used. T_{mix} was determined from the methods described previously (Figure 2.1). The T_{mix} for this protocol is ~5 min in Benignus's subjects and ~6.5 min in Garvican's subjects. The uptake kinetics of CO in all the blood compartments for this protocol are shown in Figure 2.12B. T_{sample} was considered as 1.5 min away from T_{mix} . In actual practice, the volume of CO exhaled should be collected over the duration of experiment and the volume of CO in the lungs and rebreathing system should be measured at the end of CO rebreathing.

The volume of CO bound to myoglobin is estimated from a regression relationship based on the model calculated V_{COMb} (Figure 2.13a, Equation 2.8a). In order to develop this regression relation, the model calculated V_{COMb} (in ml, BTPS), T_{sample} (in minutes) and V_{CO_t} (in ml, BTPS) from Benignus's and Garvican's subjects were used. V_{COMb} is estimated as a function of T_{sample} and V_{CO_t} (Equation 2.8). V_{COMb} is the dependent variable and T_{sample} , V_{CO_t} are the independent variables. To develop a

regression equation to estimate V_{COMb} for protocol N, the muscle blood flow (decreased by 20% of average value) and blood volume of the third skeletal vascular compartment (increased by 20% of mixed venous blood volume) was changed in 3 of the 9 Garvican's subjects. The regression equations to estimate V_{COMb} were developed for this protocol using a D_{MCO} of 0.225 ml/min/Torr/Kg of muscle mass for Benignus's subjects and 0.302 ml/min/Torr/Kg of muscle mass for Garvican's subjects. In one typical subject (S112, Benignus et al., 1994), when the D_{MCO} was increased by 50%, the regression equation (Equation 2.8a) underestimated V_{COMb} by 0.62 ml (relative to the correct value of 2.53 ml) and a decrease in D_{MCO} by 50% resulted in an overestimation of V_{COMb} from the regression equation by 0.65 ml. S112 was chosen for analysis of variations in D_{MCO} on the regression equations proposed, as the value for V_{COMb} calculated from the regression equation (Equation 2.8) for this subject was close to the value for V_{COMb} from the model. The effects of changes in ventilation (+50%) on estimation of V_{COMb} from the regression equations were negligible. The errors in ${}^E\hat{M}_{Hb}$ are less than 1% from this protocol (Table 2.5, Figure 2.2.13) from any blood sampling site. Thus, protocol N results in lower errors in estimation of ${}^E\hat{M}_{Hb}$ compared to protocols B and P without involving any compensatory errors (Figure 2.14).

$$V_{COMb} = \left\{ \begin{array}{l} 0.223 \cdot T_{sample} + 0.024 \cdot V_{COI} - 1.129 ; \text{ For Protocol N} \dots\dots 2.8a \\ 0.400 \cdot T_{sample} + 0.057 \cdot V_{COI} - 4.685 ; \text{ For Protocol B} \dots\dots 2.8b \\ 0.091 \cdot T_{sample} + 0.013 \cdot V_{COI} \quad ; \text{ For Protocol P} \dots\dots 2.8c \end{array} \right\} \dots\dots 2.8$$

The major source of error in calculation of ${}^E\hat{M}_{Hb}$, from protocols B and P are due to errors in the estimation of V_{COMb} . Independent of the site of sampling, low errors in estimates of M_{Hb} from protocols B and P can be obtained by using the suggested regression equations (Equation 2.8b-c).

Protocol B: A regression equation to estimate V_{COMb} is developed for this protocol based on the model estimates of V_{COMb} from 24 (Benignus's and Garvican's subjects) healthy humans (Figure 2.13A, Equation 2.8b). To develop this regression relation, the model calculated V_{COMb} (in ml, BTPS), T_{sample} (in minutes) and V_{COI} (in ml, BTPS) from these

subjects (Benignus et al., 1994; Garvican et al., 2010) were used. V_{COMb} is the dependent variable and T_{sample} , V_{CO_i} are the independent variables. For Benignus's subjects, T_{sample} was 1.5 min away from the model determined T_{mix} (See methods, Figure 2.1) and for Garvican's subjects T_{sample} provided by the investigators were used. The D_{MCO} values used for the two data sets simulated (Benignus et al., 1994; Garvican et al., 2010) were same as those used in protocol N. In one typical subject (S112, Benignus et al., 1994), the effects of changing D_{MCO} on estimation of V_{COMb} from the regression equation were analyzed. When the D_{MCO} was increased by 50%, the regression equation (Equation 2.8b) underestimated V_{COMb} by 0.93 ml from its actual value and a decrease in D_{MCO} by 50% resulted in an overestimation of V_{COMb} from the regression equation by 1.2 ml from its actual value. The errors in calculation of $^E\hat{M}_{Hb}$ are less than 1.1% (independent of blood site sampled) when the regression equation is used (Equation 2.8b, Table 2.5). For this protocol, it would also be recommended that the volume of CO in the rebreathing system be measured at the T_{sample} instead of estimating it from Equation 2.5.

Protocol P: A regression equation to estimate V_{COMb} is proposed to improve the estimation of M_{Hb} from this CO rebreathing method, based on the model estimates of V_{COMb} from 24 healthy subjects (Figure 2.13C, Equation 8c). To develop this regression relation, the model calculated V_{COMb} (in ml, BTPS), T_{sample} (in minutes) and V_{CO_i} (in ml, BTPS) from the subjects of Benignus et al. (1994) and Garvican et al. (2010) were used. V_{COMb} is the dependent variable and T_{sample} , V_{CO_i} are the independent variables. For Benignus's subjects, T_{sample} was 1.5 min away from the model determined T_{mix} and for Garvican's subjects T_{sample} provided by the investigators were used. In one typical subject (S112, Benignus et al., 1994), when the D_{MCO} was increased by 50%, the regression equation (Equation 2.8c) underestimated V_{COMb} by 0.54 ml from its actual value and a decrease in D_{MCO} by 50% resulted in an overestimation of V_{COMb} from the regression equation by 0.61 ml from its actual value. In this protocol, the effects of changes in ventilation on estimation of V_{COMb} from the regression equation were negligible and it would be suggested that the volume of CO exhaled be measured up to T_{sample} . Errors less

than 1% (Table 2.5) without involving any compensatory errors are obtained when the regression equation (Equation 2.8c) is used to calculate ${}^E\hat{M}_{Hb}$.

Predicted values for T_{mix} , T_{sample} , and sampling blood sites to estimate M_{Hb} with low errors: In this study additional analysis of the simulations of the three CO rebreathing protocols (B, P, and N) was done to determine the effects of T_{mix} , T_{sample} , and the sampling blood site on estimation of M_{Hb} .

Effects of mixing time (T_{mix}): In order to determine the effects of T_{mix} on estimation of M_{Hb} , ${}^M\hat{M}_{Hb}$ was calculated for protocols B, P and N from arterial (ar), capillary other tissue (cot), capillary muscle (cm) and muscle venous (vm) blood compartments by assuming different values for T_{mix} . ${}^M\hat{M}_{Hb}$, the M_{Hb} estimated using the exact values from the model (Equations 2.1-2.4, Table 2.2) for $V_{CO\ L+S}$, $V_{CO\ ex}$, and V_{COMb} was calculated for the Benignus's subjects. In calculations of ${}^M\hat{M}_{Hb}$, T_{mix} was assumed as 1, 3, 5, 7, 9, 11, 13, 15 and 38 minutes. The difference between T_{sample} and T_{mix} was always 1.5 min. For each protocol, the errors in calculation of ${}^M\hat{M}_{Hb}$ from different blood sites and T_{mix} was plotted for all the subjects (Figure 2.17-2.18). The error at each T_{sample} was calculated on comparing ${}^M\hat{M}_{Hb}$ with ${}^A M_{Hb}$. In protocol B, low errors in estimation of M_{Hb} were obtained from blood sites "ar" and "ot" at a minimum value of T_{mix} of 7.5 min ($T_{sample} = 9$ min). The minimum value of T_{mix} to obtain low errors in ${}^M\hat{M}_{Hb}$ from blood sites "cm" and "vm" was 38 min ($T_{sample} = 39.5$ min). Thus, in this protocol estimation of M_{Hb} from a blood sample taken from an artery or an ear lobe at 9 min, would result in a lower error than taking a blood sample from a vein or finger tip at 40 mins. Similar error analysis for protocols P (Figure 2.18) and N (Figure not shown for protocol N) were done. Error analysis for protocols P and N revealed that low errors in estimation of M_{Hb} were obtained irrespective of the blood site sampled at a minimum value of T_{mix} of 5.0 min ($T_{sample} = 6.5$ min) and 6.5 min ($T_{sample} = 8$ min), respectively. These results suggest that irrespective of the protocol, site of blood sampling and intersubject variability, a minimum value of T_{mix} after which the effects of T_{mix} on

estimation of M_{Hb} are minimal is 7.5 min. Results of the simulations to look at the effects of changing various factors like myoglobin concentration, V_{CO_2} , D_{MCO} , duration of rebreathing, muscle blood flow and muscle blood volume on T_{mix} are reported in the discussion sections of this chapter in the section “*Mixing time of CO in the vascular space*”

Effects of sampling time (T_{sample}): To determine the effects of T_{sample} on estimation of M_{Hb} , $^M\hat{M}_{Hb}$ was calculated for protocols B, P and N from four blood compartments (ar, cot, cm, vm) for Benignus’s subjects by varying the T_{sample} . $^M\hat{M}_{Hb}$ was calculated at T_{sample} ’s which were 1.5, 3, 5, 7, 9 and 11 minutes from the determined T_{mix} of each subject (Figure 2.15, shown for protocol N). T_{mix} for each subject for a given CO rebreathing protocol was determined from the model using the methods described previously (Figure 2.1). Error analysis for protocols P (Figure not shown) and N (Figure 2.15) suggested that low errors in estimation of M_{Hb} were obtained irrespective of the blood site sampled, when the difference between T_{mix} and T_{sample} was between 1.5-3 min. For protocol B (Figure not shown), low errors in estimation of M_{Hb} were obtained from blood sites “ar” and “cot” when the difference between T_{mix} and T_{sample} was between 1.5-3 min. In protocol B to obtain low errors in estimation of M_{Hb} from blood sites “cm” and “vm”, the difference between T_{mix} and T_{sample} was between 8-10 min. Summarizing results on error analysis of M_{Hb} with changes in T_{mix} , and T_{sample} from different blood sites in these 15 healthy subjects (Benignus et al., 1994) and using the information from the plateaus observed in %HbCO’s of blood compartments of the experimental data from 9 healthy, recreationally-active subjects (Garvican et al., 2010); a minimal value of T_{sample} to obtain low errors in \hat{M}_{Hb} can be suggested. It is suggested that low errors in \hat{M}_{Hb} can be obtained for any protocol at a T_{sample} of 9 min using a blood sample from ear lobe, finger tip, or an artery in the forearm.

Effects of blood sampling site: In this study $^M\hat{M}_{Hb}$ was calculated from four blood compartments for all three CO rebreathing protocols (B, P and N) at different T_{mix} and

T_{sample} values. Low errors in \hat{M}_{Hb} were obtained when the blood was sampled from arterial (assumed to represent blood sample from an artery in a fore arm), capillary other tissue (assumed to represent blood sample from an ear lobe) and muscle capillary (assumed to represent blood sample from a finger tip) sites (Table 2.5, Figure 2.13, Figure 2.17-2.18).

In general analysis of protocols B, P and N suggest that, using a sample taken from blood sites “ar”, “cot” or “cm” at 9 min and estimating V_{COMb} from the proposed regression equations (Equation 2.8) will ensure estimation of M_{Hb} with low errors.

DISCUSSION

The main aim of this study was to use a validated mathematical model to determine any potential sources of errors in estimation of M_{Hb} (\hat{M}_{Hb}) from the existing *CO* rebreathing methods. After validating the model, my goal was to evaluate any potential errors in these methods and to suggest modifications that mitigate those errors. The validated mathematical model was used to simulate the two commonly used *CO* rebreathing methods in healthy human subjects. For these methods, \hat{M}_{Hb} was determined using the exact values from the model for $V_{\text{CO L+S}}$, $V_{\text{CO ex}}$, and V_{COMb} ($^M\hat{M}_{Hb}$) and using the approximated values based on the published formulas for calculating $V_{\text{CO L+S}}$, $V_{\text{CO ex}}$, and V_{COMb} ($^E\hat{M}_{Hb}$). The errors in estimation of M_{Hb} were calculated by comparing the values of $^M\hat{M}_{Hb}$ and $^E\hat{M}_{Hb}$ to the known hemoglobin mass of the subjects, $^A M_{Hb}$. On comparison, it was found that the values of $^M\hat{M}_{Hb}$ were in agreement with $^A M_{Hb}$ independent of the sampling blood site while the values from $^E\hat{M}_{Hb}$ were dependent on the sampling blood site and $^E\hat{M}_{Hb}$ either inaccurately estimated (overestimation or underestimation) $^A M_{Hb}$ or was close to $^A M_{Hb}$ based on compensating errors. Inaccuracies in estimation of volume of *CO* bound to myoglobin was found to be the major source of error in calculation of $^E\hat{M}_{Hb}$ from the existing *CO* rebreathing methods. In this study, I also propose a new *CO* rebreathing method which I predict will estimate M_{Hb} with small

errors. Also, for experimentalists who wish to use the existing *CO* rebreathing methods, I suggest modifications to these methods for calculating $^E\hat{M}_{Hb}$ with low errors.

Model Limitations

Model validation of %HbCO levels: The model was validated by comparing the model predicted and experimentally measured values of %HbCO (%HbCO_{ar}, %HbCO_{cm}, %HbCO_{vm}) from three blood sites (arterial, capillary, venous). The experiments of Garvican et al. (2010) were simulated, and the predicted mean %HbCO \pm SD values from all the three blood compartments at different time points were within the 95% confidence limits of the experimental data (Figures 2.3-2.4). However, individual comparison of %HbCO vs. time revealed that in 3 of the 9 subjects the model predicted faster uptake of *CO* in the muscle venous compartment, and higher %HbCO_{vm}, during the initial few minutes of both the *CO* rebreathing protocols (Figure 2.16). After ~5 minutes, the predicted %HbCO_{vm} was in agreement with the experimental values. Model prediction of fast uptake of *CO* in the muscle venous compartment would result in a smaller predicted T_{mix} in these subjects when compared to the experimentally determined T_{mix} . This behavior of the model would suggest an erroneously small T_{mix} for ~33% of the population when compared to the data obtained from experiments. I was able to match the predicted %HbCO_{vm} with experimental values by decreasing the muscle blood flow by 20% and increasing blood volume in the third vascular compartment of the muscle (V_{bm3}) by 20% of the mixed venous blood volume (Figure 2.16). In these 3 subjects, changing the values for muscle blood flow and V_{bm3} did not affect the values of %HbCO_{vm} after 5 minutes or the uptake of *CO* in other blood compartments.

In my model, I used average values reported in the literature (Bruce and Bruce, 2008; Erupaka et al., 2010) for blood flow and V_{bm3} (as the values for these parameters were not provided by the investigators). The blood flow rates are heterogeneous at different compartments of vasculature and, for some subjects, may be lower than the average values used for the integrated muscle compartment in the model. In addition to this, the coefficient of variation in muscle blood flow or any physiological parameter might be 20%. On this basis, decreasing the muscle blood flow to match the experimental

data of 3 subjects may be justifiable. Also, V_{bm3} is assumed to be larger by up to 20% of the mixed venous blood volume in some subjects than the average values used in the model. Thus, when the volume of this compartment was increased, the model matched the slower uptake of CO by muscle observed in the experimental data. The regression equations to estimate V_{COMb} for protocols B, P, and N were developed using the simulations from Garvican's subjects, including the 3 for whom the values of blood flow and V_{bm3} were changed. Thus this limitation of the model to predict uptake of CO in the muscle venous compartment for some subjects should not affect the regression equations proposed.

Model parameters: Values for parameters in the model were either provided by the investigators, or estimated from regression equations developed from healthy populations (Bruce and Bruce, 2008; Erupaka et al., 2010). For some parameters which were not provided to us by the investigators or estimating the value from a regression equation was not possible (like estimating alveolar ventilation), average values from the literature for healthy populations were used. In my simulations using the same average value for all the subjects for some parameters like alveolar ventilation, the muscle diffusion capacity of CO (D_{MCO}) and lung volume, may affect the model calculated values of V_{COMb} , $V_{CO S+L}$ and $V_{CO ex}$. Thus whenever possible, in all my simulations intersubject variability was taken into account while estimating the values for unknown parameters which were not provided to us by the investigators (Garvican et al., 2010; Benignus et al., 1994). Like in cases where the subject specific values for alveolar ventilation were not measured (Garvican et al., 2010), the ventilation in each subject was adjusted so that an arterial PO_2 of 98 Torr was obtained on breathing room air at the control or steady state. For Garvican's subjects, \hat{M}_{Hb} calculated using equations 2.1a-2.4 were in agreement with $^A M_{Hb}$ for both the CO rebreathing methods. However, for Schmidt and Prommer method $^E \hat{M}_{Hb}$ underestimated $^A M_{Hb}$ by ~6%. In addition to inaccurate estimation of V_{COMb} , assumptions made in estimation of alveolar ventilation may have contributed to larger errors in $^E \hat{M}_{Hb}$ from Schmidt and Prommer method when compared to Burge and Skinner method. The values for D_{MCO} may differ among the subjects, thus the D_{MCO}

was varied as a function of muscle mass to take into account differences in muscle mass of subjects (Garvican et al., 2010, Benignus et al., 1994). An average value of lung volume was used for simulating the three CO rebreathing protocols (B, P and N) in all the subjects (Bruce and Bruce, 2003; Erupaka et al., 2010). To determine the effects of changes in lung volume on estimation of M_{Hb} , protocol N was simulated in Benignus's subjects with changing the lung volume as a function of age, body weight and height of the subject (Petersen et al., 1975). For each subject ${}^M\hat{M}_{Hb}$ was calculated (Equations 2.1-2.4) using the estimated value of lung volume as a function of age, body weight and height. No significant differences were found in the values of ${}^M\hat{M}_{Hb}$ (results not shown) compared to the ${}^M\hat{M}_{Hb}$ calculated using the same average value of lung volume in different subjects. For protocols B and P, the effects of changing the lung volume (as a function of age, body weight and height) on calculation of ${}^M\hat{M}_{Hb}$ were not analyzed in this study. The small or no influence of lung volume on estimation of M_{Hb} has also been confirmed by the experiments and calculations of Steiner and Wehrin (2010).

Effects of various factors on estimation of hemoglobin mass, \hat{M}_{Hb}

Volume of CO bound to myoglobin: Analysis of simulations of all three protocols in Benignus's subjects reveals that $\sim 6\%$, 2% , and 3% of V_{CO_i} is bound to myoglobin in protocols B, P, and N respectively. On average if V_{COMb} is ignored in the estimation of V_{COHb} , then protocols B, P, and N overestimate M_{Hb} by $\sim 7\%$ ($T_{sample} = 12$ min), 2.2% ($T_{sample} = 6$ min), and $\sim 3.3\%$ ($T_{sample} = 7$ min), respectively. If a larger T_{sample} (say $T_{sample} = 12$ min) is used in protocols P and N then the error in \hat{M}_{Hb} due to ignoring V_{COMb} may be slightly greater by $\sim 1\%$, but would not be as large as the error in protocol B. In protocols P and N, CO is exhaled after rebreathing ends causing a decrease in the amount of CO entering the tissues and resulting in lower values for V_{COMb} at any T_{sample} when compared to protocol B. Thus at any given T_{sample} when compared to protocol P, V_{COMb} is larger in protocol B. Also, when compared to protocol P the underestimation of V_{COMb} is larger in protocol B, thus resulting in a higher estimate of M_{Hb} from protocol B for any subject. Thus in the existing CO rebreathing methods when compared to protocol P, \hat{M}_{Hb}

is always greater from protocol B either due to ignoring V_{COMb} (Gore et al.,2006; Schmidt and Prommer,2005; Steiner and Wehrin,2010) or due to underestimating the volume of CO bound to Mb using the Prommer and Schmidt's formula (Equation 2.7) (Garvican et al., 2010; Schmidt and Prommer,2007), which either ways results in an overestimation of M_{Hb} . However in protocol B, if the volume of CO bound to myoglobin is accounted accurately, then the estimates of M_{Hb} are close to the values of $^A M_{Hb}$ (Figure 2.8, Table 2.5).

Prommer and Schmidt (2007) make an assumption that there is continuous flow of CO from Hb to Mb at a constant rate. Certainly there is continuous flow of CO from Hb to Mb (Bruce and Bruce, 2003), but the rate of flow of CO is not constant (Figure 2.6). This assumption results in inaccuracies in calculation of V_{COMb} which may combine with other errors to either result in overestimation of M_{Hb} (Table 2.4), underestimation of M_{Hb} (See results) or correct estimation of M_{Hb} based on compensatory errors (Table 2.4). Also the formula (Equation 2.7) proposed by Prommer and Schmidt (2007) is greatly influenced by the choice of (i) site of sampling due to the use of %HbCO levels and (ii) values for T_{mix} , and T_{sample} due to the two assumptions made while developing their formula.

In protocol B, the %HbCO_{cm} or %HbCO_{vm} levels rise slowly, resulting in a larger T_{mix} (Figure 2.2a). In this protocol assuming that negligible amount of CO is bound to Mb at T_{mix} results in underestimation of V_{COMb} . Thus, using Prommer and Schmidt's formula (Equation 2.7) to estimate V_{COMb} overestimates M_{Hb} in protocol B. In protocol P using Prommer and Schmidt's formula to estimate V_{COMb} from venous blood results in an overestimation of M_{Hb} , which is due to the underestimation of V_{COMb} from their assumption of constant CO flux. Estimation of M_{Hb} from other blood compartments is based on compensatory errors. Also, the errors in estimation of V_{COMb} from different blood compartments are evident due to the effects of incomplete circulatory mixing (Figure 2.5). For protocol P, my modeling results agree with findings of Prommer and Schmidt (2007) that ~2% of V_{CO_t} is bound to Mb. In this article (Prommer and Schmidt,

2007), it should be noted that the ear lobe was the sampled blood site and the precise volume of CO exhaled was measured.

In this study, I proposed regression equations to estimate V_{COMb} from T_{sample} and V_{CO_t} for different protocols using V_{COMb} values calculated by the model for Benignus's (healthy) and Garvican's (healthy, recreationally-active) subjects. In the case of Garvican's subjects, volume of CO bound to Mb will be greater compared to Benignus's subjects because T_{sample} and V_{CO_t} are larger in recreationally-active subjects. Though this result cannot be proven experimentally, it is suggested by the fact that the recreationally-active populations will have more muscle mass, resulting in larger amount of myoglobin being available to bind to CO . The regression equations to estimate V_{COMb} were developed for each protocol using a D_{MCO} of 0.225 ml/min/Torr/Kg of muscle mass for Benignus's subjects and 0.302 ml/min/Torr/Kg of muscle mass for Garvican's subjects. For all the protocols, I analyzed the effects of changing D_{MCO} ($\pm 50\%$) on estimation of V_{COMb} from the regression equation (see Results). For protocols P and N, the effects of changes in ventilation on estimation of V_{COMb} from the regression equations were negligible.

Mixing time of CO in the vascular space (T_{mix}): The mixing times of protocol B and protocol P are in agreement with articles published in the literature (Burge and Skinner, 1995; Gore et al., 2006; Schmidt and Prommer, 2005). These articles used approximated methods to determine T_{mix} , where as my model allowed a more complete analysis of mixing, as it was based on pairwise differences from five blood sites (Figure 2.1). In order to determine the effects of T_{mix} on estimation of M_{Hb} , $^M\hat{M}_{Hb}$ was calculated for protocols B, P and N from various blood compartments for Benignus's subjects by varying the T_{mix} . Analysis of these results suggested that irrespective of the protocol, site of blood sampling and intersubject variability, a minimum value of T_{mix} after which the effects of T_{mix} on estimation of M_{Hb} are minimal is 7.5 min.

The simulations discussed in this paragraph were not presented in the results section. In this study I also looked at the effects of changing various factors like myoglobin (Mb) concentration, V_{CO_i} , D_{MCO} , duration of rebreathing, muscle blood flow and muscle blood volume on T_{mix} in one of the Benignus's subjects (S112, Benignus et al, 1994). An increase in concentration of Mb resulted in a larger T_{mix} for any CO rebreathing protocol. Thus, untrained (sedentary) subjects and populations with lower muscle mass will have a smaller T_{mix} when compared to trained (athletes, recreationally-active) subjects and populations with larger muscle mass. Administering smaller doses of CO resulted in lower values for %HbCO and smaller T_{mix} in any CO rebreathing protocol because of the 0.1% HbCO threshold criterion to determine T_{mix} . One of the major reasons for obtaining a larger T_{mix} in CO rebreathing methods is due to the slow diffusion of CO from the vascular space to the tissue spaces containing myoglobin. The rate of diffusion of CO from the vascular space to the myoglobin containing tissues is dependent on the D_{MCO} and the pressure gradients of CO between the blood and tissue compartments. It is however suggested that the minimum dose of CO to be administered is 1 ml/Kg for men and 0.8 ml/Kg for women, to allow measurements of %HbCO. When compared to trained subjects the amount of CO injected into the rebreathing bag is smaller in untrained subjects, thus resulting in untrained subjects having a smaller T_{mix} when compared to the trained subjects. Also, women will have a lower T_{mix} when compared to men as the dose of CO administered in the CO rebreathing studies is smaller in women than men. For any CO rebreathing protocol, a lower value for D_{MCO} results in a smaller T_{mix} . When a smaller value of D_{MCO} is used, the amount of CO flowing into the tissues from the vascular space is smaller and thus mixing of CO takes place faster in the vascular space. As the CO flux from the vascular space to the muscle tissues is dependent on D_{MCO} , using a lower D_{MCO} value results in a smaller T_{mix} than using a higher D_{MCO} value. A CO dilution technique with longer duration of CO rebreathing has larger T_{mix} when compared to a CO rebreathing method involving smaller durations of CO rebreathing. Depending on D_{MCO} value, the volume of CO diffusing from the blood compartments to the muscle tissue compartment is directly proportional to the duration of CO rebreathing method. Longer the duration of rebreathing, larger is the volume of CO flowing into the muscle tissues from the vascular space and slower is the mixing of CO in

the vascular space- thus resulting in a larger T_{mix} . Thus for any given subject, protocol B has the largest T_{mix} followed by protocol N and protocol P. Populations with lower muscle blood flow tend to have a larger T_{mix} when compared to populations with normal or lower blood flows. An increase in muscle blood volume also results in an increase in T_{mix} . Thus a variation in one or more than one of these various factors may explain the range of values reported for T_{mix} in the literature. These results also suggest that trained populations may have a larger T_{mix} than untrained populations.

Blood sampling site: $^M\hat{M}_{Hb}$ and $^E\hat{M}_{Hb}$ were calculated in Benignus's subjects for the three CO rebreathing protocols B, P and N (Tables 2-4) from the arterial (ar-artery in fore arm), capillary other tissue (cot-ear lobe), capillary muscle (cm-finger tip) and muscle venous (vm- vein in forearm) blood compartments. Errors in $^M\hat{M}_{Hb}$ from blood compartments "ar" and "cot" of protocol B and all other compartments of protocol P were less than 1%. Errors in $^M\hat{M}_{Hb}$ from blood sites "cot" and "vm" in protocol B were <2%. The reason for slightly larger errors in $^M\hat{M}_{Hb}$ from compartments "cot" and "vm" in protocol B is due to the sensitivity of M_{Hb} to changes in $\% \Delta HbCO$ (Equation 2.1) and due to incomplete mixing of CO in blood (Figure 2.2a). A variation of $\Delta HbCO$ by $\pm 0.1\%$ will result in a variation of M_{Hb} by ∓ 12 g. Despite a difference of $\sim 0.1\%$ between the $\% HbCO$'s, considering a sample from blood site "cot" or "vm" one can expect that the $^A M_{Hb}$ will be overestimated or underestimated by ~ 12 g (Figure 2.2a). In protocol P, $^E\hat{M}_{Hb}$ was lower from blood sites ar, cot and cm when compared to $^E\hat{M}_{Hb}$ from blood site vm. These results are due to incomplete mixing of CO in blood and are in agreement with other studies (Garvican et al., 2010; Gore et al., 2006). Suggested sampling sites to obtain low errors in estimation of M_{Hb} for protocol B are arterial or ear lobe blood sites. For protocols P and N, arterial, ear lobe or finger tips are the suggested blood sites to obtain low errors in M_{Hb} . Based on the analysis of simulation results from all the blood compartments and experimental data (Garvican et al., 2010), despite low errors in $^M\hat{M}_{Hb}$ or $^E\hat{M}_{Hb}$ (Table 2.3, 2.5) from protocol B, P and N, blood site "vm" is not suggested as it is not a reliable sampling site.

Irrespective of the protocol, low errors in estimation of M_{Hb} were obtained from arterial, capillary other tissue and muscle capillary sites (Table 2.5). My results for suggested reliable sampling sites for protocols B and P are in agreement with the preferred sampling blood sites of Garvican et al. (2010). For a given CO rebreathing method, Garvican et al. (2010) chose their blood site in each subject based on the least coefficient of variation in M_{Hb} at different time points. Suggestions for reliable sampling blood sites from my study are more credible than theirs as reliable sampling blood sites were determined based on obtaining lowest errors in estimates of M_{Hb} , when compared to $^A M_{Hb}$ from three different CO rebreathing methods and four different blood sites in 24 (15 Benignus's and 9 Garvican's subjects) healthy humans. Thus, suggestions for reliable blood sampling sites to obtain low errors in estimation of M_{Hb} based on experimental data and analysis of simulations are ear lobe or pre warmed finger tips. If obtaining samples from ear lobe or finger tips is not possible, then arterial blood should be sampled. Considering the difficulties in obtaining samples from arterial blood sites, despite low errors arterial blood site is reserved as the next best site for sampling. Though all the protocols estimate M_{Hb} with errors less than 2% using %HbCO values from venous blood (Table 2.3, Table 2.5), it is suggested that venous blood sites should be avoided because this compartment takes more time to reach equilibration with other compartments. Usage of one of the suggested blood sampling sites will improve the reliability and accuracy of the CO rebreathing methods to estimate M_{Hb} and allow standardization of the method.

Sampling time: To determine the effects of T_{sample} on estimation of M_{Hb} , $^M \hat{M}_{Hb}$ was calculated for protocols B, P and N from various blood compartments for Benignus's subjects by varying the T_{sample} relative to T_{mix} . Summarizing the simulation results from Benignus's subjects and using the information of plateaus attained in %HbCO levels from the experimental data of Garvican's subjects, it is suggested that low errors in \hat{M}_{Hb} can be obtained for any protocol at a T_{sample} of 9 min using a blood sample from ear lobe, finger tip, or an artery in the forearm. Using finger tips for blood sampling may have slightly larger errors (Table 2.3, Table 2.5) compared to using ear lobe or arterial blood sites in protocol B. Sampling at the suggested T_{sample} will allow determination of \hat{M}_{Hb}

with low errors and also avoid taking multiple samples which will decrease the cost of the experiment, inconvenience to the subject and duration of the experiment.

Effects of plasma skimming: Due to a process known as plasma skimming the red blood cells (RBC) are not evenly distributed within the vascular tree and the hematocrit in the microvascular beds is considerably lower than that of the larger vessels (Burge and Skinner, 1995). Plasma skimming is a phenomenon in which, due to low flow rates in the microvascular beds like capillaries, the RBC's stick together, thus increasing the viscosity, and remaining at the centre of the vessel. Thus, the blood closest to the vessel wall has lower hematocrit and the fraction of blood volume that is occupied by the RBC's is lower in the microvascular beds when compared to larger blood vessels. As an effect of plasma skimming, it would be expected that \hat{M}_{Hb} calculated using %HbCO measurements from a capillary blood site may be an overestimate of the actual hemoglobin mass. However, this process of plasma skimming should not effect the estimation of M_{Hb} from a specific blood site, if the blood is sampled for %HbCO after mixing of CO is complete and the %HbCO's from all the blood compartments are similar or equal. As it is difficult to determine the true T_{mix} , using the suggested sampling time of 9 min should allow accurate estimation of M_{Hb} . Though the process of plasma skimming is not implemented in the model, it should be noted that the model was able to predict the %HbCO's from different blood compartments, which were in agreement with the experimental data. Also the techniques using tagged RBC's (CO, ^{51}Cr) have been reported to accurately estimate the RBC volume, but underestimate the plasma and blood volume (Burge and Skinner, 1995). Thus, a correction factor as proposed by Burge and Skinner (1995) may have to be applied to estimate blood volume using the CO rebreathing methods.

Proposed new CO rebreathing method

In this study I have proposed a new CO rebreathing method (Figure 2.12A) to estimate M_{Hb} with low errors irrespective of the site of sampling. In this section I summarize the procedure to determine \hat{M}_{Hb} using this new method. Prior to CO rebreathing the subject breathes 100% O_2 for approximately 5 minutes. The initial

%HbCO levels from ear lobe, pre warmed finger tip or an artery in fore arm should be measured. The subject then rebreathes CO in 100% O_2 for 3.5 min. A known volume of CO is injected into the rebreathing system (3 L) at the beginning of CO rebreathing. The time at which CO is injected into the rebreathing circuit is considered as the experiment start time (T_0). The volume of CO administered is based on the gender and fitness level of the subject (Schmidt and Prommer, 2005). The concentration of CO in the rebreathing system at the end of rebreathing (3.5 min from T_0) is measured in ml, ATPD and then converted to BTPS. The volume of CO exhaled from end of rebreathing to T_{sample} (9 min from T_0) is measured in ml, BTPS. The %HbCO levels at T_{sample} are measured from the arterial, capillary other tissue, or capillary muscle blood compartments. V_{COMb} (in ml, BTPS) is estimated using the proposed regression equation (Equation 2.8a, Figure 2.13A). The V_{CO} administered (V_{CO_i}) is in ml, ATPD and should be converted to BTPS. T_{sample} is in minutes. M_{Hb} is calculated using equation 2.1.

Modifications to the existing CO rebreathing methods

Protocol B: In this method, inaccuracies in estimation of V_{COMb} result in larger errors in \hat{M}_{Hb} when compared to other CO rebreathing methods. Also, the long duration of CO rebreathing in 100% O_2 (40 min) causes inconvenience to the subjects. Thus the main disadvantages of this method are inaccurate estimation of V_{COMb} , larger T_{mix} and long durations of rebreathing. However, using the regression equation (Equation 2.8b, Figure 2.13b) suggested in this study to estimate V_{COMb} will lower the errors in $^E\hat{M}_{\text{Hb}}$ (Table 2.5) when compared to using the Prommer and Schmidt's formula (Equation 2.7, Table 3) or ignoring V_{COMb} . Despite larger T_{mix} , making a measurement from arterial or ear lobe (other tissue capillary) blood sites at a sampling time of 9 min, will allow determination of \hat{M}_{Hb} with low errors (Figure 2.17). Also the duration of the experiment can be decreased to 9 minutes as low errors in \hat{M}_{Hb} are obtained at the suggested sampling site and time. In addition to the suggested modifications, this method is complemented with other advantages like there will be no additional errors introduced in $^E\hat{M}_{\text{Hb}}$ due to inaccuracies in measurement of $V_{\text{CO ex}}$ (as CO is not exhaled in this method). In this

method despite intersubject variability, the magnitude of the size of error in calculation of \hat{M}_{Hb} is low from any blood site (Figure 2.17). Thus this method can be anticipated to determine \hat{M}_{Hb} with low errors for a range of subjects. Also I suggest that the $V_{CO} L+S$ be measured at the suggested sampling time, instead of calculating it from Equation 2.5.

Protocol P: The advantages of this method are that it has a smaller T_{mix} , smaller duration of CO rebreathing and lower volume of CO bound to myoglobin when compared to other rebreathing methods. However, the choice of 2 min duration of rebreathing in this method was not based on experimental or mathematical model driven results. Also, the model was able to validate the %HbCO's measured from different blood compartments for the Schmidt and Prommer's experiment conducted by Garvican et al. (2010), using the blood volumes calculated for the Burge and Skinner's method in the same experiment. This result suggests that the estimates of M_{Hb} from Schmidt and Prommer's method were inaccurate. In this CO rebreathing method, the values of ${}^E\hat{M}_{Hb}$ are based on compensatory errors in calculation of V_{COMb} and $V_{CO} ex$ (Table 2.4). To avoid errors in ${}^E\hat{M}_{Hb}$, it is suggested that $V_{CO} ex$ should be measured during the experiment and V_{COMb} should be calculated using the regression equation proposed in this study for protocol P (Equation 2.8c, Figure 2.13c). Unlike protocol B, in this method the magnitude of the size of error in calculation of \hat{M}_{Hb} from any blood site is dependent on the intersubject variability (Figure 2.17). The subject specific factors like ventilation, age, fitness level, body weight, blood volume, or D_MCO , to which the magnitude of error is sensitive, is not known and have not been analyzed in this study. Also the choice of duration of CO rebreathing in protocol N is based on results (low errors in M_{Hb}) obtained from simulation analysis.

CONCLUSIONS

In this study a validated mathematical model was used to determine any potential sources of errors in estimation of M_{Hb} (\hat{M}_{Hb}) from the existing CO rebreathing methods. Inaccuracies in estimation of volume of CO bound to myoglobin was found to be the

major source of error in calculation of \hat{M}_{Hb} from these methods. Using the regression equations developed in this study to estimate the volume of *CO* bound to myoglobin will allow estimation of M_{Hb} with low errors from any *CO* rebreathing method. Also estimating M_{Hb} using the new *CO* rebreathing method (Protocol N) or from the existing *CO* rebreathing methods with the suggested modifications for estimation of volume of *CO* bound to myoglobin, sampling time, and blood site, will allow estimation of M_{Hb} with low errors and allow comparison of hemoglobin mass determined from different studies using different *CO* rebreathing methods possible.

SUMMARY

Routine measurements of hemoglobin mass (M_{Hb}) are made to study the alterations in oxygen delivery during exercise training and acclimatization to altitude. Carbon monoxide (*CO*) rebreathing technique is a popularly used method to determine M_{Hb} in humans. The two commonly used *CO* rebreathing methods to determine M_{Hb} were proposed by Burge and Skinner (1995) and Schmidt and Prommer (2005). The potential sources of errors in determination of M_{Hb} from these methods are not known. The main aim of this study was to use a validated mathematical model to simulate the commonly used *CO* rebreathing methods and determine any potential sources of errors in estimation of M_{Hb} using these methods. For the two *CO* rebreathing methods, my previously published mathematical model (Erupaka et. al., 2010) was validated for experimentally measured %HbCO and M_{Hb} from arterial, capillary and venous blood sites of human subjects (Garvican et al., 2010). The validated model was used to simulate the existing *CO* rebreathing methods in 24 human subjects with a known M_{Hb} . M_{Hb} in these subjects was also estimated using the approximations made in the existing *CO* rebreathing methods for calculating volume of *CO* bound to myoglobin, volume of *CO* exhaled and the volume of *CO* in the rebreathing system. On analysis of my simulations, it was found that inaccuracies in estimation of volume of *CO* bound to myoglobin was the major source of error in determination of M_{Hb} . To determine M_{Hb} with low errors from the *CO* rebreathing methods, the validated mathematical model was applied in this study to propose a new *CO* rebreathing method and suggest modifications to the existing *CO* rebreathing methods.

Table 2.1: Symbols and their definitions		
Symbol	Definition	
Blood sites	Blood sites sampled for determination of hemoglobin mass	
	ar	Arterial blood site (artery in forearm)
	cm	Muscle tissue capillary blood site (finger tip)
	cot	Nonmuscle tissue capillary blood site (ear lobe)
	vm	Muscle tissue venous blood site (vein in forearm)
%HbCO	Percent carboxyhemoglobin level	
	%HbCO _{ar}	%HbCO in arterial blood
	%HbCO _{cot}	%HbCO in capillary blood of nonmuscle tissues
	%HbCO _{cm}	%HbCO in capillary blood of skeletal muscle tissues
	%HbCO _{vm}	%HbCO in venous blood of skeletal muscle tissues
M_{Hb}	Hemoglobin mass	
$^A M_{Hb}$	Known value of M_{Hb} from experiments (Input parameter to the model)	
\hat{M}_{Hb}	Estimated M_{Hb}	
	$^M \hat{M}_{Hb}$	\hat{M}_{Hb} estimated using the values from the model
	$^E \hat{M}_{Hb}$	\hat{M}_{Hb} estimated using the approximations from the experiments
T_{mix}	Estimated mixing time of CO in vascular space	
T_{sample}	Blood sampling time	
V_{COHb}	Volume of CO bound to hemoglobin	
V_{COMb}	Volume of CO bound to myoglobin	
$V_{CO L+S}$	Volume of CO in the lungs and rebreathing system at T_{sample}	
$V_{CO ex}$	Volume of CO exhaled	

Table 2.2 : Estimation of hemoglobin mass (${}^M\hat{M}_{Hb}$, ${}^E\hat{M}_{Hb}$)				
Variable	Model		Experiment	
	Protocol B	Protocol P	Protocol B	Protocol P
\hat{M}_{Hb}	${}^M\hat{M}_{Hb} = K \cdot {}^M V_{COHb} \cdot \frac{100}{1.58\Delta HbCO_i}$		${}^E\hat{M}_{Hb} = K \cdot {}^E V_{COHb} \cdot \frac{100}{1.58\Delta HbCO_i}$	
V_{COHb}	${}^M V_{COHb} = V_{COt} - V_{CO\ L+S} - V_{CO\ ex} - V_{COMb}$		${}^E V_{COHb} = V_{COt} - V_{CO\ L+S} - V_{CO\ ex} - V_{COMb}$	
V_{COt}	Total volume of CO administered		Total volume of CO administered	
$V_{CO\ L+S}$	Equation 2.4	Equation 2.4	Equation 2.5	Equation 2.4
$V_{CO\ ex}$	0	Equation 2.3	0	Equation 2.6
V_{COMb}	Equation 2.2	Equation 2.2	Equation 2.7	Equation 2.7

Table 2.3: Mean values with standard deviations of various variables and mean errors in calculation of ${}^M\hat{M}_{Hb}$ from Benignus's subjects (15 healthy male humans) for simulations of protocols B and P.			
Variable		Protocol B	Protocol P
T_{mix}		11.5 ± 2.561	3.54 ± 0.159
T_{sample}		13 ± 2.561	5.04 ± 0.159
Actual hemoglobin mass (${}^A M_{Hb}$)(g)		779.9 ± 167.8	779.9 ± 167.8
V_{CO} administered (ml)		83.88 ± 13.44	83.88 ± 13.44
V_{CO} Lung + rebreathing system (ml)		1.279 ± 0.161	1.116 ± 0.339
V_{CO} exhaled (ml)		0.0	1.440 ± 0.342
V_{COMb} (ml)		5.174 ± 1.683	1.581 ± 0.382
V_{COHb} (ml)		77.43 ± 12.62	79.74 ± 13.05
Arterial	$\Delta HbCO$ (%) *	6.411 ± 0.899	6.718 ± 1.053
	mean % error ⁺	0.118 ± 0.151	-0.865 ± 0.363
Capillary_{OT}	$\Delta HbCO$ (%) *	6.415 ± 0.900	6.732 ± 1.055
	mean % error ⁺	0.057 ± 0.140	-0.974 ± 0.365
Capillary_M	$\Delta HbCO$ (%) *	6.307 ± 0.899	6.716 ± 1.056
	mean % error ⁺	1.619 ± 0.079	-0.769 ± 0.365
Venous_M	$\Delta HbCO$ (%) *	6.291 ± 0.906	6.601 ± 1.055
	mean % error ⁺	1.883 ± 0.209	-0.392 ± 0.402

* All $\Delta HbCO\%$ are the values estimated by the model at T_{sample} .

⁺ %errors in estimates of M_{Hb} calculated from the model (${}^M\hat{M}_{Hb}$) compared to ${}^A M_{Hb}$

Table 2.4: Mean values with standard deviations of estimated V_{COMb} using Equation 2.7 and errors in calculation of ${}^E\hat{M}_{Hb}$ from Benignus's subjects for simulations of protocols B and P.			
Blood site	Protocol*	V_{COMb} (ml)	mean % error ⁺
Arterial	B	3.134 ± 0.603	2.051 ± 1.599
Capillary _{OT}	B	3.201 ± 0.619	1.901 ± 1.582
Capillary _M	B	2.154 ± 0.590	4.870 ± 1.378
Venous _M	B	1.896 ± 0.550	5.479 ± 1.288
Arterial	P	1.872 ± 0.568	-0.056 ± 0.37
Capillary _{OT}	P	2.120 ± 0.613	-0.474 ± 0.41
Capillary _M	P	2.031 ± 0.723	-0.159 ± 0.49
Venous _M	P	-1.749 ± 0.77	4.958 ± 0.702

*See Table 2.3 for T_{mix} , T_{sample} , actual M_{Hb} (${}^A M_{Hb}$), V_{CO} administered, and $\Delta HbCO\%$. The volume of CO exhaled is 0 ml and 0.513 ± 0.088 ml for protocols B and P respectively. The volume of CO in the lungs and rebreathing system is 1.845 ± 0.296 ml in protocol B and 0.513 ± 0.088 ml in protocol P.

⁺ %errors in estimates of M_{Hb} calculated from the experiments (${}^E\hat{M}_{Hb}$) compared to ${}^A M_{Hb}$

Table 2.5: Mean values with standard deviations of errors in ${}^E\hat{M}_{Hb}$ from Benignus's subjects for simulations of protocols B, P and N.			
Blood site	Protocol N* <i>mean % error⁺</i>	Protocol B <i>mean % error⁺</i>	Protocol P <i>mean % error⁺</i>
Arterial	-0.249 ± 0.502	-0.694 ± 1.026	0.322 ± 0.504
Capillary_{OT}	-0.305 ± 0.488	-0.755 ± 1.014	0.212 ± 0.486
Capillary_M	-0.730 ± 0.576	0.793 ± 0.897	0.419 ± 0.485
Venous_M	-0.056 ± 0.453	1.053 ± 0.774	0.801 ± 0.424

*The mean values for T_{mix} , T_{sample} , volume of CO exhaled, and volume of CO in the lungs + rebreathing system for the new protocol are 4.54 ± 0.19 , 6.04 ± 0.19 , 1.00 ± 0.15 and 1.26 ± 0.26 respectively. V_{COMb} for all protocols are estimated from the regression equations.

⁺ %errors in estimates of M_{Hb} calculated from the ${}^E\hat{M}_{Hb}$ (as described below) compared to ${}^A M_{Hb}$. ${}^E\hat{M}_{Hb}$ was calculated using estimations of V_{COMb} from the regression equations (Equation 2.8) and V_{CO} L+S (Equation 2.5), V_{CO} exhaled (Equation 2.6) from the experiment formulas.

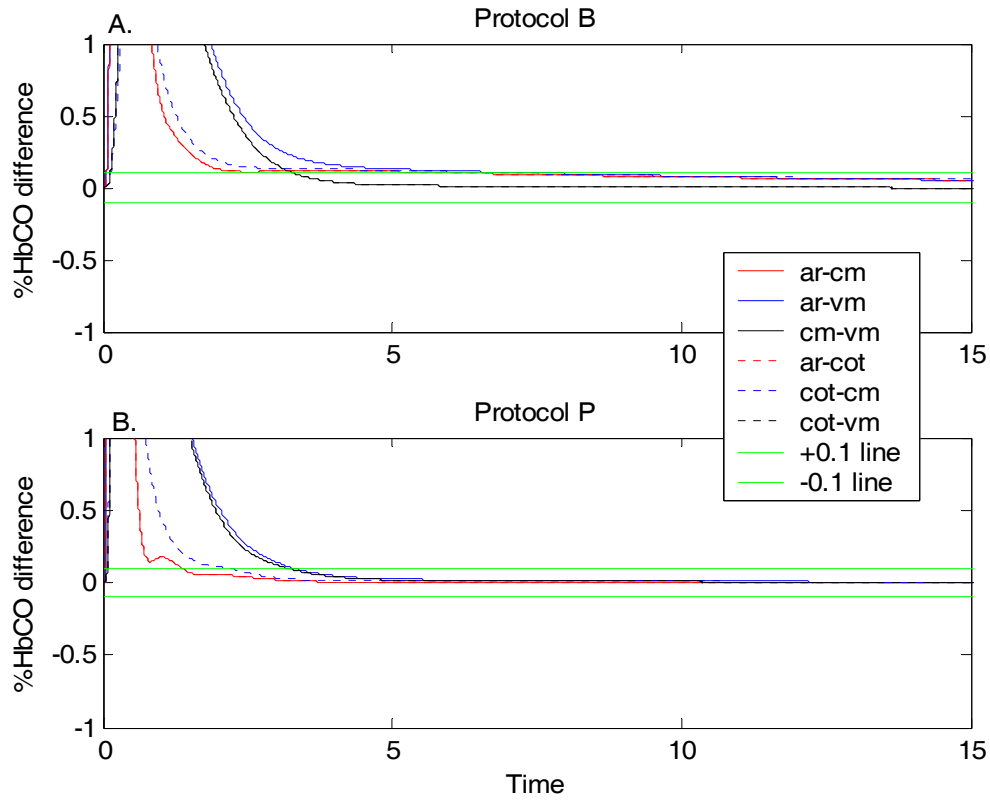


Figure 2.1: Determination of T_{mix} in (A) protocol B and (B) protocol P. The pairwise differences in %HbCO within four different blood compartments were plotted at different times. The time at which the %HbCO difference line crosses the reference line was determined as the mixing time, T_{mix} .

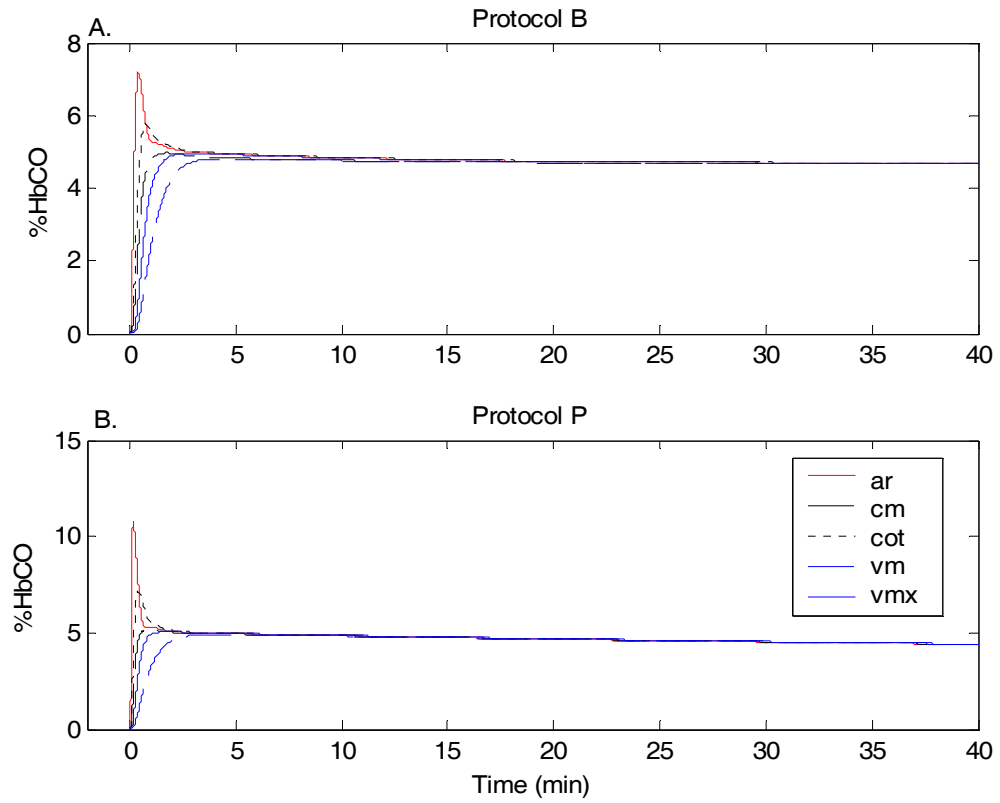


Figure 2.2: Uptake kinetics of CO in (A) protocol B and (B) protocol P. The $\%HbCO$ levels in different vascular compartments of the model arterial (ar), capillary muscle (cm), capillary other tissue (cot), muscle venous (vm) and mixed venous (vmx).

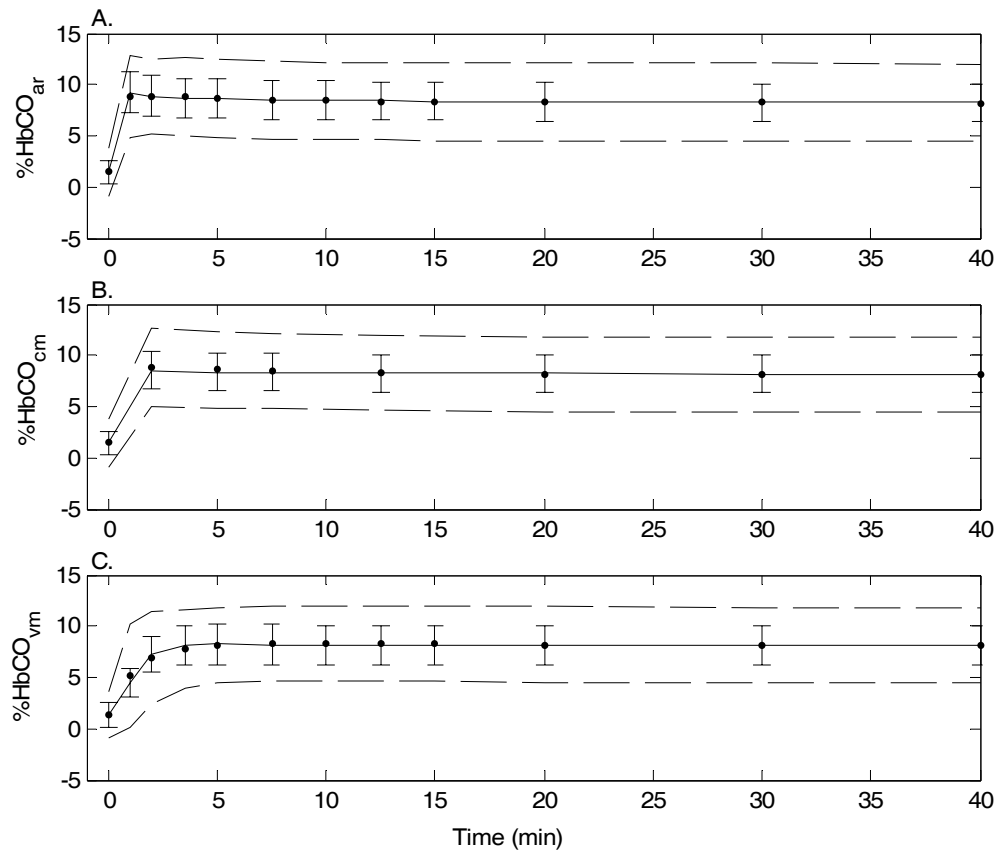


Figure 2.3: Comparison of model predicted %HbCO with experimental data from three blood sites: (A) arterial-ar, (B) capillary muscle -cm, (C) venous muscle-vm, for Burge and Skinner method. The solid lines with error bars are the model predicted mean %HbCO with \pm SD, from individual simulations of 9 subjects. Mean %HbCO from the experiments is represented with symbol ‘•’. The dashed lines are the 95% confidence limits of the experimental data.

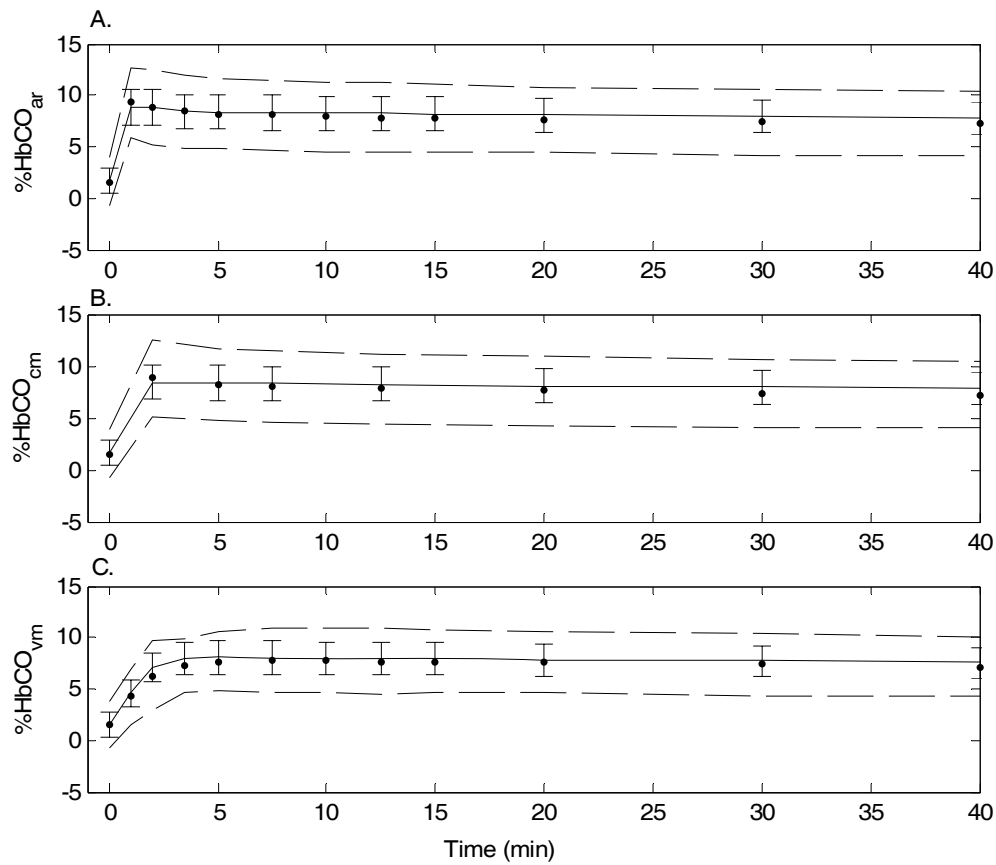


Figure 2.4: Comparison of model predicted $\%HbCO$ with experimental data from three blood sites: (A) arterial-ar, (B) capillary muscle -cm, (C) venous muscle-vm, for Schmidt and Prommer method. The solid lines with error bars are the model predicted mean $\%HbCO$ with $\pm SD$, from individual simulations of 9 subjects. Mean $\%HbCO$ from the experiments is represented with symbol '•'. The dashed lines are the 95% confidence limits of the experimental data.

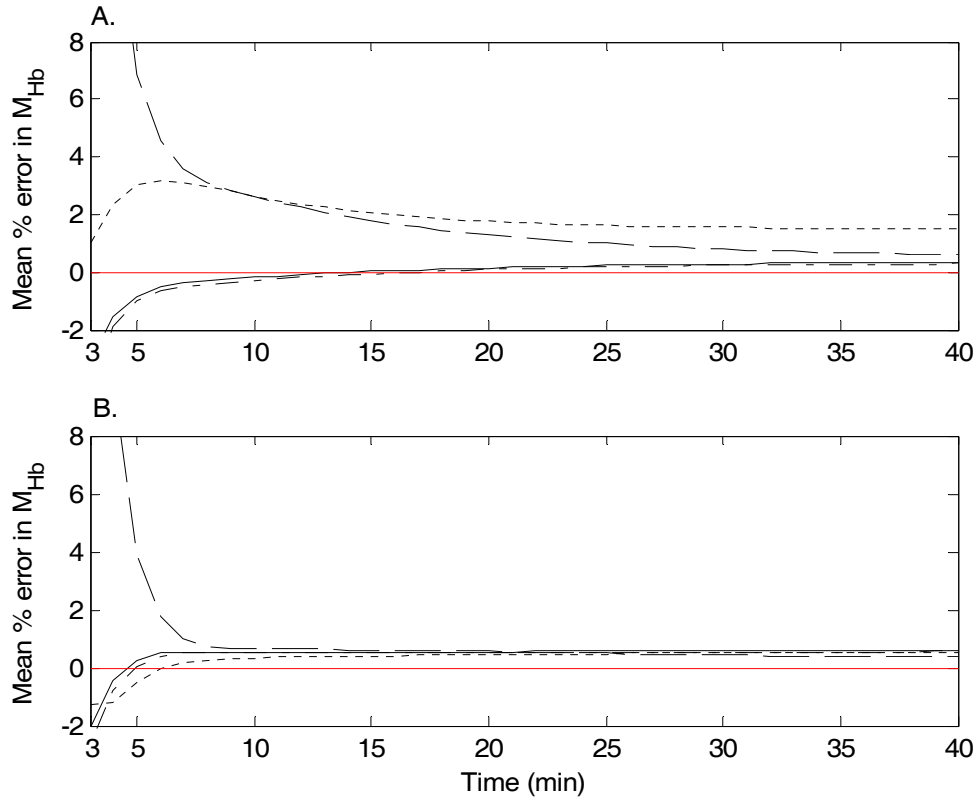


Figure 2.5: Mean % error in estimated Hb mass using exact data from the model (i. e., V_{COHb}) vs. time for blood sampled from arterial (—), capillary other tissue (— · —), capillary muscle (····) and muscle venous (— —) blood sites for (A) Burge and Skinner method and (B) Prommer and Schmidt method. Value at each time point represents mean percent error from simulations of Garvican’s 9 subjects. The red solid line is the zero line.

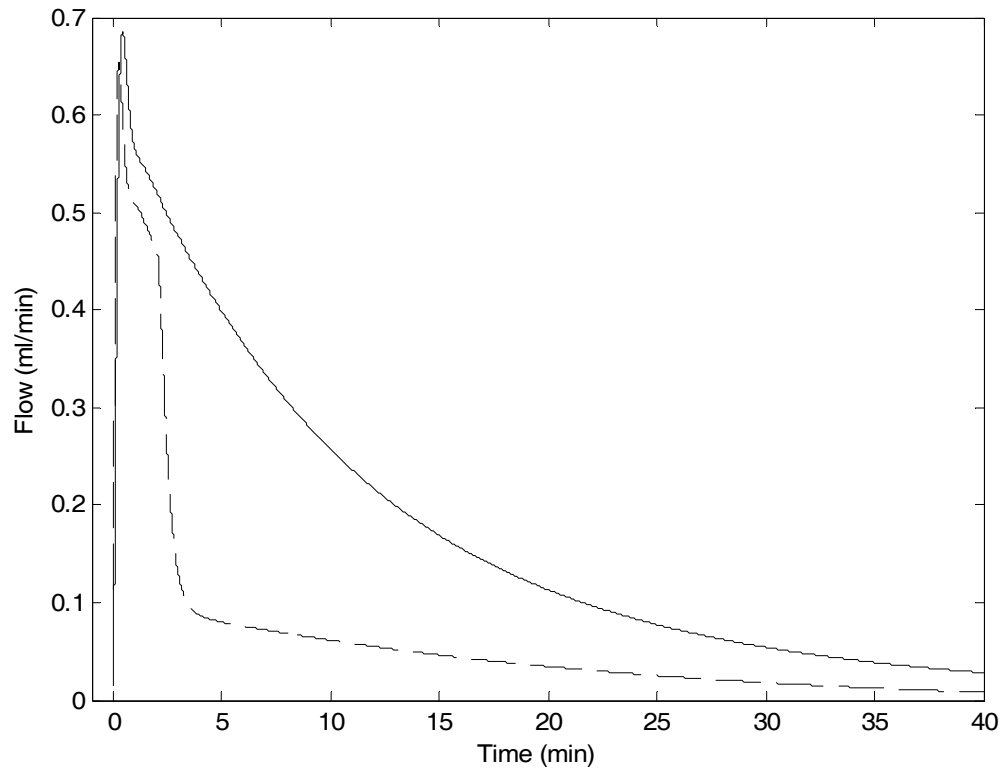


Figure 2.6: *CO* flux from blood to muscle tissues in the two commonly used *CO* rebreathing methods. *CO* flux (ordinate) from blood to muscle tissue in protocol B (solid line) and Protocol P (dashed line) is not constant.

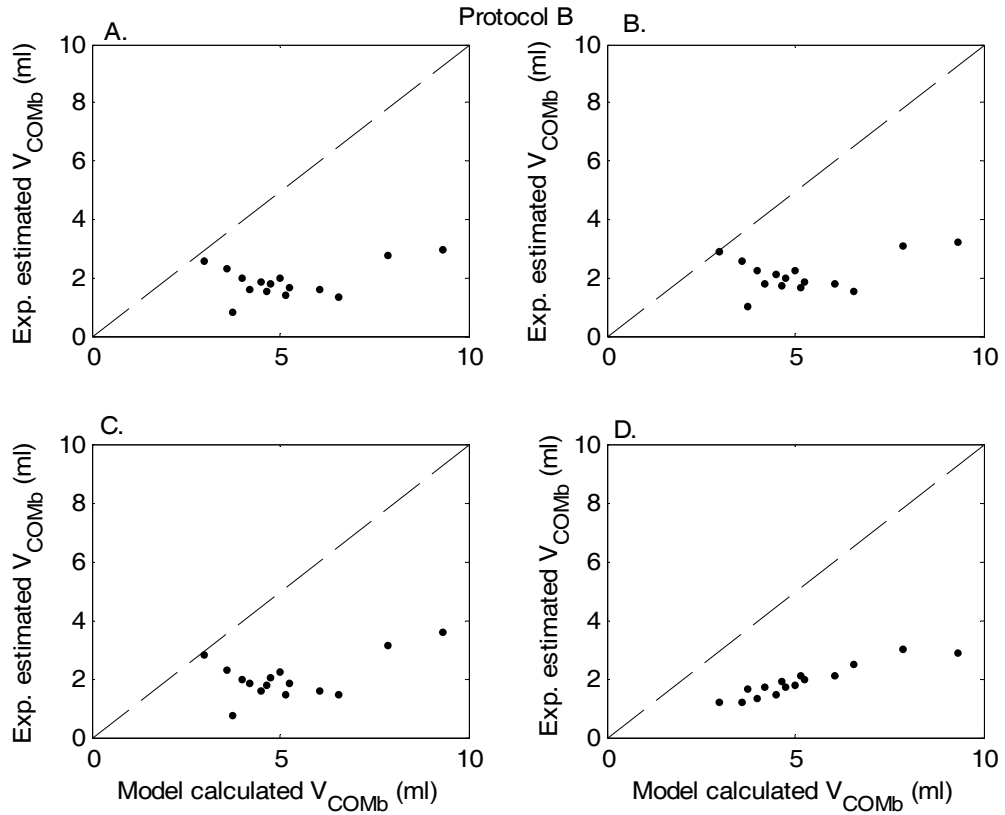


Figure 2.7: Comparison of model calculated V_{COMb} (abscissa) with Prommer and Schmidt's estimated V_{COMb} (ordinate) in (A) arterial, (B) capillary other tissue, (C) capillary muscle and (D) muscle venous blood sites for protocol B. Dashed lines are the identity lines. Each point represents one subject.

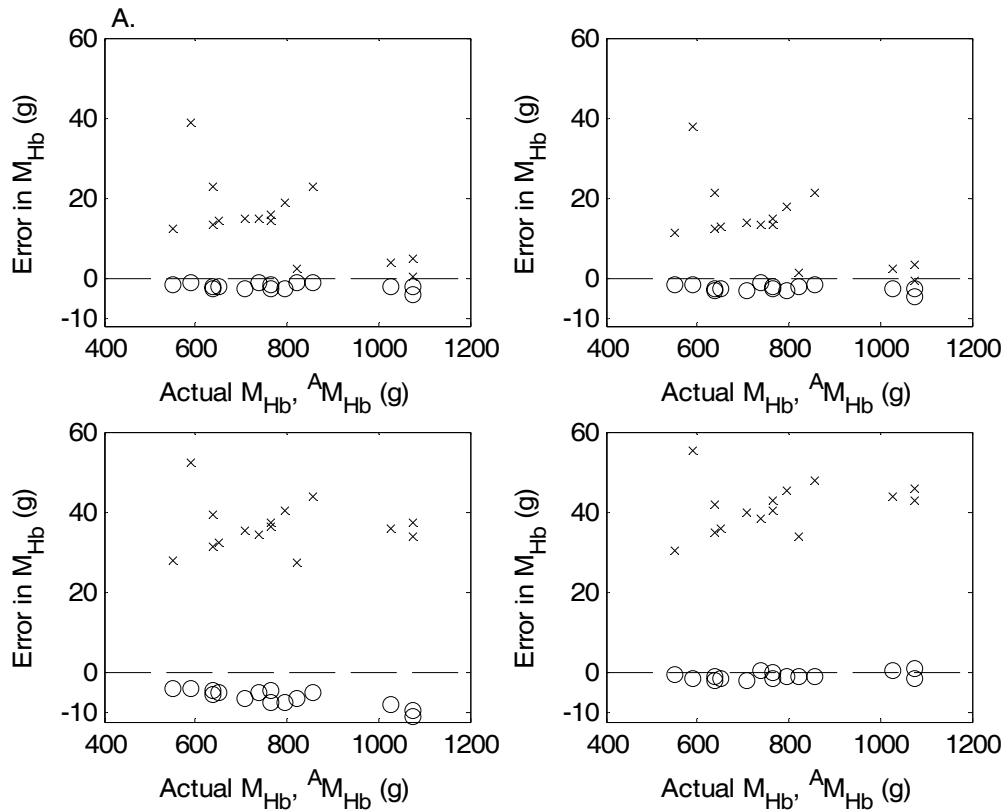


Figure 2.8: Errors in estimation of M_{Hb} . Comparison of the actual known M_{Hb} , $^A M_{Hb}$ with M_{Hb} estimated using the exact values from the model, $^M \hat{M}_{Hb}$ and M_{Hb} estimated using the approximations used in the existing *CO* rebreathing methods, $^E \hat{M}_{Hb}$ for samples taken from different blood sites (A) arterial, (B) capillary other tissue, (C) capillary muscle and (D) muscle venous for protocol B. Dashed lines are the zero reference lines. Each point represents one subject.

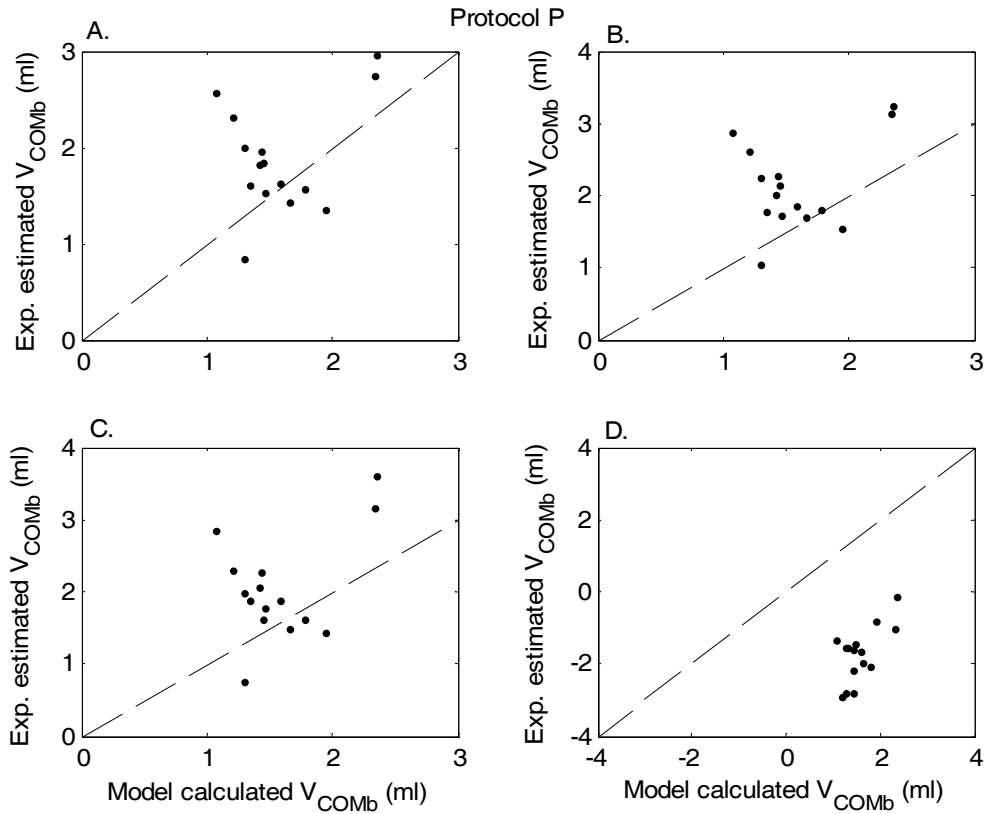


Figure 2.9: Comparison of model calculated V_{COMb} (abscissa) with Prommer and Schmidt's estimated V_{COMb} (ordinate) in (A) arterial, (B) capillary other tissue, (C) capillary muscle and (D) muscle venous blood sites for protocol P. Dashed lines are the identity lines. Each point represents one subject.

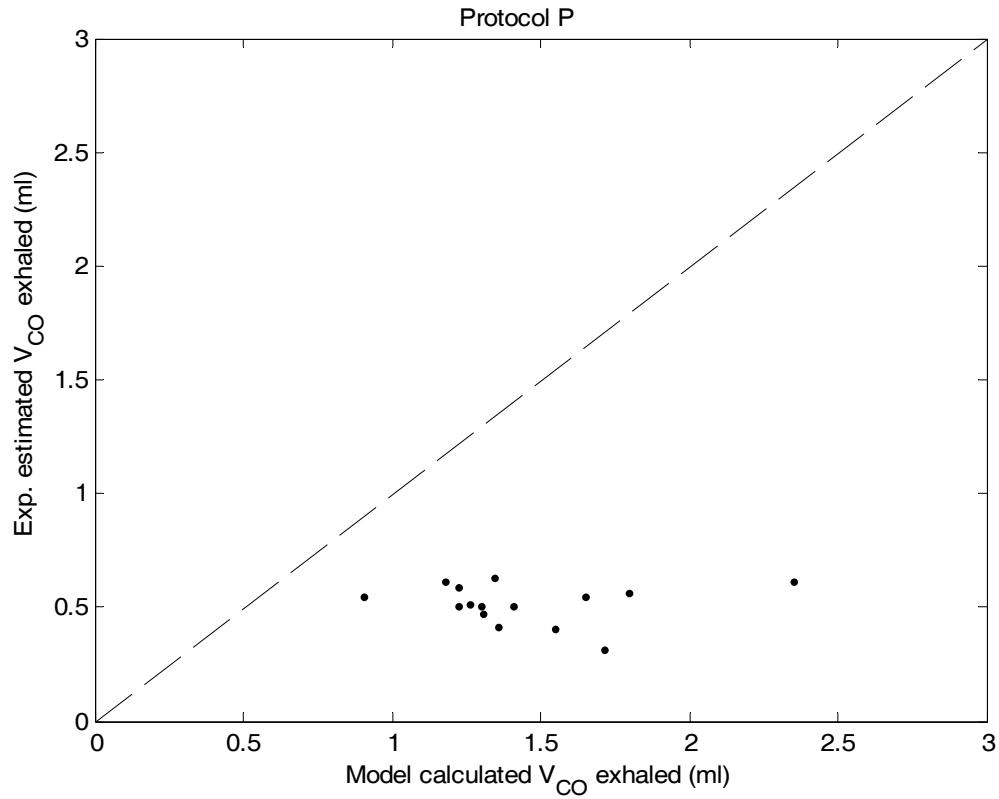


Figure 2.10: Comparison of model calculated V_{CO} exhaled (abscissa) with Prommer and Schmidt's estimated V_{CO} exhaled (ordinate) in protocol B. Dashed line is the identity line. Each point represents one subject.

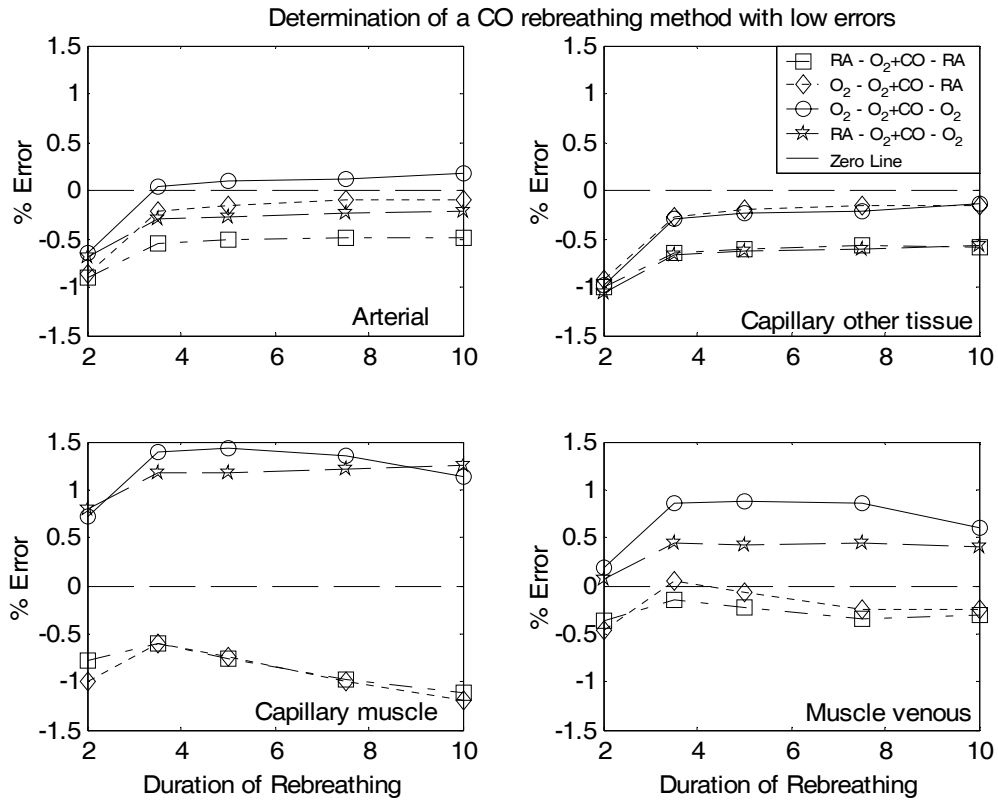


Figure 2.11: Effects of varying durations of CO rebreathing in 100% O_2 and the ambient conditions before or after CO rebreathing on errors in estimation of M_{Hb} . Errors in estimates of M_{Hb} (y-axis) from various blood compartments for different durations of rebreathing shown on x-axis (2, 3.5, 5, 7.5, 10 min) are represented by (A) '□' on breathing room air before and after CO rebreathing in 100% O_2 , (B) '◇' breathing 100% O_2 before CO rebreathing in 100% O_2 followed by breathing room air (C) '○' breathing 100% O_2 before and after CO rebreathing in 100% O_2 and (D) '☆' breathing room air before CO rebreathing in 100% O_2 followed by 100% O_2 . Dashed lines are the zero reference lines.

New Protocol (Protocol N):

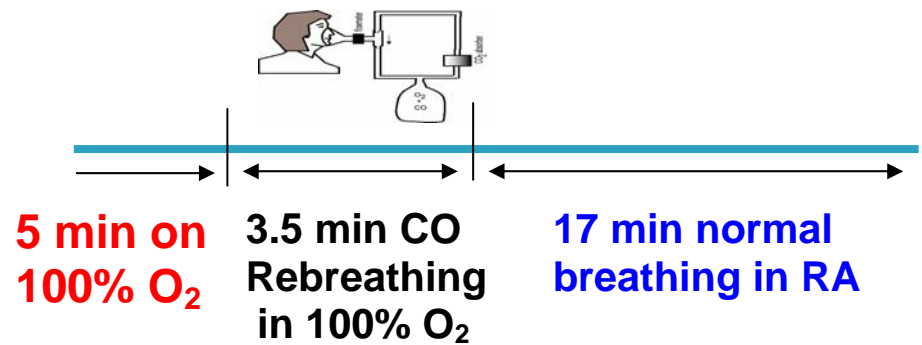


Figure 2.12A: Protocol N

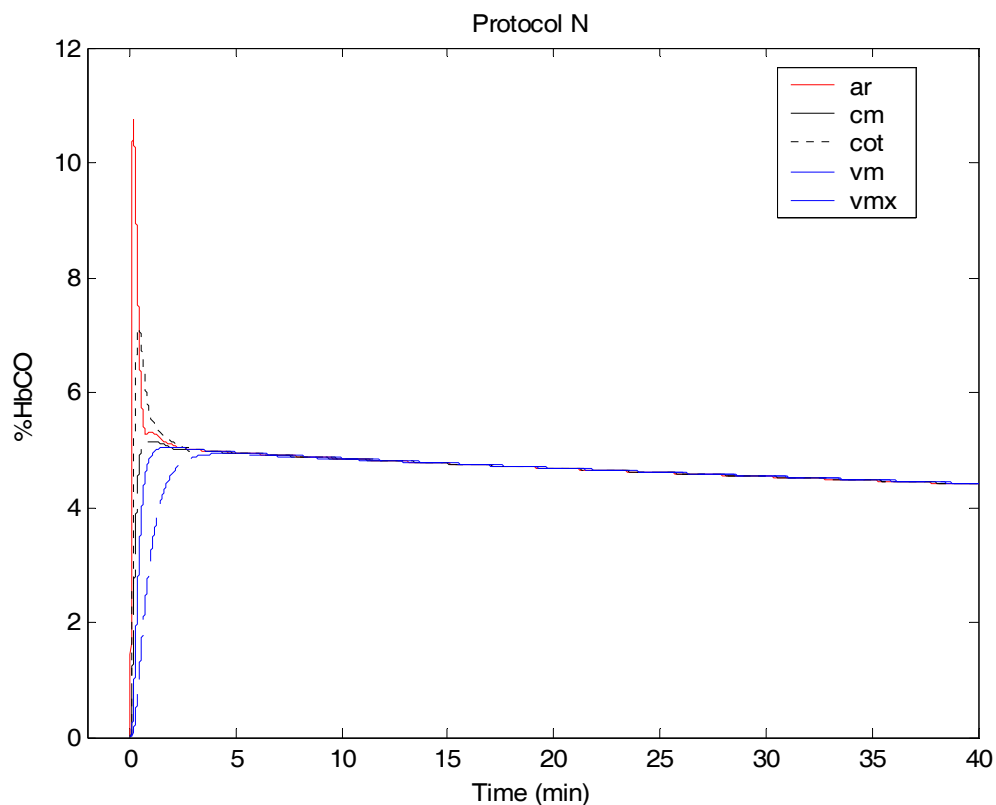


Figure 2.12B: Uptake kinetics of *CO* in protocol N for one typical subject. The %*HbCO* levels in different vascular compartments of the model arterial (ar), capillary muscle (cm), capillary other tissue (cot), muscle venous (vm) and mixed venous (vmx).

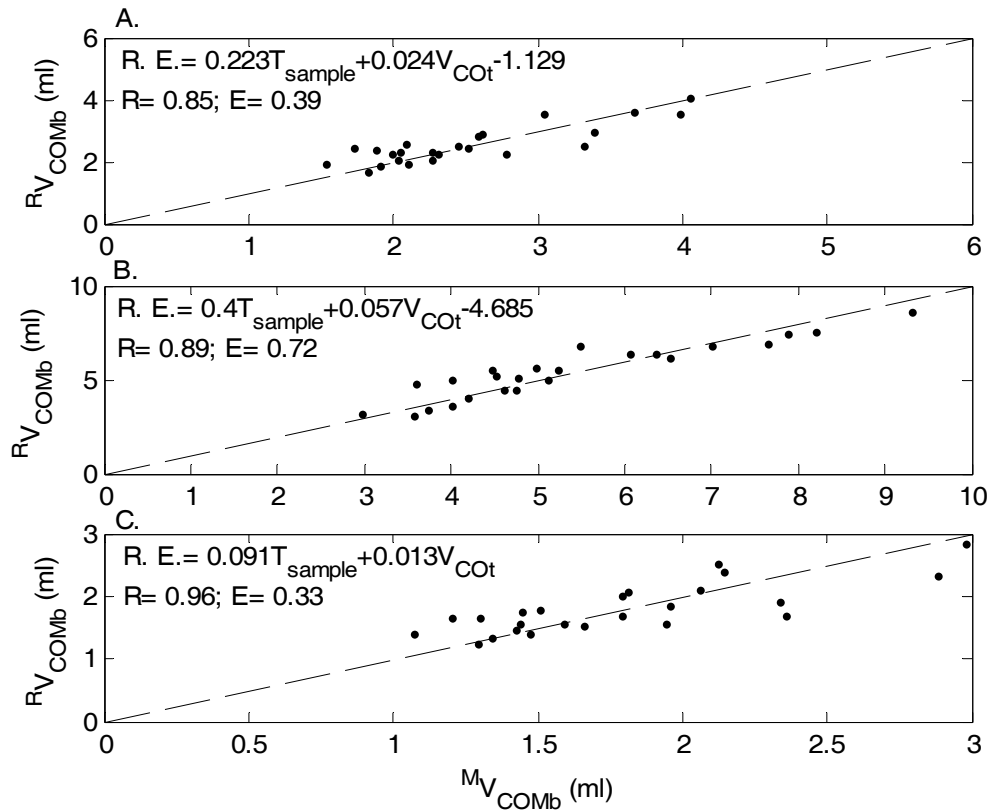


Figure 2.13: Proposed regression equations to estimate V_{COMb} for calculation of M_{Hb} from (A) Protocol N, (B) Protocol B and (C) Protocol P. Model calculated V_{COMb} as abscissa and regression estimated V_{COMb} as ordinate. R is the regression coefficient and E is the error in the estimate. Dashed lines are the identity lines. Each point represents one subject.

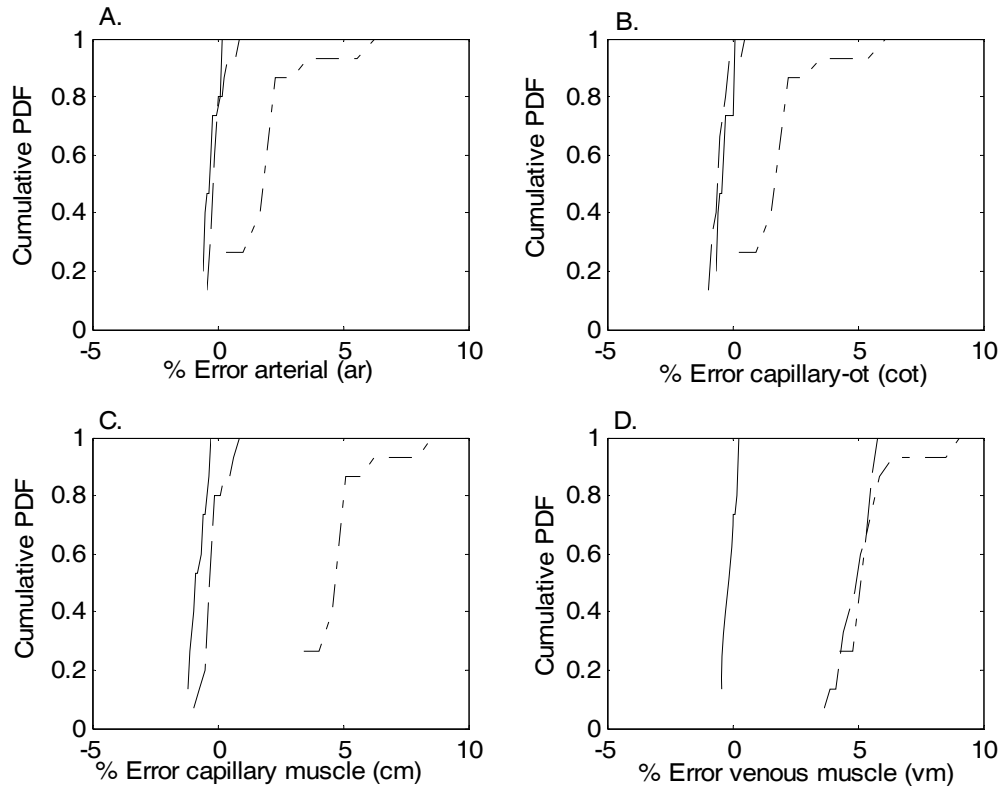


Figure 2.14: Comparison of errors from different blood sites for protocols B (dash-dotted line), P (dashed line) and N (solid line). Shown on x-axis and y-axis are the errors in \hat{M}_{Hb} and cumulative probability density functions for data from the 15 subjects (Benignus et al., 1994) from (A) arterial, (B) capillary-other tissue, (C) capillary muscle and (D) muscle venous blood sites.

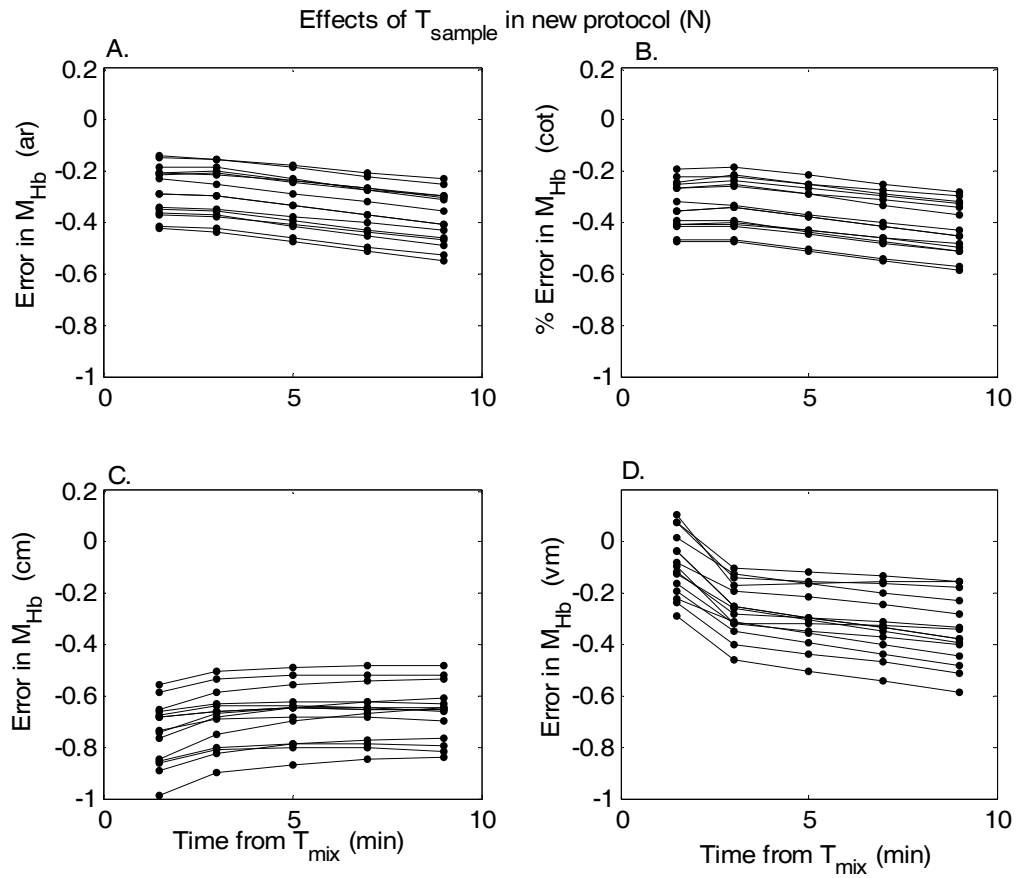


Figure 2.15: Effects of T_{sample} on estimation of M_{Hb} in protocol N. Errors in calculation of $^M \hat{M}_{\text{Hb}}$ (ordinate) from (A) arterial, (B) capillary-other tissue, (C) capillary muscle and (D) muscle venous blood compartments are plotted at different times (abscissa) in Benignus's subjects. Each line represents one subject.

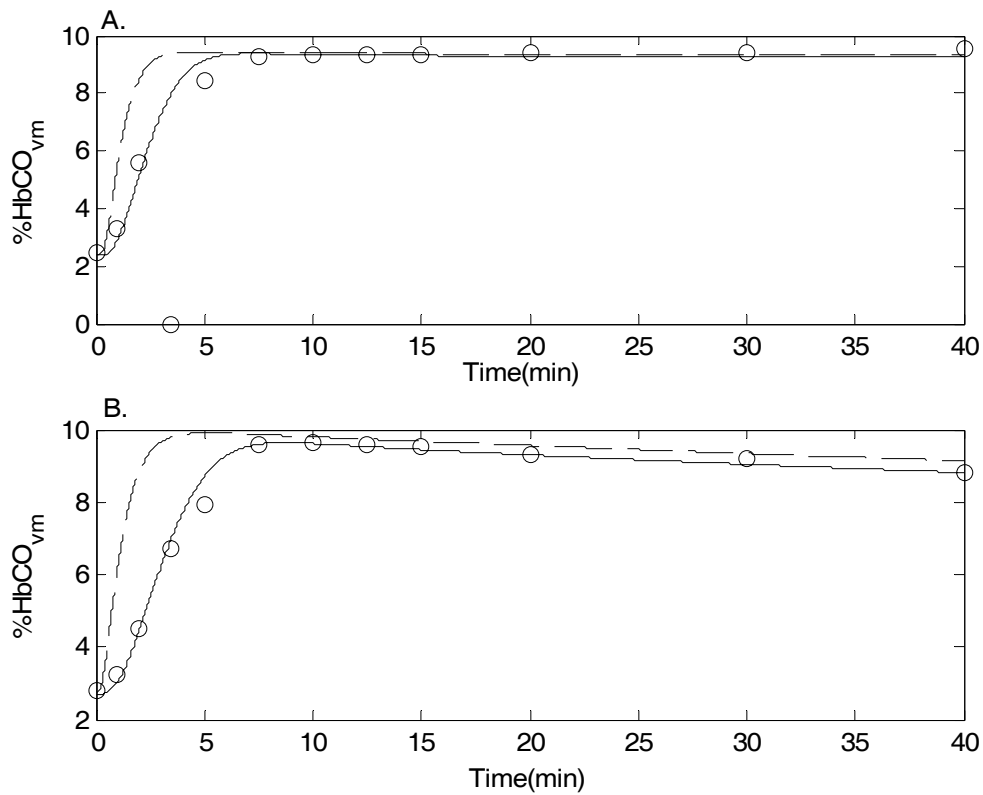


Figure 2.16: Model fit of a healthy, recreationally-active female human subject from Garvican et al.(2010). The %venous HbCO levels in the (A) Burge and Skinner methods and (B) Schmidt and Prommer method from the experiment of Garvican et al., 2010 (o), model fit using average values for blood volume of venous blood compartment of the muscle and muscle blood flow (dashed line) and model fit using the increased blood volume of venous blood compartment of the muscle and decreased muscle blood flow (solid line). The venous blood compartment volume was increased by 20% of mixed venous blood volume and the muscle blood flow was decreased by 20%.

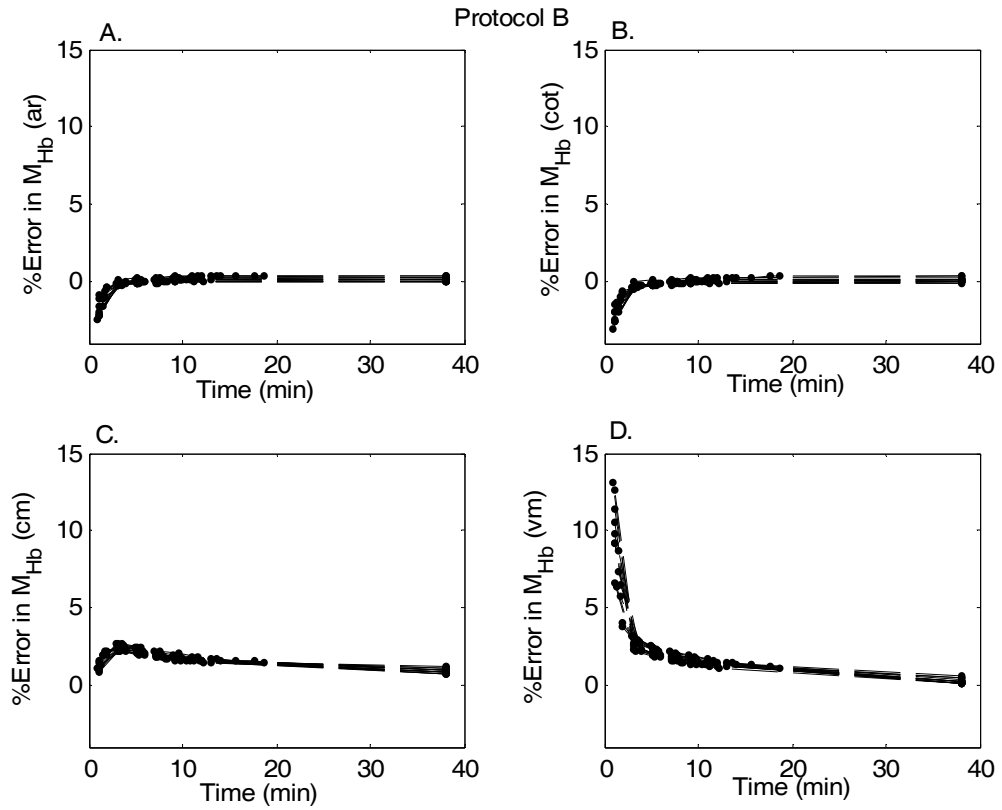


Figure 2.17: Effects of T_{mix} on estimation of M_{Hb} in protocol B. Errors in calculation of $^M \hat{M}_{Hb}$ (ordinate) from (A) arterial, (B) capillary-other tissue, (C) capillary muscle and (D) muscle venous blood compartments are plotted at different times (abscissa) in Benignus's subjects. Each line represents one subject.

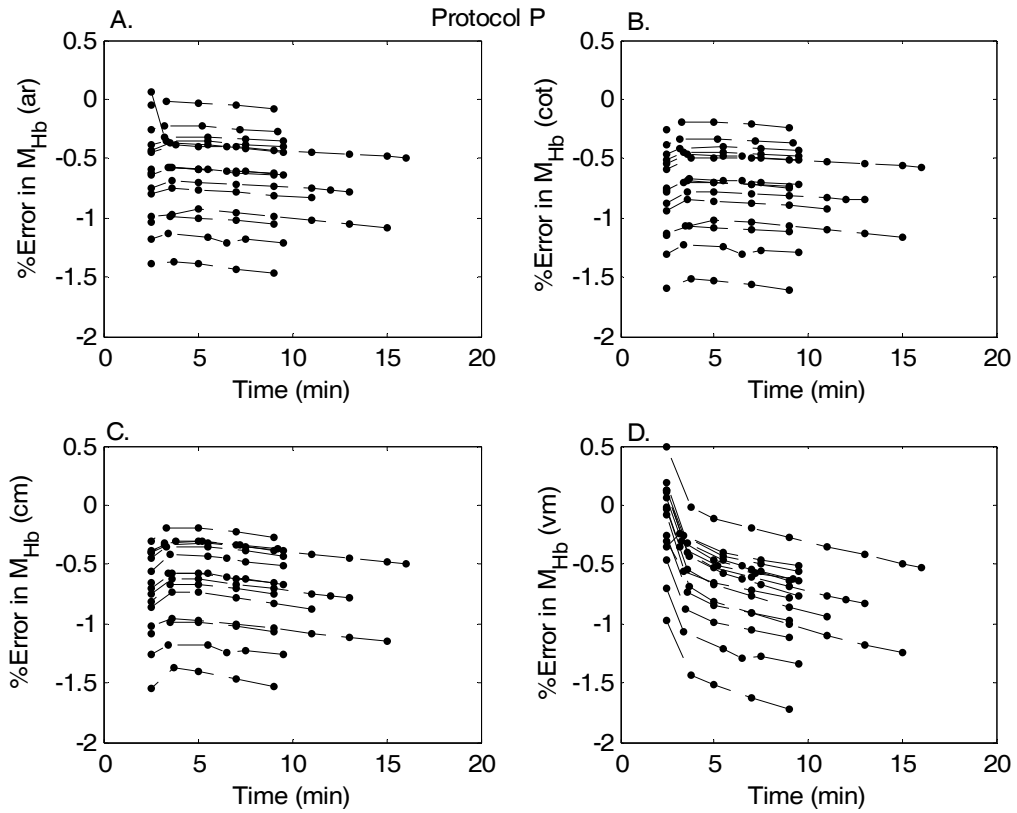


Figure 2.18: Effects of T_{mix} on estimation of M_{Hb} in protocol P. Errors in calculation of $^M \hat{M}_{Hb}$ (ordinate) from (A) arterial, (B) capillary-other tissue, (C) capillary muscle and (D) muscle venous blood compartments are plotted at different times (abscissa) in Benignus's subjects. Each line represents one subject.

Chapter 3: Enhanced Mathematical Model

Contents of this chapter will be submitted as a manuscript

INTRODUCTION

The third specific aim is to compare the current treatment strategies available to treat *CO* poisoned victims and determine the best treatment strategy ensuring fastest *CO* removal and O_2 delivery after *CO* poisoning. As stated in chapter 1, the best approach to accomplish this aim would be to use a validated mathematical model capable of estimating *CO* burden (%HbCO, %MbCO), O_2 levels and CO_2 levels in different blood (arterial, capillary, venous) and tissue (brain, heart, skeletal muscle, nonmuscle) compartments for various *CO* exposures and treatment sessions in healthy populations. Understanding the O_2 and CO_2 dynamics (transport and utilization of O_2 or CO_2 from and within blood vessels and tissues) in the brain, heart and skeletal muscle during different treatments plays a key role in designing treatments. This is because brain, heart and skeletal muscle (during exercise) tissues are highly oxidative organs and produce metabolites like CO_2 . Limitation of O_2 supply below a certain level to these organs due to *CO* leads to collapse of vital cell functions, accumulation of metabolites and eventually cell death (Erecińska and Silver, 2001; Folbergrová et al., 1990; Zauner et al., 2002).

The major limitations of the previously developed model (Erupaka et al., 2010) are that the brain tissue is represented as a part of the lumped other tissue compartment and the model lacks control of ventilation and regulation of blood flow in conditions of changing O_2 or CO_2 concentrations. Thus due to these major limitations, this model cannot be applied to compare O_2 levels in the brain compartment during different treatments and to understand the role of CO_2 during isocapnic (arterial PCO_2 maintained at a constant level) and poikilocapnic (uncontrolled arterial PCO_2) treatments. There are other whole body mathematical models developed in the literature but have limitations (Stuhmiller and Stuhmiller, 2005; Ursino et al., 2001; Wolf and Garner, 2007; Zhou et al., 2007). Many of these models cannot be applied because mass balance of *CO* or regulation of blood flow has not been incorporated in these models for conditions like *CO* exposure or HBO_2 (Ursino et al., 2001; Wolf and Garner, 2007; Zhou et al., 2007). Models which have incorporated *CO* mass balance equations ignore the fact that a significant amount of *CO* can diffuse into the muscle tissues (Stuhmiller and Stuhmiller, 2005). Thus, the best available mathematical model that can be applied to

implement the third specific aim is the model developed in our lab (Erupaka et al., 2010). However, this model should be enhanced by adding the necessary features and validated for various conditions of changing O_2 and CO_2 concentrations to allow simulations of various treatment protocols.

The mathematical model described in this chapter is an expansion of the previous model (Erupaka et al., 2010). This previously developed and published model (Erupaka et al., 2010) was upgraded by adding a cardiac compartment to the original model of Bruce et al. (2008). Significant enhancements made to the previous upgraded model (Erupaka et al., 2010) are addition of: (i) brain compartment (Figure 3.1), (ii) mass balance equations for CO_2 , (iii) control of ventilation, (iv) regulation of blood flow: cardiac output, cerebral blood flow, myocardial blood flow, skeletal muscle tissue and non-muscle tissue blood flow with changes in arterial O_2 saturation (S_{O_2}), PO_2 , PCO_2 , %HbCO and (v) Bohr effect on O_2 dissociation curve and Haldane effect on CO_2 dissociation curve.

METHODS

ACSL 11.8 was used to implement this model. For numerical integration, Runge-Kutta-Fehlberg variable step size algorithm with error flagging was used and the maximum allowable step size was 0.001 min. Simulations were performed in double precision and a 30 minute stabilization period was initiated with every simulation run for the baseline simulation to reach a steady state. New algorithms were added to implement Bohr effects and previously used algorithms (described as special functions in Erupaka et al., 2010) were modified.

Model Description

Addition of brain compartment: A brain compartment (Figure 3.1) comprising three vascular subcompartments (bb_1, bb_2, bb_3) and two tissue subcompartments (b_1, b_2) was added to my previously published model (Erupaka et al., 2010). This concept of two tissue subcompartments with three vascular subcompartments was introduced, validated and published for the skeletal muscle by Bruce et al. (2008). Later this concept was

extended to the cardiac muscle tissue by Erupaka et al. (2010). In this chapter, the same concepts of a two tissue subcompartments described by Bruce et al. (2008) were implemented to add a brain tissue compartment to the model. The brain tissue in my previous model (Erupaka et al., 2010) was lumped with the nonmuscle tissues. A separate brain compartment was implemented to estimate extent of CO induced hypoxia during CO exposure and O_2 delivery during different therapy protocols. Also, knowledge of O_2 and CO_2 (CO_2 mass balance equations described later in the text) levels in the brain will enable better control of ventilation in the model. The structure of the brain compartment (Figure 3.1) is similar to that of the skeletal and cardiac muscle compartments of previous models developed in our lab (Bruce et al., 2008; Erupaka et al., 2010). The relative volumes of brain tissue subcompartments and blood subcompartments were chosen by trial and error from various volume distributions, which were tested to optimize the model predictions for brain blood and brain tissue PO_2 's in various conditions (Table 3.1-3.2). The mass balance equations for O_2 and CO for the brain compartment (Eqs. 3.1-3.10) are similar to that of the cardiac and skeletal muscle tissue (Appendix A of Erupaka et al., 2010), except that the brain tissue compartments do not contain myoglobin. After adding the brain compartment, the brain tissue and venous PO_2 's were validated for conditions of hypoxic hypoxia, CO hypoxia, hyperoxia and hyperbaric oxygen (See section “*Model Validation*”). The O_2 and CO mass balance equations written for brain compartment are as described below:

Brain Tissue Subcompartment 1, (b_1):

$$\frac{dC_{b_1}O_2(t)}{dt} = \frac{Flux_{b_1}O_2(t)}{V_{b_1}} + \frac{D'_b O_2 \cdot (C_{b_2}^d O_2(t) - C_{b_1}^d O_2(t))}{D_{xb}} - \frac{MR_{b_1}O_2(t)}{V_{b_1}} \dots\dots\dots (3.1)$$

$$\frac{dC_{b_1}CO(t)}{dt} = \frac{Flux_{b_1}CO(t)}{V_{b_1}} + \frac{D'_b CO \cdot (C_{b_2}^d CO(t) - C_{b_1}^d CO(t))}{D_{xb}} \dots\dots\dots (3.2)$$

$C_{b_1}O_2(t)$ and $C_{b_1}CO(t)$ are the tissue concentrations of O_2 and CO in brain tissue subcompartment, b_1 of volume V_{b_1} . $Flux_{b_1}O_2(t)$ and $Flux_{b_1}CO(t)$ are the O_2 and CO fluxes from blood to brain tissue subcompartment 1. $C_{b_1}^d O_2(t)$, $C_{b_2}^d O_2(t)$, $C_{b_1}^d CO(t)$, and $C_{b_2}^d CO(t)$ are the dissolved O_2 and CO concentrations

in tissue subcompartments 1 and 2, respectively. D_{xb} is the mean intercapillary distance in the brain tissue. $D'_b O_2$ and $D'_b CO$ are the intertissue brain diffusion coefficients for O_2 and CO . $MR_{b_1} O_2(t)$ is the metabolic rate of O_2 in tissue compartment b_1 .

Brain Tissue Subcompartment 2, (b_2):

$$\frac{dC_{b_2} O_2(t)}{dt} = \frac{Flux_{b_2} O_2(t)}{V_{b_2}} + \frac{D'_b O_2 \cdot (C_{b_1}^d O_2(t) - C_{b_2}^d O_2(t))}{D_{xb} \cdot \left(\frac{V_{b_2}}{V_{b_1}} \right)} - \frac{MR_{b_2} O_2(t)}{V_{b_2}} \dots\dots\dots(3.3)$$

$$\frac{dC_{b_2} CO(t)}{dt} = \frac{Flux_{b_2} CO(t)}{V_{b_2}} + \frac{D'_b CO \cdot (C_{b_1}^d CO(t) - C_{b_2}^d CO(t))}{D_{xb} \cdot \left(\frac{V_{b_2}}{V_{b_1}} \right)} \dots\dots\dots(3.4)$$

$C_{b_2} O_2(t)$ and $C_{b_2} CO(t)$ are the tissue concentrations of O_2 and CO in brain tissue subcompartment, b_2 of volume V_{b_2} . $Flux_{b_2} O_2(t)$ and $Flux_{b_2} CO(t)$ are the O_2 and CO fluxes from blood to brain tissue subcompartment 2. $MR_{b_2} O_2(t)$ is the metabolic rate of O_2 in tissue compartment b_2 .

Brain Blood compartment 1, (bb_1):

$$V_{bb_1} \frac{dC_{bb_1} O_2(t)}{dt} = \dot{Q}_b(t) \cdot (C_{ar} O_2(t) - C_{bb_1} O_2(t)) - O_2 Flux_{b_1}(t) \dots\dots\dots(3.5)$$

$$V_{bb_1} \frac{dC_{bb_1} CO(t)}{dt} = \dot{Q}_b(t) \cdot (C_{ar} CO(t) - C_{bb_1} CO(t)) - CO Flux_{b_1}(t) \dots\dots\dots(3.6)$$

$C_{bb_1} O_2(t)$ and $C_{bb_1} CO(t)$ are the blood concentrations of O_2 and CO in brain vascular subcompartment 1, bb_1 of volume V_{bb_1} . $\dot{Q}_b(t)$ is the brain blood flow and $C_{ar} O_2(t)$, $C_{ar} CO(t)$ are the concentration of O_2 and CO in the arterial blood. $O_2 Flux_{b_1}(t)$ and $CO Flux_{b_1}(t)$ are the O_2 and CO fluxes from blood compartment 1 to brain tissue subcompartment 1.

Brain Blood compartment 2, (bb_2):

$$V_{bb_2} \frac{dC_{bb_2} O_2(t)}{dt} = \dot{Q}_b(t) \cdot (C_{bb_1} O_2(t) - C_{bb_2} O_2(t)) - O_2 Flux_{b_2}(t) \dots\dots\dots(3.7)$$

$$V_{bb2} \frac{dC_{bv2}CO(t)}{dt} = \dot{Q}_b(t) \cdot (C_{bv1}CO(t) - C_{bv2}CO(t)) - COFlux_{b2}(t) \dots \dots \dots (3.8)$$

$C_{bv2}O_2(t)$ and $C_{bv2}CO(t)$ are the blood concentrations of O_2 and CO in brain vascular subcompartment 2, bb_2 of volume V_{bb2} . $O_2Flux_{b2}(t)$ and $COFlux_{b2}(t)$ are the O_2 and CO fluxes from blood compartment 2 to brain tissue subcompartment 2.

Brain Blood compartment 3, (bb_3):

$$V_{bb3} \frac{dC_{bv3}O_2(t)}{dt} = \dot{Q}_b(t) \cdot (C_{bv2}O_2(t) - C_{bv3}O_2(t)) - O_2Flux_{b3}(t) \dots \dots \dots (3.9)$$

$$V_{bb3} \frac{dC_{bv3}CO(t)}{dt} = \dot{Q}_b(t) \cdot (C_{bv2}CO(t) - C_{bv3}CO(t)) - COFlux_{b3}(t) \dots \dots \dots (3.10)$$

$C_{bv3}O_2(t)$ and $C_{bv3}CO(t)$ are the blood concentrations of O_2 and CO in brain vascular subcompartment 3, bb_3 of volume 3 to brain tissue subcompartment 1. $O_2Flux_{b3}(t)$ and $COFlux_{b3}(t)$ are the O_2 and CO fluxes from blood compartment 1 to brain tissue subcompartment 1.

Auxiliary equations for brain tissue (b_1, b_2) and blood (bb_1, bb_2, bb_3) subcompartments:

$$V_{b1} = Fv_b \cdot V_{bt}$$

$$V_{b2} = (1 - Fv_b) \cdot V_{bt}$$

V_{b1} , V_{b2} are the tissue volumes of brain tissue subcompartment 1 and 2, respectively. V_{b1} is the product of brain tissue volume distribution fraction, Fv_b and total brain tissue volume, V_{bt}

$$V_{bb} = volfrac_b \cdot V_{bt}$$

V_{bb} is the total blood volume in the vascular compartments of brain tissue. It is the product of the fraction of volume of brain tissue compartment attributed to blood, $volfrac_b$ and V_{bt}

$$V_{bb1} = F_{vb} \cdot V_{bb}$$

$$V_{bb2} = (1 - F_{vb}) \cdot V_{bb}$$

$$V_{bb3} = D_{bvb_on} \cdot V_{bb1}$$

V_{bb1} , V_{bb2} , V_{bb3} are the blood volumes of arterial, capillary and venous subcompartments of brain tissue.

$$MR_b O_2 = 1.21 \cdot MR_b O_{2/gram} \cdot V_{bt}$$

$$MR_{b1} O_2(t) = \begin{cases} (MR_b O_2) \cdot \left(\frac{V_{b1}}{V_{b1} + V_{b2}} \right) & \text{if } P_{b1} O_2(t) \geq 26 \\ (MR_b O_2) \cdot \left(\frac{V_{b1}}{V_{b1} + V_{b2}} \right) \cdot \left(\frac{P_{b1} O_2(t)}{K_b O_2 + P_{b1} O_2(t)} \right) & \text{if } P_{b1} O_2(t) < 26 \end{cases}$$

$$MR_{b2} O_2(t) = \begin{cases} (MR_b O_2) \cdot \left(\frac{V_{b2}}{V_{b1} + V_{b2}} \right) & \text{if } P_{b2} O_2(t) \geq 26 \\ (MR_b O_2) \cdot \left(\frac{V_{b2}}{V_{b1} + V_{b2}} \right) \cdot \left(\frac{P_{b2} O_2(t)}{K_b O_2 + P_{b2} O_2(t)} \right) & \text{if } P_{b2} O_2(t) < 26 \end{cases}$$

$MR_b O_2$, $MR_{b1} O_2(t)$, $MR_{b2} O_2(t)$ are the metabolic oxygen consumptions of an average brain tissue, brain tissue subcompartment 1, and brain tissue subcompartment 2, respectively. MRO_2 of the tissue compartment decreases as a function of tissue PO_2 , after a tissue PO_2 of 26 Torr.

$$Flux_{b1} O_2(t) = O_2 Flux_{b1}(t) + O_2 Flux_{b3}(t)$$

$$Flux_{b2} O_2(t) = O_2 Flux_{b2}(t)$$

$$O_2 Flux_{b1}(t) = Db_{b1} O_2(t) \cdot (P_{ab} O_2(t) - P_{b1} O_2(t))$$

$$Db_{b1} O_2(t) = \frac{PS_{b1} O_2(t) \cdot S_{O_2} \cdot V_{b1}}{1.04}$$

$$P_{ab} O_2(t) \text{ , (Erupaka et al, 2010; Appendix A, See Section 2.7, special functions}$$

(F.5))

$$PS_{b1} O_2(t) = PS_{bav_rest} \cdot \frac{\dot{Q}_b(t)}{\dot{Q}_{b0}}$$

$$\dot{Q}_{b0} = \dot{Q}_{b/gram} \cdot V_{bt}$$

$$O_2 Flux_{b2}(t) = Db_{b2} O_2(t) \cdot (P_{bb} O_2(t) - P_{b2} O_2(t))$$

$$Db_{b2} O_2(t) = \frac{PS_{b2} O_2(t) \cdot S_{O_2} \cdot V_{b2}}{1.04}$$

$$PS_{b_2}O_2(t) = PS_{bcap_rest} \cdot \frac{\dot{Q}_b(t)}{\dot{Q}_{b0}}$$

$P_{ab}O_2(t)$, $P_{bb}O_2(t)$ (Erupaka et al., 2010; Appendix A, See Section 2.7, *special functions* (F.5))

$$Flux_{b_1}CO(t) = COFlux_{b_1}(t) + COFlux_{b_3}(t)$$

$$Flux_{b_2}CO(t) = COFlux_{b_2}(t)$$

$$COFlux_{b_1}(t) = Db_{b_1}CO(t) \cdot (P_{ab}CO(t) - P_{b_1}CO(t))$$

$$P_{ab}CO(t) = 0.5(P_{ar}CO(t) + P_{bv_1}CO(t))$$

$$COFlux_{b_2}(t) = Db_{b_2}CO(t) \cdot (P_{bb}CO(t) - P_{b_2}CO(t))$$

$$P_{bb}CO(t) = 0.5(P_{bv_1}CO(t) + P_{bv_2}CO(t))$$

$$COFlux_{b_3}(t) = Db_{b_3}CO(t) \cdot (P_{cb}CO(t) - P_{b_1}CO(t))$$

$$P_{cb}CO(t) = 0.5(P_{bv_2}CO(t) + P_{bv_3}CO(t))$$

$$Db_{b_1}CO(t) = D_B CO \cdot \left(\frac{Db_{b_1}O_2(t)}{Db_{b_2}O_2(t)} \right)$$

$$D_B CO(t) = D_M CO \cdot \left(\frac{Db_{b_2}O_2(t)}{Db_{m_2}O_2(t)} \right)$$

$$Db_{b_2}O_2(t) = \frac{PS_{b_2}O_2(t) \cdot S_{O_2} \cdot V_{b_2}}{1.04}$$

$$PS_{b_2}O_2(t) = PS_{bcap_rest} \cdot \frac{\dot{Q}_b(t)}{\dot{Q}_{b0}}$$

$$Db_{b_2}CO(t) = D_B CO$$

$$Db_{b_3}O_2(t) = Db_{b_1}O_2(t) \cdot D_{bvb_on}$$

$$D_{bb_3}CO(t) = D_B CO \cdot \left(\frac{Db_{b_3}O_2(t)}{Db_{b_2}O_2(t)} \right)$$

$$C_{b_1}^d O_2(t) = C_{b_1} O_2(t)$$

$$C_{b_1}^d CO(t) = C_{b_1} CO(t)$$

$$C_{b_1} O_2(t) = S_{O_2} \cdot P_{b_1} O_2(t)$$

$$C_{b1}CO(t) = S_{CO} \cdot P_{b1}CO(t)$$

All other equations are similar to those of skeletal and cardiac tissue compartments (Appendix A of Erupaka et al., 2010), except that there is no O_2 or CO bound to myoglobin in brain tissue compartments. See Table 3.1 and Appendix A of Erupaka et al. (2010) for definitions of all other parameters and variables.

Addition of mass balance equations for CO_2 : Mass balance equations for CO_2 in all compartments were added to model transport and production of CO_2 from and within various blood vessels, lungs and various tissues. This modification was added to allow control of ventilation and regulation of blood flow with changes in CO_2 levels. Addition of this feature to the model will also allow evaluation of the role of CO_2 in managing a treatment after CO poisoning occurs. The mass balance equations for CO_2 are similar to that of O_2 (Appendix A of Erupaka et al., 2010), except that CO_2 is produced as a metabolite on O_2 utilization. In the blood compartments Hb binds to CO_2 to form carbaminohemoglobin ($HbCO_2$). Thus the total CO_2 in any vascular compartment is expressed as dissolved CO_2 , in the form of bicarbonate and as bound to Hb while the total CO_2 in any tissue compartment is expressed as dissolved CO_2 and in the form of bicarbonate (HCO_3^-) (Stuhmiller and Stuhmiller, 2005; Ursino et al., 2001; Wolf and Garner, 2007; Zhou et al., 2007).

Mass balance equations for CO_2 in Lung (Alveolar (L)) compartment :

$$V_L \frac{dC_A CO_2(t)}{dt} = (P_i CO_2(t) - P_A CO_2(t)) \times \frac{\dot{V}_A(t)}{P_B} - CO_2 flux_{LB}(t) \dots \dots \dots 3.11$$

$$CO_2 flux_{LB}(t) = \dot{Q}(t) \cdot (1 - SF) \cdot (C_{ep} CO_2(t) - C_{mx} CO_2(t - d_v))$$

V_L is the lung volume, \dot{V}_A is the alveolar ventilation, \dot{Q} is the cardiac output, SF is the pulmonary shunt fraction (SF=0 for HBO₂ conditions), $C_i CO_2$ is the concentration in compartment 'i' and $P_i CO_2$ is the partial pressure of CO_2 in compartment 'i'. Like the mass balance equations of oxygen (Appendix A of Erupaka et al., 2010), I assume that the end pulmonary PCO_2 ($P_{EP}CO_2$) is equal to the alveolar PCO_2 ($P_A CO_2$).

Mass balance of CO_2 in any vascular compartment 'i':

$$V_{b_i} \frac{dC_i CO_2(t)}{dt} = \dot{Q}_i(t) \cdot (C_{i_{in}} CO_2(t) - C_{i_{out}} CO_2(t)) - CO_2 Flux_i(t) \dots \dots \dots 3.12$$

$$C_i CO_2(t) = {}^{dissolved} C_i CO_2(t) + {}^{HCO_3^-} C_i CO_2(t) + {}^{HbCO_2} C_i CO_2(t)$$

$${}^{dissolved} C_i CO_2(t) = S_b CO_2 \cdot P_i CO_2$$

$${}^{HCO_3^-} C_i CO_2(t) = S_b CO_2 \cdot P_i CO_2 \cdot 10^{(pH_i - 6.1)}$$

$${}^{HbCO_2} C_i CO_2(t) = 0.2413 C_{Hb} + (0.31 C_{Hb} \cdot (1 - S_i O_2))$$

$CO_2 Flux_i(t) = 0$ for arterial and mixed venous blood compartments

V_{b_i} is the blood volume of compartment 'i', $S_b CO_2$ is solubility of CO_2 in blood, $S_i O_2$ is the O_2 saturation of blood compartment 'i' ($0 \leq S_i O_2 \leq 1$), pH_i is the pH in the blood compartment 'i' and C_{Hb} is the concentration of Hb. Calculation of ${}^{HbCO_2} C_i CO_2(t)$ indirectly depends on $P_i CO_2$, as $S_i O_2$ is calculated at every time step (0.001 min) taking into account the effects of $P_i CO_2$, pH_i and %HbCO_i (Bohr effect on the oxygen dissociation curve).

Mass balance of CO_2 in any tissue of two subcompartments (i1, i2):

$$\frac{dC_{i1} CO_2(t)}{dt} = \frac{Flux_{i1} CO_2(t)}{V_{i1}} + \frac{D'_i CO_2 \cdot (C_{i2}^d CO_2(t) - C_{i1}^d CO_2(t))}{D_{xi}} + \frac{MR_{i1} CO_2(t)}{V_{i1}} \dots \dots \dots 3.13$$

$$C_{i1} CO_2(t) = {}^{dissolved} C_{i1} CO_2(t) + {}^{HCO_3^-} C_{i1} CO_2(t)$$

$${}^{dissolved} C_{i1} CO_2(t) = S_i CO_2 \cdot P_{i1} CO_2$$

$${}^{HCO_3^-} C_{i1} CO_2(t) = S_i CO_2 \cdot P_{i1} CO_2 \cdot 10^{(pH_{i1} - 6.1)}$$

The mass balance equation for CO_2 is given for the first tissue subcompartment. V_{i1} is the volume of tissue compartment 'i1', $D'_i CO_2$ is the intertissue diffusion coefficient of CO_2 , D_{xi} is the intercapillary distance in the tissue compartment, $S_i CO_2$ is the solubility of CO_2 in tissue, $MR_{i1} CO_2$ is the rate of CO_2 production in tissue subcompartment i₁, and pH_{i1} is pH in the tissue compartment 'i'.

Auxiliary equations for CO_2 mass balance equations:

$$Flux_{b1} CO_2(t) = CO_2 Flux_{b1}(t) + CO_2 Flux_{b3}(t)$$

$$Flux_{b2} CO_2(t) = CO_2 Flux_{b2}(t)$$

$$CO_2Flux_{b1}(t) = Db_{b1}CO_2(t) \cdot (P_{ab}CO_2(t) - P_{b1}CO_2(t))$$

$$P_{ab}CO_2(t) = 0.5(P_{ar}CO_2(t) + P_{bv1}CO_2(t))$$

$$CO_2Flux_{b2}(t) = Db_{b2}CO_2(t) \cdot (P_{bb}CO_2(t) - P_{b2}CO_2(t))$$

$$P_{bb}CO_2(t) = 0.5(P_{bv1}CO_2(t) + P_{bv2}CO_2(t))$$

$$CO_2Flux_{b3}(t) = Db_{b3}CO_2(t) \cdot (P_{cb}CO_2(t) - P_{b3}CO_2(t))$$

$$P_{cb}CO_2(t) = 0.5(P_{bv2}CO_2(t) + P_{bv3}CO_2(t))$$

$$MR_iCO_2(t) = MR_iO_2(t) \cdot RQ_i$$

$$D_iCO_2(t) = 18 \cdot D_iO_2(t)$$

$$MR_{ot}CO_2(t) = MR_{CO_2}(t) - (MR_BCO_2(t) + MR_{CM}CO_2(t) + MR_MCO_2(t))$$

$MR_{ot}CO_2(t)$, $MR_{CO_2}(t)$, $MR_BCO_2(t)$, $MR_{CM}CO_2(t)$ and $MR_MCO_2(t)$ are the rates of CO_2 production in the non-muscle tissue, whole body, brain tissue, cardiac muscle and skeletal muscle, respectively. Values for RQ_i and fac are given in table 3.1. The diffusion coefficient for CO_2 ($D_iCO_2(t)$) is reported to be at least 18 times greater than that of O_2 ($D_iO_2(t)$) in the normoxic and normocapnic conditions (Zhou et al., 2007). In my model this relation of a constant ratio between $D_iCO_2(t)$ and $D_iO_2(t)$ is assumed to be valid for all conditions like hyperoxia, hypoxia, hypercapnia, CO hypoxia, hypocapnia etc.

After implementing the mass balance equations for CO_2 , tissue and blood PCO_2 from various compartments were validated for situations of normoxic normocapnia, hypercapnia, hyperoxia, and hyperbaric oxygen (See section “*Model Validation*”).

Addition of control of ventilation: The uptake and removal of CO is dependent on the ventilation of the subject. For the same duration and concentration of CO exposure, a subject with higher ventilation will inhale more CO and will have higher %HbCO levels at the end of exposure, when compared to a subject with lower ventilation. In CO exposure studies of humans (Chiodi et al., 1941) and animals (Doblar et al., 1977; Santiago and Edelman, 1976), it has been observed that the ventilation does not change

significantly from the control values at least up to a %HbCO of 55. But during treatment with normobaric oxygen (NBO₂), isocapnic NBO₂ or hyperbaric oxygen (HBO₂), the ventilation would be significantly different from the control values (Becker et al., 1996; Fisher et al., 1999; Lambertsen et al., 1952, 1953; Nishimura et al., 2007). Inhalation of O₂ results in a decreased brain blood flow due to cerebral vasoconstriction. Decreased brain blood flow causes an increase in brain tissue PCO₂. Increases in brain tissue PCO₂ are sensed by the central chemoreceptors and the respiratory centers in the brain send signals to cause an increase in ventilation. Higher ventilation during treatment (NBO₂, isocapnic NBO₂, or HBO₂) for a CO poisoned patient would mean that more CO will be exhaled, thereby resulting in faster removal of CO from the body. Thus to appropriately estimate uptake and removal of CO during an exposure and treatment, it is essential to implement control of ventilation in my model.

Many mathematical models (Duffin et al., 2000; Longobardo et al., 2002; Stuhmiller and Stuhmiller, 2005; Ursino et al., 2001; Topor et al., 2004; Wolf and Garner, 2007; Zhou et al., 2007) have implemented control of ventilation as the sum of peripheral (\dot{V}_{PERI}) and central ventilation (\dot{V}_{CENT}). But the gains or threshold used in their equations were specific to situations like hypoxic hypoxia, sleep stages or hyperoxia. Also most of these models estimated minute ventilation (Duffin et al., 2000; Longobardo et al., 2002; Stuhmiller and Stuhmiller, 2005; Ursino et al., 2001; Topor et al., 2004; Wolf and Garner, 2007). In my model, I need to estimate alveolar ventilation (\dot{V}_A) during normoxia, CO hypoxia, NBO₂, isocapnic NBO₂, and HBO₂. Thus to implement ventilation control in my model, I used the concepts of Garner and Wolf (2007) and implemented alveolar ventilation as the sum of peripheral and central component (Eqs. 3.14-3.16). Tidal volume, dead space and minute ventilation were estimated from regression equations based on alveolar ventilation (Bruce et al., 2011, under review). Minute ventilation was calculated in the model to allow comparison of model estimates of ventilation with the experimental data. The parameters in the equations for control of ventilation (Wolf and Garner, 2007) were first adjusted to match normoxic values of ventilation. Later the values of the parameters were fine tuned to match hypoxic, hypercapnic and hyperoxic (NBO₂, isocapnic NBO₂, and HBO₂) data. The details of the

experiments used to determine the gains and threshold of the ventilation control equations (Eqs. 3.14-3.16) are described in the “*model validation*” section of this chapter. The equations for the control of ventilation are:

$$\dot{V}_A(t) = \dot{V}_{CENT}(t) + \dot{V}_{PERI}(t) \dots \dots \dots 3.14$$

$$V_{CENT}(t) = 2.07 \cdot (P_{bt} CO_2(t) - 46) \dots \dots \dots 3.15$$

$$V_{PERI}(t) = 0.72 \cdot (P_{cb} CO_2(t) - 37.8) + \left(\frac{360}{P_{cb} O_2(t) - 26.2} - 5.04 \right) \cdot F_{CO_2}(t) \dots 3.16$$

$$P_{bt} CO_2(t) = P_{b2} CO_2(t + D_c) ; D_c = \frac{k_c}{\dot{Q}(t)}$$

$$F_{CO_2}(t) = \begin{cases} \left(5 - 4 \left(\frac{P_{cb} CO_2(t)}{40} \right)^4 \right)^{-1} & \text{for } \left(\frac{P_{cb} CO_2(t)}{40} \right) \leq 1 \\ \left(\frac{P_{cb} CO_2(t)}{40} \right)^3 & \text{for } \left(\frac{P_{cb} CO_2(t)}{40} \right) > 1 \end{cases}$$

$$P_{cb} CO_2(t) = P_{ar} CO_2(t + D_p) ; D_p = \frac{k_p}{\dot{Q}(t)}$$

where,

$P_{b2} CO_2(t)$ is the PCO_2 of the brain tissue in subcompartment 2 and $P_{ar} CO_2(t)$ is the arterial PCO_2 . D_p and D_c are the peripheral and central time delays. See Table 3.1 for values of k_c and k_p . $\dot{Q}(t)$ is the cardiac output.

Addition of regulation of blood flow: Cardiac output (\dot{Q}) and blood flow to various tissues is regulated constantly with changes in arterial PO_2 , PCO_2 and %HbCO levels (low or high O_2 and CO_2 , high CO). Cardiac output and blood flow to other vital organs like brain and heart is reported to increase with increasing %HbCO levels (Benignus et al., 1992; Chiodi et al., 1941; Dobljar et al., 1977; Einzig et al., 1980; Kleinert et al., 1980; Koehler et al., 1984; Langston et al., 1996; Paulson et al., 1973; Rucker et al., 2002; Santiago et al., 1986; Zhu and Weiss, 1995). In NBO_2 or HBO_2 conditions and hypocapnia, cardiac output and brain blood flow is reported to decrease due to peripheral vasoconstriction (Floyd et al., 2003; Lambertsen et al., 1953; Ohta, 1986; Topor et al., 2004; Zhou et al., 2007; Weaver et al., 2009). During hypoxic hypoxia and hypercapnia, cardiac output and brain blood flow (\dot{Q}_B) is reported to increase due to peripheral

vasodilatation (Topor et al., 2004; Wolf and Garner, 2007; Zhou et al., 2007). Thus to model dynamics of O_2 , CO_2 and CO during exposure and various treatments, regulation of blood flow should be implemented.

Regression equations were developed to predict changes in cardiac output (Figure 3.2) and brain blood flow (Figure 3.3) with increases in %HbCO levels (Benignus et al., 1992; Chiodi et al., 1941; Doblar et al., 1977; Koehler et al., 1984; Langston et al., 1996; Paulson et al., 1973; Rucker et al., 2002; Santiago et al., 1986). Piecewise linear regression fits were made to predict percent changes in cardiac output (Figure 3.2d) and brain blood flow (Figure 3.3) as a function of %HbCO. The previous model (Erupaka et al., 2010) was developed to simulate CO exposures <30% HbCO levels. But, the current model being developed is intended to simulate CO exposures greater than 30% HbCO levels. The previous regression equation developed in my model (Equation C5 of Appendix C, Erupaka et al., 2010) underestimated the changes in cardiac output with increases in %HbCO levels >30. Chiodi et al. (1941) reported that the changes in cardiac output are statistically different for %HbCO levels >30. To predict appropriate percent changes in \dot{Q} for %HbCO levels greater than 26%, a regression equation was developed (Figure 3.2) using the data from Chiodi et al. (1941). The regression statistics for this equation are $R^2=0.901$ and the error in the estimate, $\check{E}=7.94$. To predict changes in cardiac output for %HbCO levels less than or equal to 26%, an equation of the form $y=mx+c$ was calculated for a line formed from two data points. The first data point (1%,0.572%) for this line was from the old regression equation (Equation C5 of Appendix C, Erupaka et al., 2010) at 1% HbCO and the second data point (26%,1.772) was from the new regression relation at 26% HbCO. The value of 26% HbCO level was chosen to avoid discontinuity in the regression relation developed. To predict percent changes in \dot{Q}_b with changes in %HbCO, data from animals (Doblar et al., 1977; Koehler et al., 1984; Langston et al., 1996; Santiago et al., 1986) and humans (Benignus et al., 1992; Paulson et al., 1973; Rucker et al., 2002) were used (Figure 3.3). The regression statistics for this equation for % HbCO levels ≤ 23 are $R^2=0.951$, $\check{E}=3.37$ and for %HbCO levels >23 are $R^2=0.898$, $\check{E}=9.622$. The value of 23% HbCO level was chosen to avoid discontinuity in the regression relation developed to predict brain blood flow.

Equations for regulation of \dot{Q} and \dot{Q}_B during hypoxia, hypercapnia and hypocapnia were used from the model of Zhou et al. (2007). For conditions of NBO₂, isocapnic NBO₂ and HBO₂, \dot{Q} was estimated using a regression equation as function of P_{ar}O₂ and P_{ar}CO₂. The regression equation was developed in this study using the data from healthy human subjects (McMohan et al., 2002; Weaver et al., 2009; Whalen et al., 1965) who were exposed to NBO₂, isocapnic NBO₂ or HBO₂ and \dot{Q} was measured. The regression statistics for the equation developed are R²=0.849, \check{E} =0.314. \dot{Q}_B for conditions of high O₂ (NBO₂, isocapnic NBO₂ or HBO₂), was estimated from the relationship developed by Floyd et al. (2003). The coefficients of the regression relation developed by Floyd et al. (2003) were fine tuned to match the model predicted ventilation to that of the experiments of Becker et al. (1996) and Lambertsen et al. (1952, 1953).

Regulation of Cardiac Output (\dot{Q})

$$\tau_q \frac{d\dot{Q}(t)}{dt} + \dot{Q}(t) = \dot{Q}_0 + \Delta\dot{Q}_{O_2}(t) + \Delta\dot{Q}_{CO_2}(t) + 0.01(\dot{Q}_0 \cdot \dot{Q}_{HbCO}(t)) \dots \dots \dots 3.17$$

$$\Delta\dot{Q}_{O_2}(t) = \left\{ \begin{array}{ll} 0.09(97.4 - S_{ar}O_2(t)) & \text{if } \%S_{ar}O_2(t) \leq 99 \\ -0.001 \cdot (P_{ar}O_2(t) - P_{ar0}O_2(t)) & \text{if } \%S_{ar}O_2(t) > 99 \text{ or } P_B > 760 \end{array} \right\}$$

$$\Delta\dot{Q}_{CO_2}(t) = \left\{ \begin{array}{ll} 0.033(P_{ar}CO_2(t) - 40) & \text{if } \%S_{ar}O_2(t) \leq 99 \\ -0.143 \cdot (P_{ar}CO_2(t) - P_{ar0}CO_2(t)) & \text{if } \%S_{ar}O_2(t) > 99 \text{ or } P_B > 760 \end{array} \right\}$$

$$\dot{Q}_{HbCO}(t) = \left\{ \begin{array}{ll} 0.048(\%HbCO(t)) + 0.52 & \text{if } \%HbCO(t) \leq 26 \\ 1.772(\%HbCO(t) - 25) & \text{if } \%HbCO(t) > 26 \end{array} \right\}$$

\dot{Q}_0 is the resting cardiac output, S_{ar}O₂(t) is the arterial O₂ saturation and P_{ar}CO₂(t) is the arterial PCO₂. P_{ar}O₂(t) is the arterial PO₂ and P_B is the barometric pressure. τ_q is the first order time constant. P_{ar0}O₂(t), P_{ar0}CO₂(t) are the arterial PO₂ and PCO₂ at the control conditions. The maximal decrease in $\dot{Q}(t)$ from \dot{Q}_0 during high oxygen conditions is limited to 15% (Weaver et al., 2009).

Regulation of Brain Blood Flow (\dot{Q}_B)

$$\tau_b \frac{d\dot{Q}_B(t)}{dt} + \dot{Q}_B(t) = \Delta\dot{Q}_{B_{O_2}, B_{CO_2}}(t) + 0.01(\dot{Q}_{B_0} \cdot \dot{Q}_{B_{HbCO}}(t)) \dots \dots \dots 3.18$$

$$\Delta\dot{Q}_{B_{O_2}, B_{CO_2}}(t) = \left\{ \begin{array}{l} \text{if } \%S_{ar}O_2(t) \leq 99 \\ \dot{Q}_{B_0} + 7.7 \times 10^{-3} (97.4 - S_{ar}O_2(t)) + 0.2 \times \exp(0.033 \times P_{ar}CO_2) - 0.75 \\ \text{if } \%S_{ar}O_2(t) > 99 \text{ or } P_B > 760 \\ 73 \cdot \frac{\dot{Q}_{B_0}}{V_{bt}} - 0.0153 \cdot (P_{ar}O_2(t) - P_{ar0}O_2(t)) + 0.67 \cdot (P_{ar}CO_2(t) - P_{ar0}CO_2(t)) + 11 \end{array} \right\}$$

$$\dot{Q}_{B_{HbCO}}(t) = \left\{ \begin{array}{ll} 0.718(\%HbCO(t)) + 0.52 \cdot ff & \text{if } \%HbCO(t) \leq 23 \\ 1.487(\%HbCO(t) - 17.285) \cdot ff & \text{if } \%HbCO(t) > 23 \end{array} \right\}$$

\dot{Q}_{B_0} is the resting brain blood flow and ff is the adjustment factor introduced, so that the ventilation does not change from its control state (normoxic, normocapnia) during CO exposure (See section “model limitations”). τ_b is the first order time constant. V_{bt} is the brain tissue volume. The maximal decrease in $\dot{Q}_B(t)$ from \dot{Q}_{B_0} during high oxygen conditions is limited to 30% (Ohta, 1986).

Regulation of cardiac muscle (\dot{Q}_{CM})

$$\dot{Q}_{CM}(t) = \dot{Q}_{CM_0} \cdot \frac{\dot{Q}(t)}{\dot{Q}_0} \dots \dots \dots 3.19$$

Regulation of skeletal muscle (\dot{Q}_{SM})

$$\dot{Q}_{SM}(t) = \dot{Q}_{SM_0} \cdot \frac{\dot{Q}(t)}{\dot{Q}_0} \dots \dots \dots 3.20$$

Regulation of nonmuscle tissue blood flow (\dot{Q}_{OT})

$$\dot{Q}_{OT}(t) = \dot{Q}(t) - (\dot{Q}_B(t) + \dot{Q}_{CM}(t) + \dot{Q}_{SM}(t)) \dots \dots \dots 3.21$$

Addition of Bohr and Haldane effects: In the presence of CO, the oxygen dissociation curve shifts to the left resulting in an increased affinity of Hb for O₂. The leftward shift causes the sigmoidal curve to become more hyperbolic and impairs unloading of oxygen to the tissues. P₅₀ is the vascular PO₂ at which hemoglobin is 50% saturated. The value of P₅₀ decreases with increases in %HbCO levels in the blood (Bruce and Bruce, 2003). The

previous model (Erupaka et al., 2010) accounted for changes in P_{50} due to increase in %HbCO levels. In the new model, after implementing mass balance of CO_2 , it was necessary to include Bohr effects (PCO_2 , pH , %HbCO levels, and temperature) on the oxygen dissociation curve and Haldane effects (O_2Hb) on CO_2 dissociation curve (Collier, 1976; Lobdell, 1981; Sharan et al., 1989; Stuhmiller and Stuhmiller, 2005). The concepts from Sharan et al. (1989) were used to implement Bohr effects on oxygen dissociation curve (ODC). Algorithms were developed to calculate O_2 saturation, P_{50} and PO_2 in a vascular compartment taking into account the effects of PCO_2 , pH , %HbCO levels, and temperature on ODC (Collier, 1976; Lobdell, 1981; Sharan et al., 1989). In the algorithm the dependence of ODC on %HbCO is implemented by calculating the P_{50} , according to the theory of Collier (1976). To calculate the oxygen saturation (SO_2) or PO_2 in any blood compartment, an invertible Adair type equation with high accuracy is used (Equation 1 of Lobdell, 1981). Later the absolute SO_2 is calculated from %HbCO levels and maximal oxyhemoglobin (HbO_2). Haldane effects (O_2Hb) on CO_2 dissociation curve were implemented using the relationship published by Stuhmiller and Stuhmiller (Equation A43, 2005). The algorithms implementing Bohr and Haldane effects were validated for various conditions of normoxia, CO hypoxia, hyperoxia, hypercapnia and hypocapnia (See section “*model validation*”).

Other modifications: The metabolic rate of O_2 consumption in cardiac muscle and skeletal muscle tissue was constant if the tissue PO_2 was greater than 20 Torr and decreased (Equation 3.22) with decreasing tissue PO_2 's for values less than 20 Torr.

$$MR_{i_1}O_2(t) = \left\{ \begin{array}{ll} (MR_{i_1}O_2) \cdot \left(\frac{V_{i_1}}{V_{i_1} + V_{i_2}} \right) & \text{if } P_{i_1}O_2(t) \geq 26 \\ (MR_{i_1}O_2) \cdot \left(\frac{V_{i_1}}{V_{i_1} + V_{i_2}} \right) \cdot \left(\frac{P_{i_1}O_2(t)}{K_{i_1}O_2 + P_{i_1}O_2(t)} \right) & \text{if } P_{i_1}O_2(t) < 26 \end{array} \right\} \dots\dots\dots 3.22$$

where i_1 , i_2 represent tissue subcompartment 1 and 2 of cardiac or skeletal muscle tissues. $MR_{i_1}O_2$ is the metabolic rate of O_2 in tissue ‘t’. $P_{i_1}O_2$ is the PO_2 in compartment ‘ i_1 ’. V_{i_1} and V_{i_2} are the tissue volumes of subcompartment i_1 and i_2 . For $K_{i_1}O_2$ see Table A4 of Appendix A of Erupaka et al. (2010).

The muscle diffusion coefficient of CO (D_{MCO}) was varied in proportion to muscle mass, with a value of D_{MCO} of 0.225 ml/min/Torr/Kg of muscle mass. Lung diffusivity of CO (D_{LCO}) varied (Equation 3.23) as a function of alveolar PO_2 (P_{AO_2}) and at a P_{AO_2} of 500 Torr, D_{LCO} was half of its value at room air ($D_{LCO_{Air}}$).

$$D_{LCO} = \frac{1}{1 + \frac{P_{AO_2}}{500}} \cdot D_{LCO_{Air}} \dots \dots \dots 3.23$$

Hypoxic ventilatory depression (HVD) is a biphasic response produced during hypoxic exposure, where an initial rapid increase in ventilation is not sustained and is followed by a decline during the first 30 mins of hypoxic exposure. HVD was implemented in the model using the concepts of Ursino et al. (2001) and Zhou et al. (2007). The version of the model in which HVD was implemented, was validated for transient and steady state conditions of hypoxia (Bascom et al., 1992). After implementing and validating the mechanism of HVD, the model was used to simulate a short duration CO exposure resulting in ~20% HbCO. At the end of CO exposure the predicted change in ventilation from the normoxic condition did not agree with the experimentally measured changes in ventilation (Chiodi et al., 1941; Kizakevich et al., 2000). As this version of the model was unable to predict appropriate changes in ventilation during CO hypoxia, the mechanism of HVD was not implemented (See discussion).

RESULTS

Model validation

After implementing the above described modifications, the capability of the model to predict brain tissue and venous PO_2 's, ventilaton, tissue and blood PCO_2 's, tissue and blood pH in various compartments was assessed and compared with experimental data. The modified model was validated for various conditions. The conditions simulated were normoxia, hypercapnia, hypocapnia, hypoxic hypoxia, CO hypoxia, hyperoxia, isocapnic hyperoxia and hyperbaric oxygen. For various simulated experimental conditions, the model predicted values of various parameters (brain tissue

and venous PO_2 , ventilation, blood PCO_2 , etc) were validated against the experimentally measured values. Most of the data for validation of brain tissue PO_2 's were obtained from studies on anesthetized animals (Table 3.2), but data for validation of ventilation, blood PCO_2 , blood pH and brain venous PO_2 's were obtained from studies involving human subjects (References in the text below and Table 3.2). Developing a validated mathematical model to estimate O_2 , CO and CO_2 levels in brain, heart and skeletal muscle tissue during CO exposures and treatments, will allow me to compare O_2 delivery, CO removal and CO_2 levels during different treatments after a CO exposure.

Validation of brain tissue and blood PO_2 : Table 3.2 shows the compiled experimental data for brain tissue and venous PO_2 's from different species and conditions of measurement. Inspired levels of O_2 ($F_{I}O_2$) and barometric pressure (P_B) in the simulations were set equal to the reported experimental values or were adjusted to achieve the measured arterial PO_2 (when arterial PO_2 was reported in the study). Arterial PO_2 's for the experiments simulated ranged from 21 Torr to 2100 Torr. Alveolar ventilation, brain blood flow, brain oxygen consumption and brain CO_2 production were estimated by the model for a human subject. For all the simulations, other brain compartment related parameters (volume distribution fraction, permeability surface area product, etc) are listed in Table 3.1. The PO_2 of the third vascular subcompartment of the brain compartment, bb_3 , (Figure 3.1), was compared to sagittal sinus PO_2 reported in the experimental data. The brain tissue O_2 tensions in the experiments were mostly reported as mean values with standard deviations. I considered the reported mean PO_2 plus one standard deviation as the O_2 tension of brain tissue subcompartment 1, b_1 and the reported mean PO_2 minus one standard deviation as the O_2 tension of brain tissue subcompartment 2, b_2 . During conditions of high arterial PO_2 , the tissue PO_2 in b_2 increased but did not increase in proportion to the arterial PO_2 . This result is in agreement with the experimental studies, where an increase in tissue PO_2 was not seen in the majority of tissue during hyperoxia (Eintrei and Lund, 1986; Lumb and Nair, 2010). Thus for hyperoxic and hyperbaric conditions, O_2 tension of b_1 was compared to the reported mean PO_2 of the experiments. Figure 3.4(a-b) shows the comparison of model predictions (brain tissue and sagittal venous PO_2 's) with experimentally measured values. Predicted PO_2 's from the model

were tested for conditions of normoxia, hypoxia, hyperoxia, hyperbaric oxygen, CO hypoxia, hypocapnia, and hypercapnia. In Fig. 3.4 (a-b), the model-predicted PO_2 's for brain tissue and venous compartments fit variations in the experimentally measured PO_2 's for a variety of simulation conditions. Also, the model was used to simulate 40 mins of CO exposure to attain 40% HbCO and the brain tissue PO_2 's after 40 min of CO exposure were compared with an experimental study in rat (Hara et al., 2011). The average brain tissue PO_2 after 40 min of CO exposure at 40% HbCO was in agreement with the experimental result of Hara et al. (2011). Thus, the model predicts physiologically reasonable brain tissue and vascular O_2 tensions over a wide range of arterial PO_2 values.

Validation of tissue and blood PCO_2 : Model predicted brain tissue and blood venous PCO_2 's were tested for conditions of normoxia (Hoffman, 2001; Lambertsen et al., 1952, 1953,1953,1955; Martinez Tica et al., 1999), hypoxia (Martinez Tica et al., 1999), hyperoxia (Lambertsen et al., 1952), hyperbaric oxygen (Lambertsen et al., 1953,1955), hypocapnia (Hoffman, 2001) and hypercapnia (Hoffman, 2001; Lambertsen et al., 1953). Figure 3.4(c-d) shows the comparison of model predictions (brain tissue and sagittal venous PCO_2 's) with experimentally measured values. In hypoxia, the model-predicted brain tissue and blood PCO_2 's are slight underestimates of the experimental data. Also, in the condition of normoxia, the skeletal muscle (M) and cardiac muscle (C) tissue PCO_2 predicted by the model (M:46.9 Torr, C:50.2 Torr) are in agreement with the experimental data (M:45.4 Torr, C:54±5 Torr) reported by Hart et al.(2003) and Hoffman et al. (2001). Model estimated tissue PCO_2 's in the cardiac muscle during hypocapnia and hypercapnia closely matched the trend in the data reported by Hoffman et al. (2001). Figure 3.5 shows that the model predicted arterial and mixed venous PCO_2 's and pH measurements for normoxia, hyperoxia and hyperbaric oxygen are in agreement with the data. Considering the limited availability and variability of experimental data for blood and tissue PCO_2 tensions, the model closely represents the trends in the data.

Validation of PO_2 and PCO_2 for hyperbaric oxygen: Weaver et al. (2009) exposed 10 healthy subjects to air and oxygen at 0.85, 3, 2.5, 2, 1.3 and 1.2 ATA. Cardiac output,

whole body metabolic rate, arterial and venous blood gas, pH measurements, heart rate and many other variables were measured at the end of exposure to each pressure. I used the model to simulate their experiment for an average subject from their data (mean age, weight, height etc). Average values for heart rate, cardiac output and metabolic rate were given as the input to my model at the specified atmospheric pressures. Model predicted arterial PO_2 ($P_{ar}O_2$), PCO_2 ($P_{ar}CO_2$), pH_{ar} and venous PO_2 ($P_{mx}O_2$), PCO_2 ($P_{mx}CO_2$), pH_{mx} were compared to the experimental data at 0.85 ATA air, 0.85 ATA O_2 , 3 ATA O_2 , 2.5 ATA O_2 , 2 ATA O_2 , and 1.2 ATA O_2 , respectively (Figure 3.5). The model predicted gas tensions in the arterial and mixed venous blood compartments were compared with the arterial and venous measurements of the experimental data. It is seen from Figure 3.5 that the model estimates are in agreement with the experimentally measured values. Also, the model-predicted tissue PO_2 in the skeletal muscle compartment at 2 ATA are in agreement with the value reported by Hart et al. (2003)

Overall the model is well validated to predict tissue and blood O_2 and CO_2 tensions in brain, heart and skeletal muscle for a variety of conditions like normoxia, hypoxic hypoxia, CO hypoxia, hyperoxia, hyperbaric oxygen, hypocapnia and hypercapnia.

Validation of ventilation: Model predicted ventilation was validated for various situations like normoxia, hypoxia, isocapnic hyperoxia, poikilocapnic hyperoxia, hypercapnia and hyperbaric oxygen.

Ventilation in hypoxia: The parameters in the peripheral ventilation equation (Equation 3.16) were adjusted to isocapnic hypoxic data from Bascom et al. (1992). In this experiment, ventilatory responses to different levels of end tidal PO_2 during isocapnia in humans were measured. End tidal PO_2 was held at normoxic level (100 Torr) for the first 10 minutes, which was followed by 20 mins hypoxic exposure at 75, 65, 55, 50, or 45 Torr. PCO_2 was held at 1-2 Torr above the resting value. In the simulations, P_ACO_2 was held constant at the resting level of 39.03 Torr. Then I adjusted the inspired oxygen fraction to match the experimental oxygen saturation and PO_2 . Model estimation of

ventilation at different levels of hypoxia is in agreement with the change in ventilation observed in the experiments (Figure 3.6). In situations where I would like to simulate *CO* exposure at altitude, the lowest (maximum) PO_2 may be 75 Torr. So I concentrated on matching model estimation of ventilation to the change at 75 Torr.

Ventilation in hyperoxia: Becker et al. (1996) measured the ventilatory response to different levels of hyperoxia. In their study, ventilation in human subjects was measured after breathing 30%, 50% or 75% O_2 for 30 min, while maintaining isocapnia. The parameters in the central ventilation equation (Equation 3.15) and the brain blood flow equation coefficients were adjusted to match hyperoxic data. PCO_2 was maintained at the resting value of 39.03 Torr. At higher levels of inspired O_2 (50%,75%), the model estimation matches with the experimental data. At 30% inspired oxygen, the model estimation is lower than the experimental data. Becker et al. (1996) did not measure the ventilation at 100% O_2 . The model application will be mainly in 100% O_2 concentration, so I attempted to adjust my model parameters to match data at higher O_2 concentrations (Figure 3.7). The model estimated ventilation change at 100% O_2 is in agreement with other data from Poulin et al. (1993) and Ren et al. (2002).

In addition to isocapnic hyperoxia, the enhanced model was validated for poikilocapnic hyperoxia. Nishimura et al. (2007) exposed human subjects to subsequent stepwise increases from 21% air to 40%, 70% and 100% O_2 . O_2 level at each step was maintained for ~20 min. They measured arterial PCO_2 and ventilation at the end of each level. This experiment was simulated using the enhanced model and model estimated changes in ventilation and arterial PCO_2 at different levels of hyperoxia were compared with the experimental data. The model matches the experimental data at high inspired oxygen concentrations (Figure 3.8). There is a slight mismatch at the lower levels of inspired O_2 concentration. But as the model will be applied only in high O_2 inspired fractions, the parameter values in the ventilation equation were considered to be appropriate.

Ventilation in hyperbaric oxygen: Lambertsen et al. (1952,1953,1955) exposed human subjects to oxygen at 3.5 ATA for ~20 min and measured the ventilatory response and changes in arterial PCO_2 . They reported a 25% increase in ventilation and drop in PCO_2 of ~ 4-5 Torr compared to the control value (normoxia). Using my enhanced model to simulate their experiment resulted in an increase in ventilation of 22% and a drop in arterial PCO_2 ($P_{ar}CO_2$) of 4.29 Torr. Thus, the estimated changes in ventilation and $P_{ar}CO_2$'s predicted by model are in agreement with the experimental data.

Slopes of Ventilation (V_e) and alveolar PCO_2 (P_ACO_2) response curves in normoxia, hypoxia, and hyperoxia: In order to produce the V_e - P_ACO_2 curves at different alveolar PO_2 's ($P_AO_2=100,50,200$ Torr), I maintained the alveolar PO_2 at a constant level and the inspired fraction of CO_2 was increased in every simulation from 0% to 3%,5%,6%, or 7% for 25 min. The slopes and the intercepts for the alveolar PCO_2 (P_ACO_2) and minute ventilation (V_e) curves at each of the maintained P_AO_2 were calculated and compared with the experimental values (Table 3.3). The slopes of the V_e - P_ACO_2 curves from my model simulations are in agreement with the slopes of the V_e - P_ACO_2 curves from other experiments. I also simulated the experiments of Reynolds et al. (1972) in which ventilatory response of healthy subjects who breathed 0%, 3%, 5%, 6%, or 7% of CO_2 for 25 minutes was determined. At various inspired levels of CO_2 , I compared the change in P_ACO_2 with the change in ventilation predicted by my model with the experimental data and with other mathematical models (Figure 3.9) in the literature simulating the same experiment (Chiari et al., 1997; Sokhanvar et al., 2005, Grodins et al., 1967, Wolf and Garner, 2007). The enhanced model was unable to reproduce the transient changes in ventilation but the steady state responses predicted by the model were in agreement with the experimental data and steady state data from other mathematical models. As the application of this model will be in situations where the CO exposure duration will be atleast 20 mins, the inability of the model to reproduce transient changes in ventilation may be ignored as a limitation.

Validation of algorithm implemented to include Bohr effects: The algorithms implementing Bohr effects were validated in the model. Model calculated O_2 saturations

were compared with experimentally measured O_2 saturation (SO_2) for various values of PCO_2 , pH , and $\%HbCO$ levels (Doblar, 1977; Roughton and Darling, 1943; Sharan et al, 1989; Severinghaus, 1966; Severinghaus, 1979; Weaver et al., 2009; Whalen et al., 1965; Zhu and Weiss, 1995). The algorithm estimated O_2 saturations are in agreement with the experimentally measured values (Figure 3.10) for conditions of normoxia, CO hypoxia, hypercapnia, and hypoxia. Also as seen in figure 3.6a, for a given inspired O_2 fraction, the model estimated arterial SO_2 is in agreement with the experimentally measured SO_2 for various PO_2 's.

DISCUSSION

Model Limitations

The current model was enhanced to simulate and compare the treatment strategies currently used to treat CO poisoned victims. My previous model (Erupaka et al., 2010) was modified by adding a two subcompartment brain tissue, dynamics of CO_2 , control of ventilation and regulation of cardiac output and blood flow to various tissues. This modified model was later validated for model estimated variables (ventilation, tissue and blood PO_2 , tissue and blood PCO_2) in various conditions of normoxia, hypercapnia, hypoxia, hyperoxia, and hyperbaric oxygen. My enhanced model is the only model currently available in the literature to estimate O_2 , CO and CO_2 tensions, bicarbonate levels, pH levels, blood $HbCO$ levels, and $MbCO$ (in heart and skeletal muscle tissues) levels in all the vascular and tissue compartments in normoxia, hypoxia, CO hypoxia, hyperoxia, isocapnic hyperoxia and hyperbaric oxygen. This feature of the developed and validated model to estimate O_2 , CO and CO_2 levels in brain, heart and skeletal muscle tissue during CO exposures and treatments, will allow me to compare O_2 delivery, CO removal and CO_2 levels during different treatments after a CO exposure. In addition to the limitations discussed in the previous version of this model (Bruce et al., 2008; Erupaka et al., 2010), there are some limitations to this enhanced model which are discussed below.

Brain tissue compartment: The brain tissue compartment in this model represents the whole brain. The brain blood flow values, oxygen consumption and all other parameters used to model this compartment are for an average human brain. Thus the oxygenation levels

predicted for this compartment for various simulation conditions represent the PO_2 's in the whole brain. However it is well known that the brain is a highly heterogeneous tissue with respect to blood flow, oxygen consumption, tissue PO_2 's and vasculature (Erecińska and Silver, 2001; Floyd et al, 2003; Kolbitsch et al., 2002; Leenders et al., 1990). Imaging studies of *CO* poisoned victims have reported injury to the basal ganglia, hippocampus, and cortical white matter. In my study, the goal is to compare O_2 delivery to the brain tissue during the different treatment strategies applied and not to find a correlation between the tissue PO_2 in the various regions (white matter, gray matter, hippocampus, basal ganglia, and cortex) of the brain with the neurological outcomes or imaging studies. Though it is desirable to have a brain compartment representing various regions, applying this model to accomplish the third specific aim should not be considered as a significant limitation.

Myocardial oxygen consumption: Myocardial oxygen consumption (MOC) in the model is calculated as a function of heart rate (Equation C8, Appendix C of Erupaka et al., 2010). An increase in work load of the heart in conditions of hypoxic hypoxia (low O_2) or *CO* hypoxia would result in increased O_2 demand and supply to the heart (Erupaka et al., 2010). In the current model or the previous version of this model, myocardial oxygen consumption does not increase with increasing work load of the heart i.e., during increase in cardiac output with *CO* exposure. A regression relation to predict changes in heart rate with increasing %HbCO levels using data from Chiodi et al. (1941) was developed. The regression estimated increases in heart rate were used to increase the resting myocardial oxygen consumption in the enhanced model. Using this approach greatly underestimated the tissue PO_2 's in the heart at HbCO levels >25%, as the increase in blood flow to the heart was not sufficient to meet the increased O_2 demand. Thus to overcome the problem of O_2 supply and demand mismatch, this regression equation was not implemented in the final version of the enhanced model. The heart is a rapidly contracting muscle with a high O_2 extraction fraction and MOC at resting state, so in conditions of increased work load the heart relies on energy production via anaerobic metabolism. My model does not feature energy production through anaerobic metabolism. In my model, irrespective of the work load, MOC in the model decreases only as a function of tissue PO_2 (Equation 3.22). If the heart rate is known during *CO* exposures, then changes in MOC can be

predicted at various stages. However obtaining information on heart rate during high *CO* exposures is difficult. Thus in healthy populations the model estimated tissue PO_2 's may assumed to be slight overestimates of the actual values at %HbCO levels greater than ~35% (educated guess based on data from Chiodi et al., 1941).

Prediction of injury: The enhanced model does not directly predict the possibility of injury after a *CO* exposure. Despite treatment, neurological and myocardial problems manifest from *CO* poisoning. Occurrence of these problems after treatment may either be due to cellular injuries sustained at the time of exposure, or due to inadequacy of the therapy administered to sustain high tissue PO_2 , together with rapid clearance of *CO* and other metabolites like CO_2 . This model can be applied to compare the adequacy of the treatment administered but currently does not have the capability to predict injury sustained by the tissues at the time of exposure or before the treatment was applied.

Tissue oxygen thresholds reported in the literature for functional impairments or occurrences of injury are as follows: Intracellular acidosis is reported to occur at tissue PO_2 's less than 6 Torr (Erecińska and Silver, 2001; Zauner et al., 2002). ECG abnormalities are seen when myocardial O_2 tensions are <5 Torr (Erecińska and Silver, 2001; Zauner et al., 2002). A tissue PO_2 of <1.5 Torr would be an indicator of anaerobic metabolism (Zauner et al., 2002). Binding of *CO* to cytochrome c-oxidase (*CCO*) can be expected when tissue PO_2 approaches 1 Torr, thereby inhibiting mitochondrial respiration (Fisher and Dodia, 1981). Cell death can be inferred when a tissue PO_2 of zero is maintained (Smith et al., 2007). Based on the above thresholds, I can attempt to specify a criterion to suggest possibility of injury in the tissues. To avoid the influence of tissue injury on determination of the best treatment, the maximum %HbCO level at which tissue injury does not occur can be suggested by determining the %HbCO level at which the PO_2 's in the brain and heart tissue start to fall below a certain threshold (P_{THO_2}). But the %HbCO level determined from this approach will be dependent on the duration and concentration of *CO*, health of the subject and intersubject variability. A logistic regression (model) to develop the prognostic equation of injury using the variables affecting the incidence of injury like the *HbCO* levels, duration of exposure, myocardial and cerebral

tissue PO_2 's, metabolic rate, oxygen saturation, blood pH, arterial PCO_2 , blood lactate levels and other subject specific variables (age, gender, Hb concentrations and health of the patient) can be used. But limitations in availability of data currently make this approach unfit to predict injury. Also in conditions of severe hypoxia, the model does not take in to account the production of CO_2 in the tissues or other metabolites from the anaerobic metabolic pathway. The best my model can do is determine the time taken in various tissues to reach the pre CO exposure (control) tissue PO_2 values or the values above the threshold PO_2 's ($P_{iO_2} > P_{THO_2}$). As unconsciousness is reported in CO poisoned subjects at a %HbCO levels ≥ 40 (Parkinson et al., 2002; Stewart, 1975), I will consider the PO_2 in the tissues at the end of a simulation of CO exposure of levels reaching 40% as P_{THO_2} .

Cerebral blood flow: The blood flow to the brain has been reported to increase during CO exposure (Benignus et al., 1992; Doblar et al., 1977; Koehler et al., 1984; Langston et al., 1996; Paulson et al., 1973; Rucker et al., 2002; Santiago et al., 1986). The regression equation developed in this study to predict percent changes in brain blood flow with increasing %HbCO, was mostly from animal data. Data for humans were available only up to HbCO levels less than 20%. During CO exposure, $P_{ar}CO_2$ (arterial PCO_2) is reported to increase significantly (Doblar et al., 1977). These increases in $P_{ar}CO_2$ will further contribute to an increase in brain blood flow. The increases in brain blood flow reported in the experiments were due to the cumulative effect of increased $P_{ar}CO_2$ and %HbCO. Also the aortic body sensitivity to CO is known to be greater in animals when compared to humans (Lahiri et al., 1981). Thus, using the data from these experiments (Doblar et al., 1977; Koehler et al., 1984; Langston et al., 1996; Santiago et al., 1986) to predict brain blood flow resulted in an overestimation of the predicted values in the model (Figure 3.3). In order to compensate the overestimations, an adjusting factor "ff" (Table 3.1) was introduced. The value for this parameter "ff" was determined by (trial and error) simulating various CO exposures and ensuring that the ventilation did not change more than 4% from the pre CO exposure value (Chiodi et al., 1941; Santiago and Edelman, 1976). A value for this parameter was chosen from 0-1, e.g., choosing a value of 0.5, decreased the percent changes predicted in brain blood flow, $\dot{Q}_{B_{HbCO}}$ as a function of %HbCO by 50% (Equation 3.18). For the chosen value, CO exposures of %HbCO levels of 10, 20, 30, 40, and 50 were

simulated and the % change in ventilation at each %HbCO level from the pre CO exposure value was calculated. The value of “ff” at which the ventilation did not change more than 4% from the pre CO exposure value for the range of %HbCO levels, was considered as the value for ff (Table 3.1) in all my simulations.

Effects of HBO₂ on shunt fraction (SF): Weaver et al., (2009) reported a decrease in SF during HBO₂ conditions in humans. In the simulations of experiments of weaver et al. (2009), the values for SF reported in the experiment were used. In their experiments, the value of SF dropped to zero during HBO₂ exposure from a value of 0.15 at normobaric oxygen. However, the authors report that this observed reduction may not reflect the actual reduction in SF, due to the limitations in applying the calculations of SF to HBO₂ conditions. There have been no other experiments measuring SF in humans and modeling studies predict (Rasanen et al., 1987) a decrease in SF with increasing inspired O₂ fraction. Thus in this study, for all the HBO₂ simulations a value of zero is assumed for SF.

Implementation of hypoxic ventilatory depression: Hypoxia produces an initial rapid increase in ventilation which is not sustained and declines during the first 30 mins of hypoxic exposure (Bascom et al, 1992). This biphasic response is referred to as hypoxic ventilatory depression (HVD). The rapid increase in ventilation is reported to be produced due to stimulation of peripheral chemoreceptors. The effects of hypoxia on the central nervous system are reported to promote the decline in ventilation due to various mechanisms like changes in K⁺ and Ca²⁺ channel dynamics, neuromodulators like adenosine, GABA. In one of the version of the enhanced model, HVD was implemented to modify the gain of peripheral ventilation component. The gain was modulated as a first order differential equation of brain tissue PO₂ (Zhou et al., 2001; Ursino et al., 2001). Model predicted ventilatory responses during transient as well as steady state hypoxia were in agreement with the experimental data (Bascom et al., 1992). However when a CO exposure resulting in 20% HbCO was simulated, model predicted ventilation decreased which was not in agreement with the experimental data (Chiodi et al., 1941; Kizakevich et al., 2000). Thus, to simulate CO hypoxia with appropriate changes in ventilation, HVD was not implemented in the current version of the enhanced model. The current version of the

model (without HVD mechanism) is able to predict changes in ventilation which are in agreement with experimental data of steady state hypoxic hypoxia and *CO* hypoxia. Peripheral chemoreceptors are reported to play an insignificant role during *CO* hypoxia, atleast for %HbCO <50 (Doblar et al., 1977). Also, changes in ventilation are reported to correlate with lactate acidosis in brain which occurs at %HbCO levels > 50 (Santiago and Edleman, 1976). Thus for simulations of *CO* exposures resulting in %HbCO < 50, inability to successfully implement HVD will not influence the simulation results. The model lacks implementation of effects of H^+ on ventilation and lactate dynamics. In future, implementation of these mechanisms in addition to HVD may allow modeling appropriate changes in ventilation during *CO* hypoxia. Also, it may be necessary to develop models which implement HVD to modulate the central and peripheral chemoreceptors gains.

CONCLUSIONS

Overall, the enhanced and validated multicompartment mathematical model can be applied as a tool to accomplish the third specific aim of “comparing the current treatment strategies available to treat *CO* poisoned victims and determine the best treatment strategy ensuring fastest *CO* removal and O_2 delivery after *CO* poisoning”. Also, a significant contribution to the database of mathematical models is made by developing this validated mathematical model to estimate O_2 , *CO* and CO_2 levels in various tissues and blood vessels (brain, heart, skeletal muscle and nonmuscle tissue, arteries, veins, capillaries) for a variety of exposure conditions like hypoxia, *CO* hypoxia, hypercapnia, hypocapnia, hyperoxia, isoapnic hyperoxia, and hyperbaric oxygen.

SUMMARY

Mathematical models of human systems are excellent tools to understand and analyze physiological mechanisms, especially in situations where experiments either provide limited information about the physiological process or are unethical. To compare the current treatment strategies available to treat *CO* poisoned victims, a previously developed model (Erupaka et al., 2010) in our lab was enhanced and validated for various situations. Significant enhancements to the previously published model are addition of a two subcompartment brain tissue, mass balance equations for CO_2 , control of ventilation,

and regulation of blood flow. The enhanced model was validated for various conditions of changing O_2 or CO_2 concentrations like hypoxia, hyperoxia, hyperbaric oxygen, hypercapnia and hypocapnia. The capability of the model to predict brain tissue and venous PO_2 's, ventilation, tissue and blood PCO_2 's, tissue and blood pH in various compartments was assessed and compared with experimental data. Considering the limited availability and variability of experimental data for the various variables validated, the model predictions closely represented the trends in the experimental data. Overall, the enhanced and validated mathematical model can be applied as a tool to accomplish the third specific aim of “comparing the current treatment strategies available to treat CO poisoned victims and determine the best treatment strategy ensuring fastest CO removal and O_2 delivery after CO poisoning”.

Table 3.1: Parameters and their default values		
<i>Parameter</i>	<i>Description and references</i>	<i>Value, Units, Reference</i>
D_{bvb_on}	Ratio of $Db_{b3}O_2(t)$ and $Db_{b1}O_2(t)^+$	0.075, none
Dx_b	Mean intercapillary distance in brain tissue	0.1, cm, (Bruce et al., 2008)
Fac	Ratio of $DiCO_2$ and DiO_2	18, unitless, (Zhou et al.,2007)
ff	Brain blood flow adjustment factor during CO exposure ⁺	0.369, unitless
F_{vb}	Brain tissue volume distribution fraction ⁺	0.2, none
K_bO_2	PO_2 at which MR_bO_2 decreases by 50%	0.5, Torr, (Erupaka et al.,2010)
k_c	Central circulatory delay constant	0.9239, L, (Ursino et al., 2001)
k_p	Peripheral circulatory delay constant	0.588,L, (Ursino et al., 2001)
$MR_bO_{2/gram}$	O_2 consumption of brain	0.0365*, ml min ⁻¹ gm ⁻¹ (Mintun et al.,2001 ; Zhou et al., 2007)
$PS_{bav_rest}O_2$	Permeability surface area product of O_2 for arterioles/venules ⁺ in brain	69, ml min ⁻¹ Torr ⁻¹ gm ⁻¹
$PS_{bcap_rest}O_2$	Permeability surface area product of O_2 for capillaries ⁺ in brain	127, ml min ⁻¹ Torr ⁻¹ gm ⁻¹
$\dot{Q}_{b/gram}$	Blood flow of brain tissue	0.55, ml min ⁻¹ gm ⁻¹ (Mintun et al.,2001)
RQ_B	Respiratory quotient for brain tissue	1, unitless, (Zhou et al.,2007)
RQ_{CM}	Respiratory quotient for cardiac muscle tissue	0.8, unitless, (Zhou et al.,2007)
RQ_M	Respiratory quotient for skeletal muscle tissue	0.75, unitless, (Zhou et al.,2007)
RQ	Respiratory quotient for whole body	0.85, unitless, (Zhou et al.,2007)
SCO_2	Solubility of CO_2 in plasma	8.071×10^{-4} , ml ml ⁻¹ Torr ⁻¹ , (Ursino et al., 2001)
τ_q	First order time constant for cardiac output	15, sec, (Wolf and Garner, 2007)
τ_b	First order time constant for brain blood flow	6, sec, (Wolf and Garner, 2007)
V_{bt}	Volume of brain tissue	Male: 1425g; Female:1291g (Steven et al., 2005, Text book)
$Volfrac_b$	Fraction of volume of brain tissue compartment attributed to blood	0.04, ml/gm, (Zhou et al.,2007)

+ See text in section of the chapter entitled “*Addition of brain compartment*”

* Values with ‘*’ are in STPD and all other values are in BTPS

Source	Species	$P_{aO_2}^+$	$P_{bvO_2}^+$	$P_bO_2^+$	Condition*
Demchenko et al., 2005	Rat	-	-	25±4	0.21, 1ATA
Demchenko et al., 2005	Rat	-	-	34±5.5	0.3, 1ATA
Demchenko et al., 2005	Rat	-	-	190	1, 2ATA
Demchenko et al., 2005	Rat	-	-	287	1, 3ATA
Jamieson and Vandenbrenk, 1963	Rat	-	-	34±4	0.21, 1ATA
Jamieson and Vandenbrenk, 1963	Rat	-	-	90±13	1, 1ATA
Jamieson and Vandenbrenk, 1963	Rat	-	-	244±39	1, 2ATA
Jamieson and Vandenbrenk, 1963	Rat	-	-	452±68	1, 3ATA
Jamieson and Vandenbrenk, 1963	Human	91	38	-	0.21, 1ATA
Lambertsen et al., 1953	Human	-	40	-	1, 1ATA
Lambertsen et al., 1953	Human	2100	75	-	1, 3.5ATA
Lambertsen et al., 1953	Human	97	34.8±1.1	-	0.21, 1ATA
Lambertsen et al., 1953	Human	1740±33	66.4±5.3	-	1, 3ATA
Lambertsen et al., 1953	Human	97	36.9±1.1	-	0.21, 1ATA, 2.16% CO ₂
Lambertsen et al., 1953	Human	97	41.1±1.3	-	0.21, 1ATA, 4.31% CO ₂
Lambertsen et al., 1953	Human	97	48.2±2.3	-	0.21, 1ATA, 5.48% CO ₂
Rolette et al., 2000	Rat	145.1±11.7	-	15.1±1.8	0.3, 1ATA
Rolette et al., 2000	Rat	56.5±4.4	-	8.8±0.4	0.15, 1ATA
Rolette et al., 2000	Rat	40.7±2.3	-	6.8±0.3	0.10, 1ATA
Zauner et al., 1995	Cat	160±22	-	42±9	0.3, 1ATA
Zauner et al., 1995	Cat	36±4	-	28±5	0.15, 1ATA
Martinez et al., 1999	Rabbit	95	-	30±13	0.21, 1ATA
Martinez et al., 1999	Rabbit	30	-	11±3	0.12, 1ATA
Martinez et al., 1999	Rabbit	27	-	8±3	0.10, 1ATA
Martinez et al., 1999	Rabbit	21	-	6±3	0.08, 1ATA
Charbel et al., 1997	Human	-	-	33±11	0.21, 1ATA
Entrei and Lund, 1986	Swine	112.5±9	-	27.4	0.21, 1ATA
Entrei and Lund, 1986	Swine	189±38	-	64.37	0.35, 1ATA
Entrei and Lund, 1986	Swine	378±50	-	90.6	0.7, 1ATA
Entrei and Lund, 1986	Swine	540±29	-	105.4	1, 1ATA

P_{bvO_2} = Brain venous PO₂; P_bO_2 = Brain tissue PO₂; + Torr

*(F_IO₂, P_B); F_IO₂ = Fractional inspired O₂, P_B = Barometric pressure, 1ATA=760 Torr

Table 3.3: Slopes for the V_E - $P_A\text{CO}_2$ curves from my model and experiments		
Condition	slope- model	slope range from experiments
Normoxia, $P_{A\text{O}_2}$ =100 Torr	2.873	2.25±0.19 – 2.90±0.19 (Poulin et al., 1993) 1.88±0.82 (Honda et al., 1983) 2.4±0.94 (Fatemian and Robbins, 1998)
Hypoxia, $P_{A\text{O}_2}$ =50 Torr	4.018	3.25±0.38 – 4.76±0.37 (Poulin et al., 1993) 3.59±1.57 (Fatemian and Robbins, 1998)
Hyperoxia, $P_{A\text{O}_2}$ =200 Torr	2.216	2.39±0.25 – 2.61±0.31 (Poulin et al., 1993) 2.14±0.22 (Ren et al., 2000)

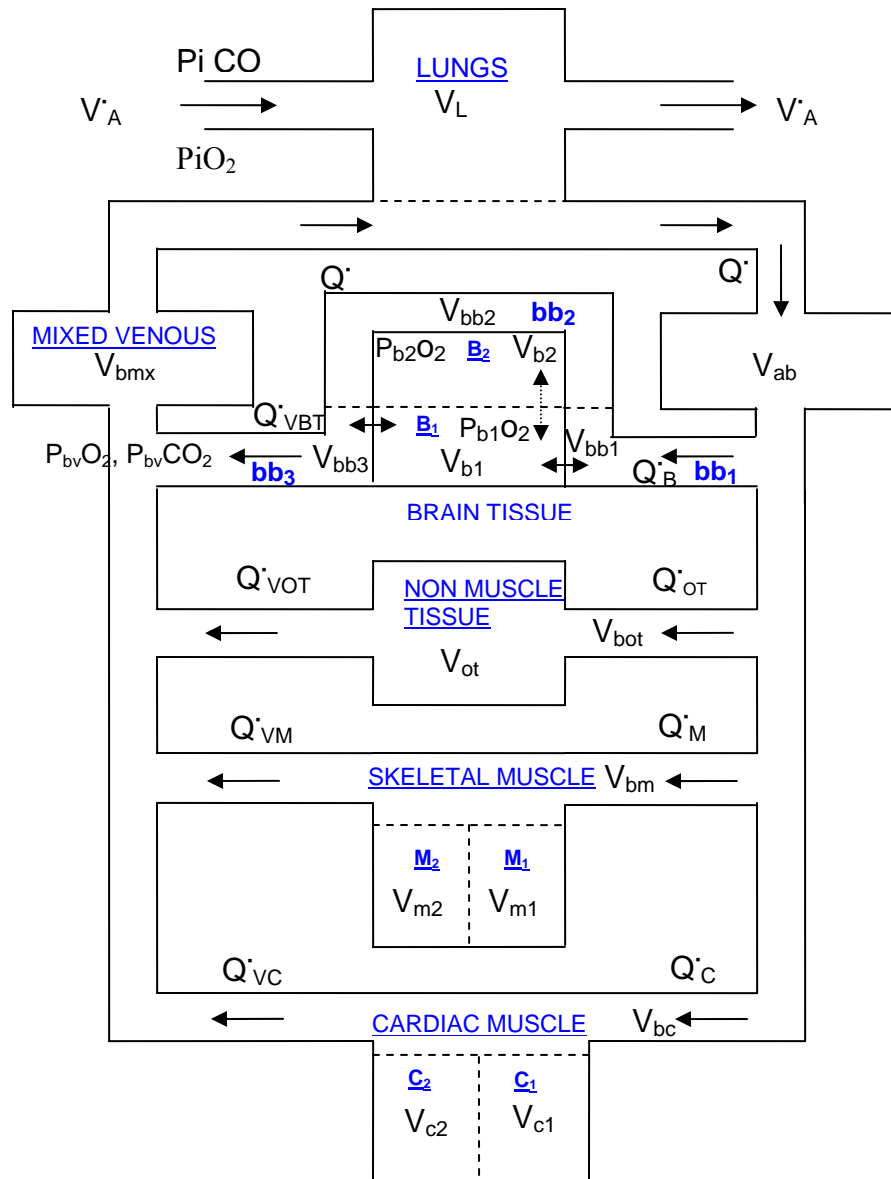


Figure 3.1: Architecture of enhanced model. The model consists of seven major compartments: lungs, arterial blood compartment, mixed venous blood compartment, brain tissue with two subcompartments, non-muscle tissue, skeletal muscle tissue with two subcompartments and cardiac tissue with two subcompartments. The brain compartment is divided into two extravascular subcompartments of volumes (V_{b1} , V_{b2}) and three vascular subcompartments of volumes (V_{bb1} , V_{bb2} , V_{bb3}). Arterial blood enters the vascular subcompartment bb_1 as \dot{Q}_B . Solid double arrows indicate blood-tissue gaseous fluxes driven by partial pressure gradients. Dotted double arrows indicate diffusive gaseous fluxes driven by concentration gradients of dissolved gases.

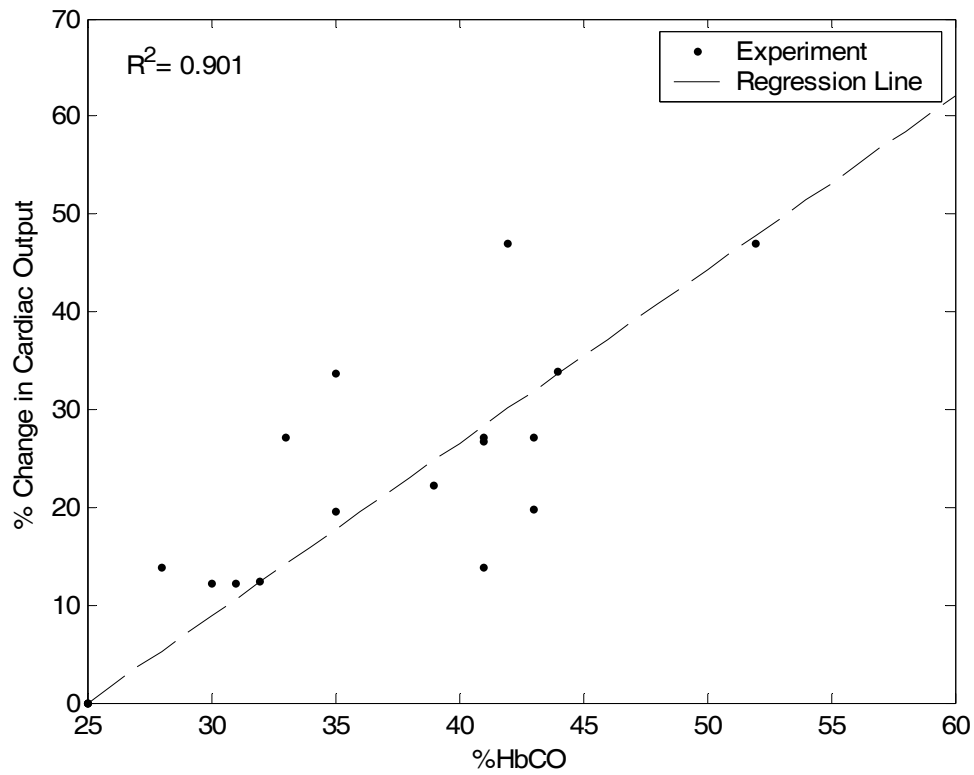


Figure 3.2: Prediction of changes in cardiac output (ordinate) with increasing %HbCO levels (abscissa). Dashed line represents the linear fit to the experimental data (•) from Chiodi et al.(1941).

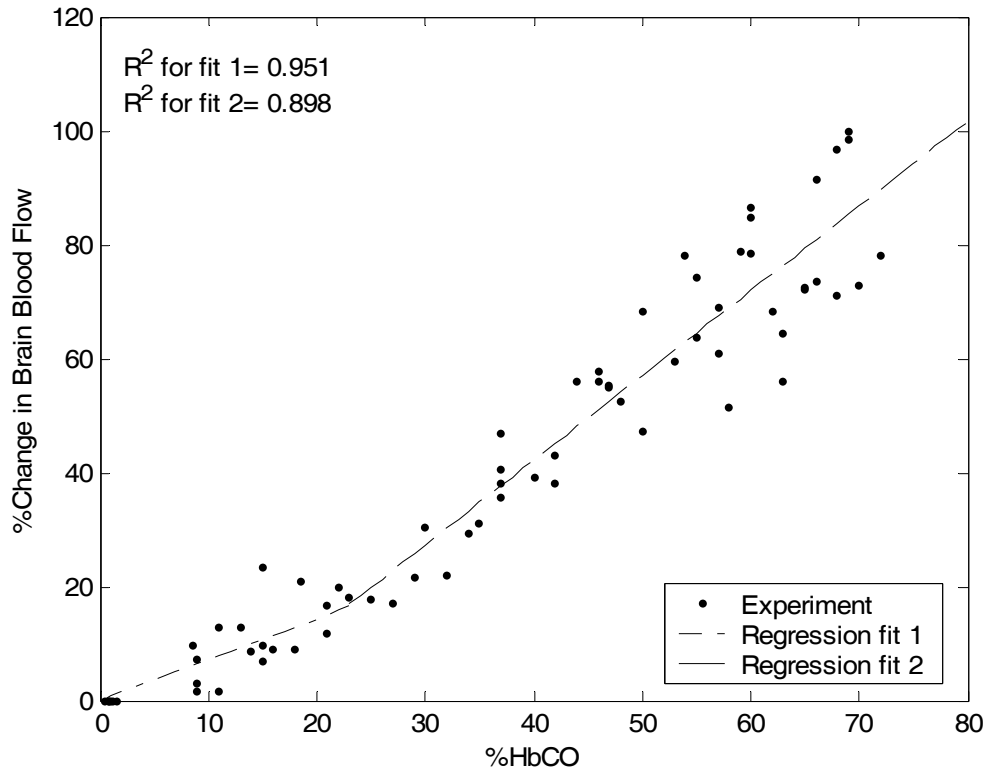


Figure 3.3: Prediction of changes in brain blood flow (ordinate) with increasing %HbCO levels (abscissa). Dashed line represents the piece wise linear fit to the experimental data (•). See text “Addition of regulation of blood flow” for references.

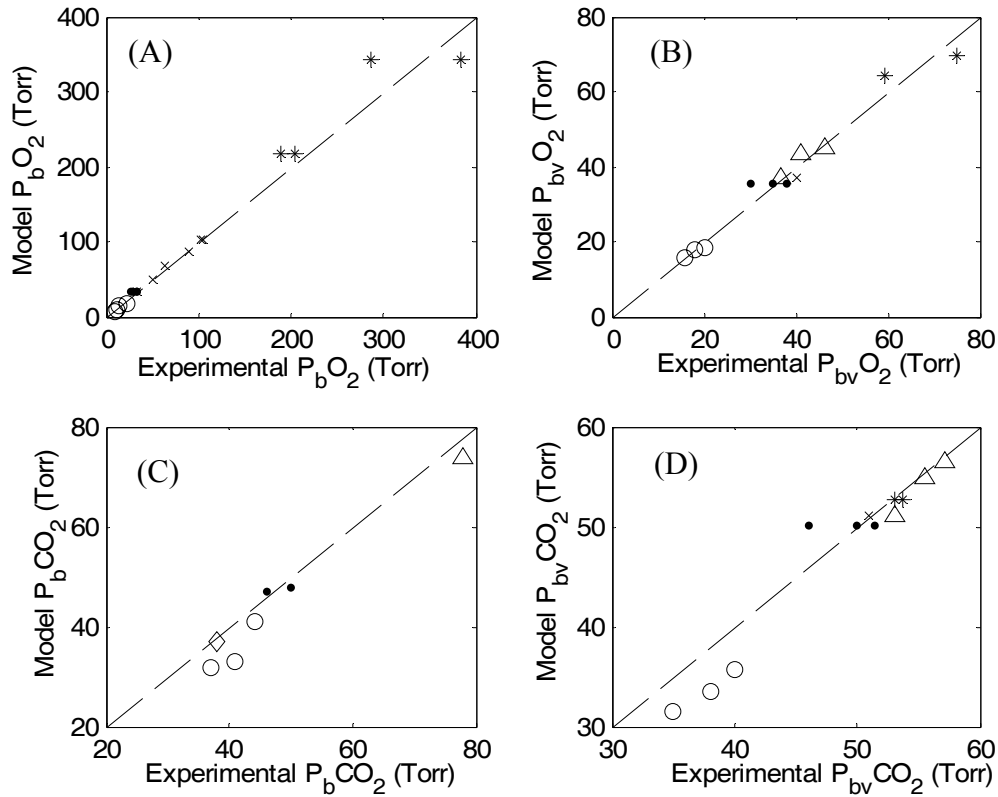


Figure 3.4: Validation of brain tissue and blood gas (O_2 , CO_2) tensions. Abscissa: Experimental gas tensions (Table 3.2, References in text “validation of tissue and blood PCO_2). Ordinate: Model predicted gas tensions. The dashed lines are identity lines (IL). (A) Brain tissue PO_2 , P_bO_2 (B) Brain venous PO_2 , $P_{bv}O_2$ (B) Brain tissue PCO_2 , P_bCO_2 , (B) Brain venous PCO_2 , $P_{bv}CO_2$. Symbols: ‘o’- Hypoxia, ‘•’-Normoxia, ‘x’- Hyperoxia, ‘*’-Hyperbaric Oxygen, ‘◊’- Hypocapnia, ‘Δ’-Hypercapnia.

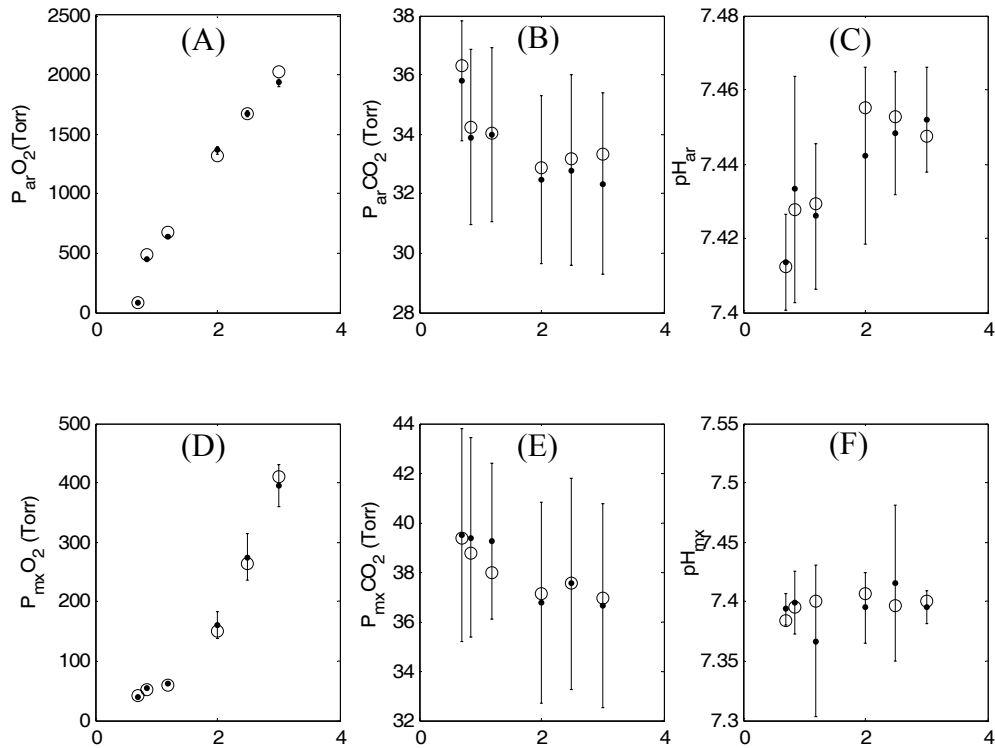


Figure 3.5: Comparison of model predicted values with experimental data: (i) arterial blood gas measurements on y-axis of upper panel (A) $P_{ar}O_2$ (B) $P_{ar}CO_2$ (C) pH_{ar} , (ii) mixed venous blood gas measurements on y-axis of lower panel (D) $P_{mx}O_2$ (E) $P_{mx}CO_2$ (F) pH_{mx} during different atmospheric pressures on x-axis. Different pressures are: 0.85 ATA air, 0.85 ATA O_2 , 1.2 ATA O_2 , 2.0 ATA O_2 , 2.5 ATA O_2 , and 3 ATA O_2 . Model estimates are represented with symbols 'o' and experimental data with symbols '•'. The error bars are the SD for experimental data (Weaver et al., 2009).

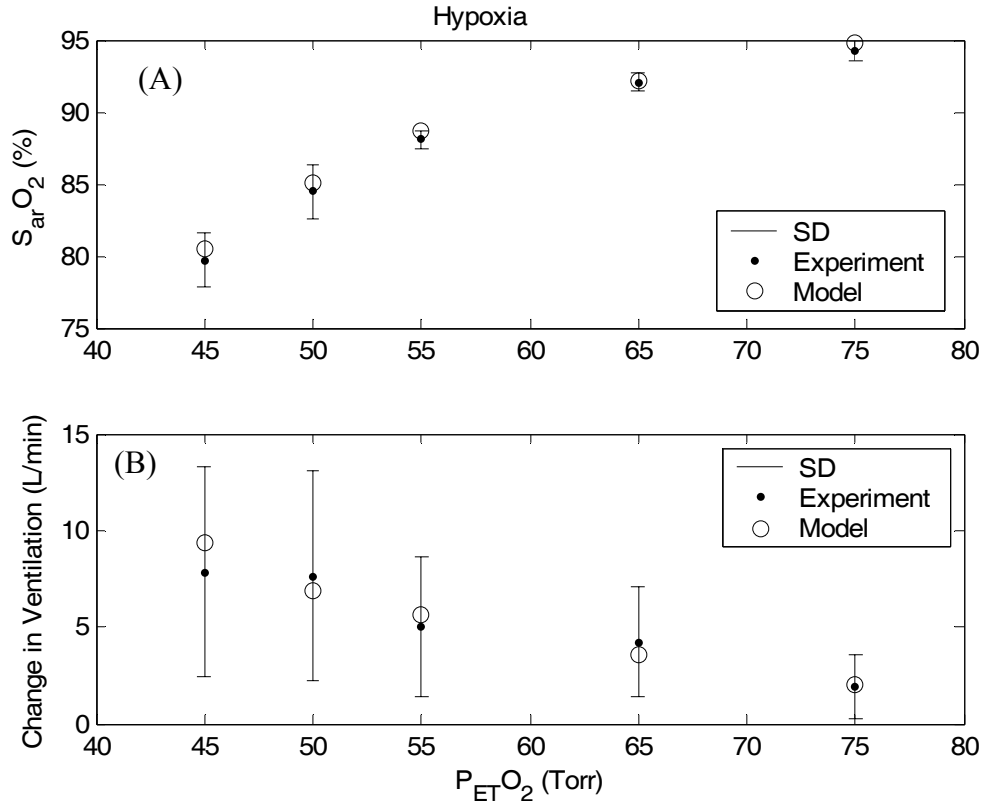


Figure 3.6: Comparison of: (A) model predicted arterial O_2 saturations ($S_{ar}O_2$) with experimentally measured data at various levels of hypoxia (B) model predicted change in ventilatory response with experimentally measured change in data at various levels of hypoxia. Model predictions represented by 'o' and experiment measurements as '•'. The error bars are the SD for experimental data (Bascom et al., 1992) and $P_{ET}O_2$ is the end tidal PO_2 .

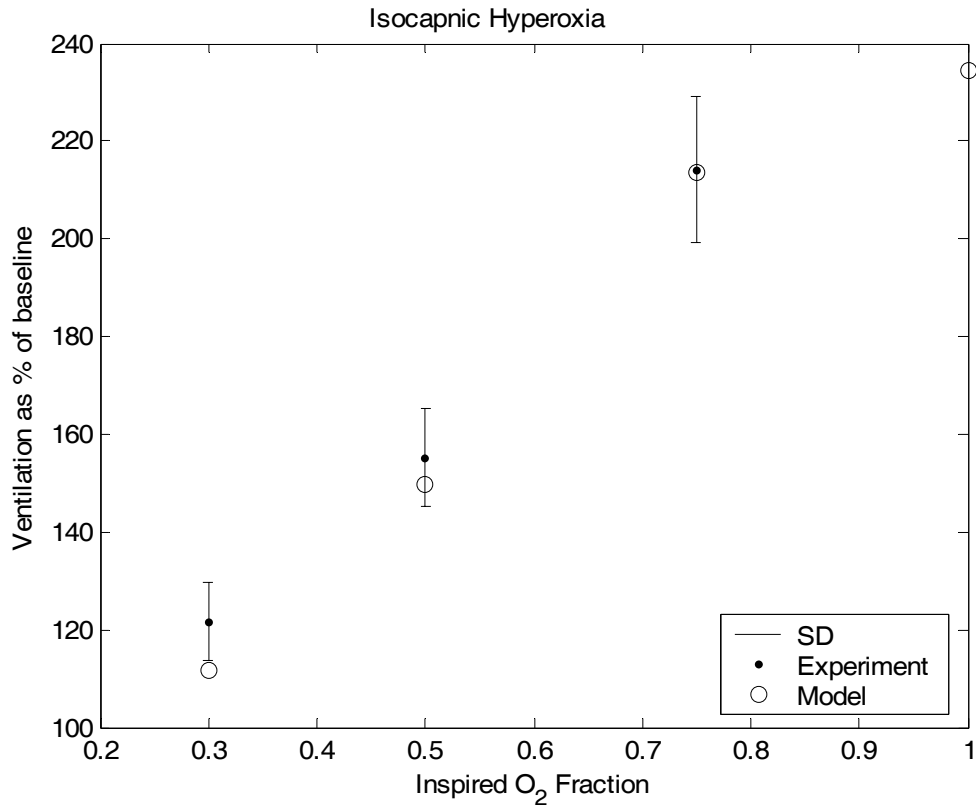


Figure 3.7: Comparison of model predicted ventilatory response with experimentally measured data at various levels of inspired oxygen fractions. Model predictions represented by 'o' and experiment measurements as '•'. The error bars are the SD for experimental data (Becker et al., 1996).

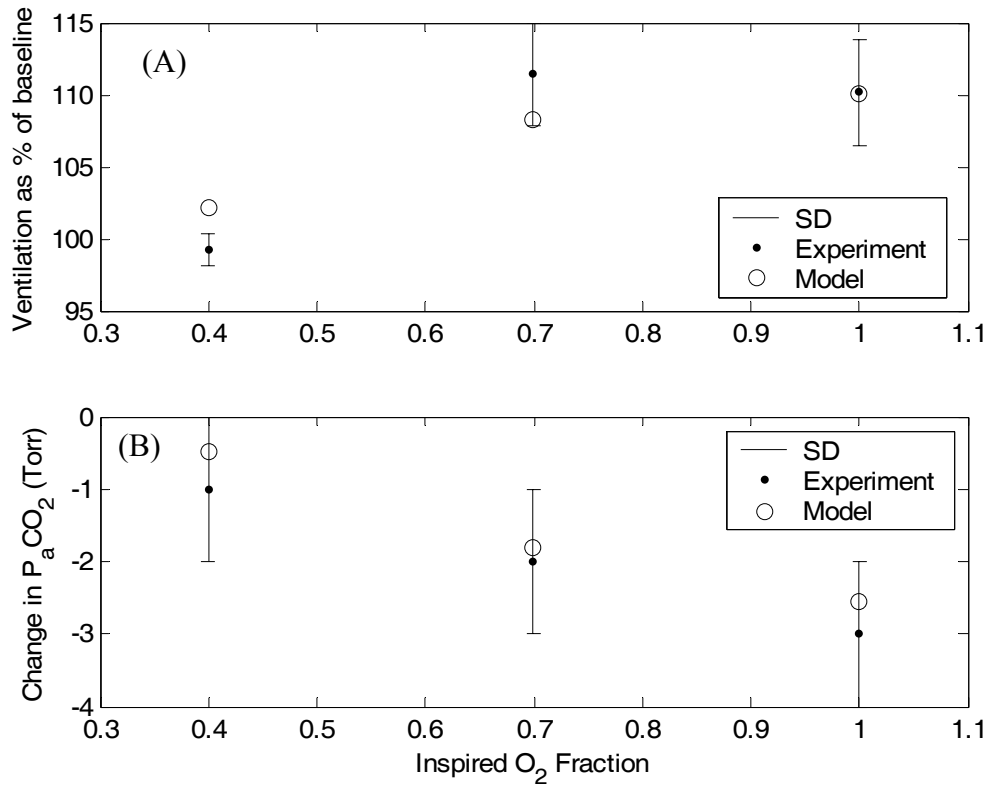


Figure 3.8: Comparison of: (A) model predicted ventilatory response with experimentally measured data at various levels of inspired oxygen fractions, (B) model predicted arterial PCO₂ changes with changes in experimentally measured data at various levels of inspired oxygen fractions. Model predictions represented by 'o' and experiment measurements as '•'. The error bars are the SD for experimental data (Nishimura et al., 2007).

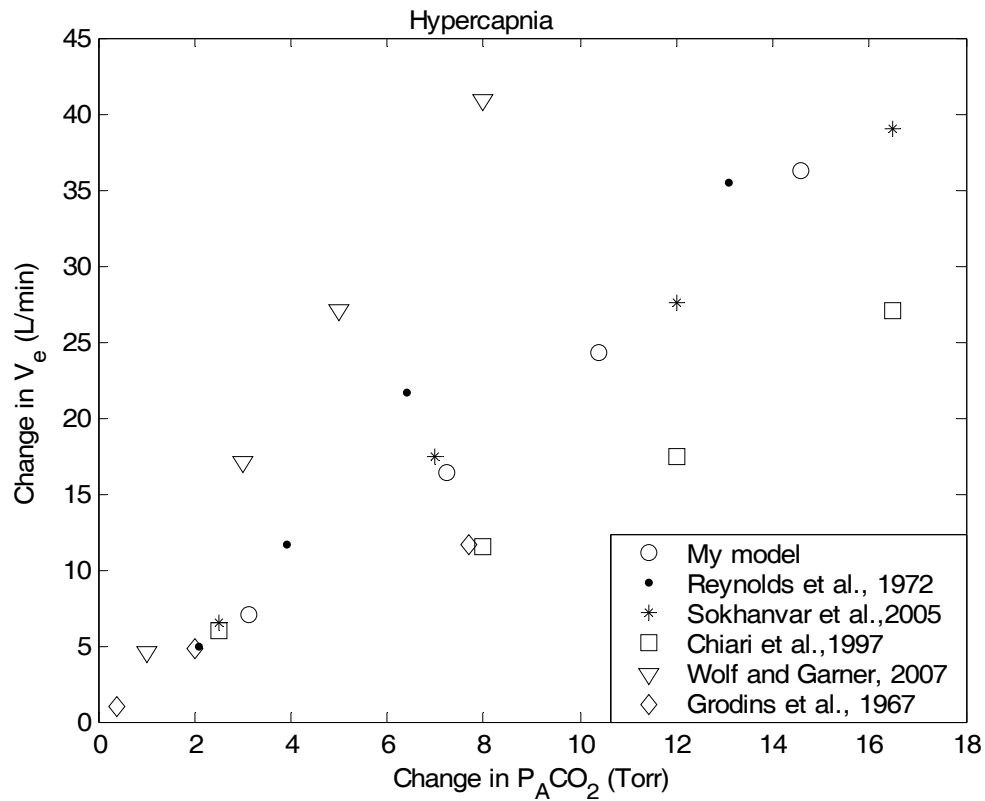


Figure 3.9: Comparison of changes in ventilation with changes in alveolar PCO_2 ($P_A CO_2$) after breathing increasing inspired concentrations of CO_2 in room air. Model predictions represented by 'o' and experiment measurements as '•'. All other symbols show predictions of other mathematical models for the same experiment of Reynolds et al. (1972).

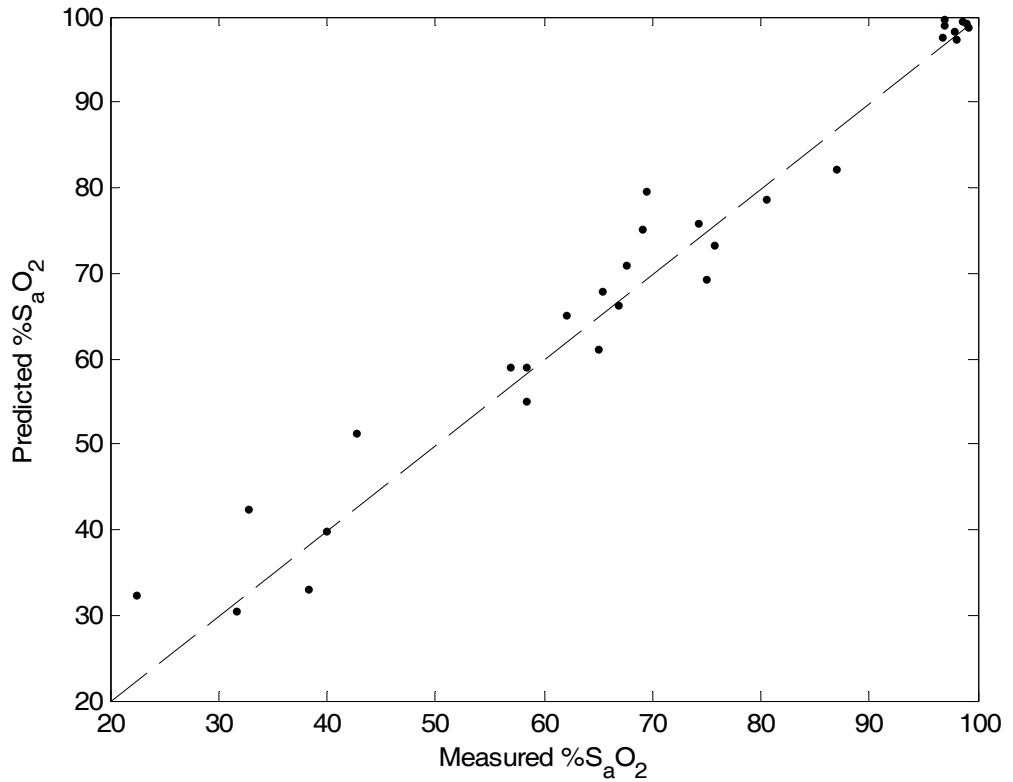


Figure 3.10: Model predicted oxygen saturation (ordinate) with experimentally measured values (abscissa) for conditions of normoxia, *CO* hypoxia, hypercapnia, and hypoxia. Dashed line is the identity line. The values for SaO₂ on the abscissa were obtained from modeling studies (Sharan et al, 1989; Severinghaus, 1966, 1979), human studies (Roughton and Darling, 1943, Weaver et al., 2009; Whalen et al., 1965) and animal studies (Doblar, 1977; Zhu and Weiss, 1995).

**Chapter 4: Computational analyses of treatments after carbon monoxide (CO)
poisoning in human**

Contents of this chapter will be submitted as a manuscript

INTRODUCTION

Carbon Monoxide (*CO*) is an odorless, colorless, tasteless gas which is responsible for a large number of accidental and intentional poisonings reported throughout the world. *CO* is generated in toxic amounts by internal-combustion engines, faulty fossil-fuel heating systems, house fires or explosions in coal mines, and emissions from modern automobiles or gasoline powered equipment in poorly ventilated spaces. Exposure to *CO* concentrations exceeding permissible exposure levels (PEL) of an average of 50 ppm over 8 hr (EHC, 1979; Raub et al., 1999) is a significant environmental and occupational health concern. Despite improved efforts in awareness and prevention, *CO* poisoning is a severely and frequently overlooked international problem (Raub et al., 1999). There are approximately 4000 deaths per year, over 40,000 emergency department visits and tens of thousands of people seeking medical attention as they lose several days to months of normal activity from *CO* exposure occurring in United States (Raub et al., 2000; Tucker and Eichold, 2005; Weaver, 1999).

CO produces tissue toxicity by impairing oxygen (O_2) delivery to the tissues. *CO* is absorbed by the respiratory tract and diffuses through the alveolar-capillary membrane and enters the blood, following a path similar to that of O_2 . *CO* poisoning causes tissue hypoxia as the binding of *CO* to the heme (*Hb*, *Mb*, *CCO*) pigments decreases the blood O_2 carrying capacity, reduces O_2 availability to tissues, and inhibits mitochondrial respiration (Piantadosi, 2004). Although *CO* poisoning does not cause a fever, other symptoms are similar to those of the flu (including nausea, severe headache, vomiting). At higher *HbCO* levels (>10%), the neurological sequelae range from mild symptoms such as headache, nausea, dizziness, and impaired manual dexterity to severe symptoms such as confusion, loss of consciousness, and brain damage due to cell death (Choi, 1983; Ernst and Zibrak, 1998; Weaver, 1999; Weaver, 2009). Loss of consciousness is reported at %HbCO levels >40 (Parkinson et al., 2002; Stewart et al., 1975). Also, myocardial injury (ECG abnormalities, elevated cardiac injury biomarkers, myocardial infarction, myocardial dysfunction) and cardiac arrest have been reported in patients with mild to severe *CO* poisoning (Anderson et al., 1967; Cosby and Bergeron, 1963; Ernst and Zibrak, 1998; Gandini et al., 2001; Henry et al., 2006; Kalay et al., 2007;

Middleton et al., 1961; Satran et al., 2005; Stewart et al., 1973; Weaver, 2009; Yanir et al., 2002).

Treatment for *CO* poisoned victims involves removing the patient from the site of *CO* exposure and then administering supplemental O_2 . O_2 hastens the dissociation of *CO* from heme proteins (*Hb*, *Mb*), thereby improving tissue oxygenation and enhancing elimination of *CO*. Choice of the treatment protocol is generally based on the measured *HbCO* levels in the venous blood and the state of consciousness of the poisoned victim. The treatment is with either normobaric hyperoxia (NBO₂), where 100% O_2 is administered if the victim is conscious and the *HbCO* levels in the blood are less than 25%, or hyperbaric hyperoxia (HBO₂) where 100% O_2 is administered, at high pressures greater than 1.5 ATA but less than 3.5 ATA (1 atmosphere = 760 mm of Hg), if the victim is unconscious or the *HbCO* levels exceed 25%. The half time elimination of *CO* on breathing room air, NBO₂ and HBO₂ at 3 ATA are ~ 320 min, 80 min and 23min, respectively (Myers et al., 1985). Thus, the choice of the treatment protocol is generally based on the measured *HbCO* levels in the venous blood, the state of consciousness of the poisoned victim and availability of equipment for treatment (hyperbaric chamber). Blood %*HbCO* is readily measurable but is thought to be an unreliable measure of poisoning severity as the symptoms and signs of intoxication correlate poorly with the level of *HbCO* measured at the time of hospital arrival. NBO₂ therapy is usually continued until the *HbCO* levels return to the near normal levels but *CO* may still be present in the tissues in the form of *MbCO* or bound to other heme structures in the cells. Specialized equipment for administration of HBO₂ is not available at all hospitals. Also, treating a *CO* poisoned victim with HBO₂ is more expensive than treating them with NBO₂ and standardized HBO₂ treatment protocols (optimal pressure, duration of treatment, and required number of sessions) for *CO* poisoning are currently unavailable and often debatable (Piantadosi, 2004; Raub et al., 2000; Weaver et al., 2002). However, mechanisms like improvement of mitochondrial oxidative metabolism and inhibition of lipid peroxidation are reported to be associated with HBO₂ and not seen with NBO₂ (Brown and Piantadosi, 1992; Piantadosi, 2004; Thom, 1990)

Precise set conditions requiring treatment with either NBO₂ or HBO₂ do not exist, often leading to disagreement with choice of treatment (Juurlink et al., 2005; Piantadosi, 2004; Raub et al., 2000). Many randomized clinical trials have been conducted to compare the merits and disadvantages of NBO₂ and HBO₂ in CO poisoned victims (Begany, 2001; Ducasse et al., 1995; Gorman, 1999; Isbister et al., 2003; Mathieu et al., 1996; Raphael et al., 1989; Scheinkestel et al., 1999; Scheinkeste et al., 2004; Thom et al., 1995; Weaver et al., 2002). Comparison of the treatment outcomes of NBO₂ and HBO₂ suggested that the trial results neither confirm nor deny the benefit of HBO₂ over NBO₂ (Juurlink et al., 2005; Piantadosi, 2004; Weaver et al., 2002). However, the clinical trials conducted varied in patient populations, durations and pressures in HBO₂ treatment protocols, durations of treatment with NBO₂, severity of poisoning and degree of follow up (Juurlink et al., 2005). Also, the potential scope of new treatments like normocapnic NBO₂ hyperventilation or normocapnic HBO₂ hyperventilation have not been tested in CO poisoning therapy management. Hyperoxia is reported to increase ventilation and decrease arterial PCO₂ (Nishimura et al., 2007). Decreases in arterial PCO₂ is accompanied by decreases in brain blood flow (Topor et al., 2004), which results in decreased O₂ delivery to the brain tissue during treatment with NBO₂ or HBO₂ (Figure 4.1). Maintaining isocapnia during NBO₂ will eliminate the effects of hypocapnia induced decreases in brain blood flow (Figure 4.1), thereby increasing oxygen delivery to the brain. Fisher et al. (1999) and others (Ishida et al., 2007; 1999; Kreck et al., 2001; Rucker et al., 2002; Takeuchi et al., 2000) have reported (in dogs as well as humans) that treatment with normocapnic NBO₂ increases the rate of CO elimination and improves O₂ delivery in CO-poisoned victims. For ethical reasons, the authors had limited HbCO levels in their subjects (Rucker et al., 2002) to 12% and whether normocapnic NBO₂ would be effective in patients with very high levels of HbCO is still unknown.

These ambiguities and variations in the clinical trials or treatment procedures give rise to many unresolved issues in treatment of CO poisoning (Juurlink et al., 2005; Piantadosi, 2004). Some of these unresolved issues are to (i) understand the advantages of NBO₂ and HBO₂ for a population varying in health status (normal, anemic, coronary artery disease, etc.), fitness level (athletes, recreationally active, sedentary), severity of

poisoning (short vs. long or low %HbCO vs. high %HbCO) and intersubject variability (age, gender, blood volume, etc.) and (ii) suggest standardized treatment regimens for NBO₂ and HBO₂ (duration of treatment, number of treatment sessions, optimal pressures, cost-benefit assessment). The main goal of my study is to compare NBO₂, HBO₂ and normocapnic NBO₂ to determine the best treatment strategy ensuring fastest CO removal and O₂ delivery after CO poisoning in healthy subjects. To achieve this goal, I will use the validated mathematical model described in chapter 3. The mathematical model has many advantages over performing clinical trials, as the model can be used to specify the treatment regimens, poisoning severity, and health status of the population, thereby allowing fair comparison among the available therapies to treat otherwise-healthy CO poisoned victims. As conducting experiments involving high CO exposures is unethical, the model can be used to simulate and compare the treatments at high %HbCO levels. In addition to comparing the treatments, various issues (Table 4.1) pertaining to treatments of otherwise-healthy CO poisoned victims will be addressed in this study.

METHODS

The validated mathematical model used in this study has been described in detail in chapter 3. This validated model was capable of predicting brain tissue and venous PO₂'s, ventilation, tissue and blood PCO₂'s, tissue and blood pH in various compartments for changing CO, O₂ or CO₂ concentrations like CO hypoxia, hypoxic hypoxia, hyperoxia, hyperbaric oxygen, hypercapnia and hypocapnia. The ability of the validated model to estimate O₂, CO and CO₂ levels in various tissues and blood vessels (brain, heart, skeletal muscle and nonmuscle tissue, arteries, veins, capillaries) during CO exposures and treatments makes it a desirable tool to accomplish the goal of this study. The mathematical model was used to simulate short (20 min) and long (480 min) CO exposures in healthy human subjects. At the end of CO exposure, NBO₂, HBO₂ or normocapnic NBO₂ treatments were simulated. The time varying tissue PO₂'s in the brain, heart and muscle compartments and CO levels in the blood, tissues and body were analyzed during CO exposures and treatments.

Model description

The mathematical model used in this study is a significant enhancement of the previous models developed in our lab (Bruce et al., 2008; Erupaka et al., 2010). This model consists of a (i) lung compartment (A), (ii) arterial blood compartment (ar), (iii) two subcompartment brain tissue (b_1, b_2) with three vascular subcompartments (bb_1, bb_2, bb_3), (iv) two subcompartment heart tissue (c_1, c_2) with three vascular subcompartments (bc_1, bc_2, bc_3), (v) two subcompartment skeletal muscle tissue (m_1, m_2) with three vascular compartments (bm_1, bm_2, bm_3), (vi) single nonmuscle tissue compartment (ot) perfused by single vascular compartment (bot) and (vii) a mixed venous blood compartment (mx). The three vascular subcompartments surrounding the tissue compartments represent the arteriole, capillary and venule blood surrounding the tissue (Bruce et al., 2008; Erupaka et al., 2010). The first tissue subcompartment is envisioned as tissue perfused extensively by small arterioles and venules in first and the third vascular subcompartments. The second tissue subcompartment is assumed to be perfused mostly by capillaries in the second vascular subcompartment. As most of the gas exchange and energy production takes place in the tissues surrounded by capillaries, the model estimated O_2 levels in the second tissue subcompartments of brain, heart and skeletal muscle tissue were analyzed in all the simulations. The model predicted tissue PO_2 's in the second tissue subcompartments of brain (Pbt_2O_2), heart (Pct_2O_2) and skeletal muscle (Pmt_2O_2) were assumed as a correlate of tissue oxygenation and were used to determine the state of O_2 delivery in the tissues during CO exposures and treatments. The CO levels in the blood (CO_{blood}), tissues (CO_{tissue}) and body (CO_{body}) during CO exposure and treatments were calculated from the model using the Equations 4.1-4.3.

$$CO_{blood} = C_{ar}CO \cdot V_{ar} + C_{bb}CO \cdot V_{bb} + C_{bc}CO \cdot V_{bc} + C_{bm}CO \cdot V_{bm} + C_{bot}CO \cdot V_{bot} + C_{mx}CO \cdot V_{mx} \dots \dots \dots 4.1$$

$$CO_{tissue} = C_{bt}CO \cdot V_{bt} + C_{ct}CO \cdot V_{ct} + C_{mt}CO \cdot V_{mt} + C_{ot}CO \cdot V_{ot} \dots \dots \dots 4.2$$

$$CO_{body} = CO_{blood} + CO_{tissue} + C_A CO \cdot V_L \dots \dots \dots 4.3$$

where, C_iCO and V_i are the concentrations of CO and volumes of compartment 'i'.

Simulation Description

ACSL 11.8 was used to simulate various CO exposures and treatments. Simulations were performed in double precision and a 30 minute stabilization period was initiated with every simulation run for the baseline simulation to reach a steady state. The values for various variables at the end of steady state were considered as the pre- CO

exposure or control values. The %HbCO levels, $P_{bt_2O_2}$, $P_{ct_2O_2}$, $P_{mt_2O_2}$, CO_{blood} , CO_{tissue} , CO_{body} , cardiac output (\dot{Q}), and alveolar ventilation (\dot{V}_A) were saved for the entire duration of the simulations to allow analysis of the data. Unconsciousness is reported to occur in *CO* poisoned subjects at a %HbCO levels ≥ 40 (Parkinson et al., 2002; Stewart, 1975). Thus to determine the tissue oxygen threshold at which unconsciousness may possibly occur, a 20 min *CO* exposure of 6400 ppm of *CO* resulting in 40% HbCO was simulated and the PO_2 's in the second tissue subcompartments of brain, heart and skeletal muscle at the end of the exposure were considered as the oxygen thresholds (P_{THO_2}) for unconsciousness and other functional impairments to occur. Simulations in this study were designed to test two specific hypotheses. Analysis of the simulation results from testing these two hypotheses will allow comparison of different treatments and also aid in understanding of the unresolved issues related to *CO* poisoning therapies stated in Table 4.1.

Hypothesis 1: I hypothesize that “treating otherwise-healthy *CO* poisoned victims with HBO_2 after a 6 hr treatment of NBO_2 will not have any benefits in improving O_2 delivery and *CO* removal.” Testing this hypothesis will allow me to compare the merits of NBO_2 and HBO_2 after *CO* poisoning occurs. Treatment duration of 6 hr is often considered as the window of opportunity in the clinical trials for comparing NBO_2 and HBO_2 (Weaver et al., 2002). This treatment window of 6 hr interval was suggested by Goulon et al. (1969) as the opportunity window for maximum benefit from HBO_2 therapy. If my hypothesis is true, then I will determine the maximum duration of NBO_2 after which administered HBO_2 therapy may still have a favorable effect in improving O_2 delivery to the tissues and speeding removal of *CO* from blood and tissues.

Hypothesis 2: I hypothesize that “irrespective of the poisoning severity treating an otherwise-healthy *CO* poisoned victim with isocapnic (normocapnic) NBO_2 will always have a favorable effect in improving O_2 delivery and enhancing *CO* removal, when compared to treating the victim with poikilocapnic NBO_2 ”

Data set used for simulations of CO exposures and treatment protocols

Benignus et al. (1994) exposed fifteen healthy, male human subjects to high concentrations of CO for short durations. This data set was used to simulate CO exposures and three different treatments namely, poikilocapnic NBO_2 , poikilocapnic HBO_2 and normocapnic NBO_2 . In this experiment (Benignus et al., 1994), measurements of age, body weight, height, blood volume, hemoglobin concentration, cardiac output, initial %HbCO and lung diffusivity coefficient of CO were provided by the investigators for each subject (Table 4.2). Alveolar ventilation was estimated by the model. Total body oxygen consumption was calculated as 3.2 ml/Kg. D_MCO was varied in proportion to muscle mass, with a value of D_MCO of 0.225 ml/min/Torr/Kg of muscle mass. Values for all other parameters that were not provided by the investigators have been referenced in my previous publication (Erupaka et al., 2010). From this data set of 15 subjects, only 6 subjects (S108, S112, S115, S118, S119 and S120) were simulated in this study (Table 1 of Benignus et al., 1994; Table 4.2 of this chapter). Subject 115 (S115) was the subject with subject specific parameters close to the mean values of the data set. S108 had the highest cardiac output and S118 had the lowest muscle mass, cardiac output and blood volume. S112 had the highest muscle mass and S119 had the largest blood volume. S120 was randomly chosen from the data set. Intersubject variability in cardiac output, muscle mass, blood volume are known to influence the uptake and removal of CO . These subjects were chosen to test my hypotheses in a range of subjects.

Simulated CO exposures and treatment protocols

To test my hypotheses the validated mathematical model was used to simulate the following CO exposures and treatments. Simulation sets 1 and 2 were performed to determine if HBO_2 had any merits in removing CO from the body and improving O_2 delivery after a NBO_2 treatment for 6 hr, irrespective of the duration of CO exposure, intersubject variability and %HbCO level at the end of exposure. Simulation set 3 was performed to determine the maximum duration of NBO_2 after which administered HBO_2 therapy may still have a favorable effect in improving O_2 delivery to the tissues and speeding removal of CO from blood and tissues, irrespective of %HbCO level at the end of exposure. Simulation set 4 was performed to determine the best treatment strategy (among the available therapies) to treat otherwise-healthy CO poisoned victims to ensure

faster CO removal and O₂ delivery, irrespective of %HbCO level at the end of exposure. Among the six subjects simulated, three subjects (S108, S112, S120) had HbCO levels of ~42% during the first CO exposure level (6400 ppm). Simulating the second CO exposure level of 8000 ppm in these subjects (S108, S112, S120) resulted in HbCO levels greater than 50%. As the confidence in model's predictions for HbCO levels greater than 50% is low (See discussion), subjects S115, S118 and S119 were chosen to simulate different treatments after CO poisoning of varying HbCO levels. Short CO exposures of (i) 6400, (ii) 8000 ppm and (iii) 10000 ppm of CO for a duration of 20 min were simulated and the end of CO exposure was followed by different treatment regimens.

Simulation set 1-Short CO exposure followed by NBO₂ treatment: Six healthy subjects (S108, S112, S115, S118, S119 and S120) were exposed to a concentration of 6400 ppm of CO for a duration of 20 min. The end of CO exposure was followed by a treatment on 100% O₂ at 1 ATA (760 Torr) for 360 min (6 hr). In addition, three subjects (S115, S118, and S119) were also exposed to a concentration of (i) 8000 ppm and (ii) 10000 ppm of CO for a duration of 20 min and the end of CO exposure was followed by a treatment on 100% O₂ at 1 ATA for 360 min. Treatment on NBO₂ for 6 hr will be referred as ^{6 hr}NBO₂ in the text.

Simulation set 2-Long CO exposure followed by NBO₂ treatment: Six healthy subjects (S108, S112, S115, S118, S119 and S120) were exposed to a concentration of 450 ppm of CO for a duration of 480 min. The end of CO exposure was followed by a treatment on 100% O₂ at 1ATA for 360 min (6 hr).

Simulation set 3-Short CO exposures followed by HBO₂ treatment: Three subjects (S115, S118, and S119) were exposed to a concentration of 6400 ppm of CO for a duration of 20 min and the end of CO exposure was followed by a treatment on (i) 100% O₂ at 1ATA for 120 min (2 hr) followed by 100% O₂ at 3 ATA (HBO₂) for 90 min (referred as ^{2 hr}NBO₂-^{1.5 hr}HBO₂), (ii) 100% O₂ at 1ATA for 180 min (3 hr) followed by 100% O₂ at 3 ATA for 90 min (referred as ^{3 hr}NBO₂-^{1.5 hr}HBO₂) or (iii) 100% O₂ at 1ATA for 240 min (4 hr) followed by 100% O₂ at 3 ATA for 90 min (referred as ^{4 hr}NBO₂-^{1.5}

^{hr}HBO₂). Also these three subjects were exposed to a concentration of (i) 8000 ppm and (ii) 10000 ppm of CO for a duration of 20 min and the end of CO exposure was followed by treatment regimens described above in simulation set 3.

Simulation set 4-Short CO exposures followed by normocapnic NBO₂ treatment: Three subjects (S115, S118, S119) were exposed to a concentration of 6400 ppm of CO for a duration of 20 min and the end of CO exposure was followed by a treatment on 100% O₂ at 1ATA for 360 min, while maintaining isocapnia at the normocapnic level of the subject (referred as ^{6 hr}INBO₂). For these simulations the alveolar PCO₂ was maintained constant for the duration of treatment at the pre-CO exposure levels (normoxia, room air). In addition, these three subjects were also exposed to a concentration of (i) 8000 ppm and (ii) 10000 ppm of CO for a duration of 20 min and the end of CO exposure was followed by a 6 hr, normocapnic NBO₂ treatment.

Data analysis

For each simulation set, the %HbCO levels, CO_{blood}, CO_{tissue}, CO_{body}, tissue PO₂'s in brain (P_{bt}O₂), heart (P_{ct}O₂) and muscle tissue (P_{mt}O₂), cardiac output (\dot{Q}), and alveolar ventilation (\dot{V}_A) were analyzed. All the variables used for analyzing the simulations to determine the best treatment are defined in Table 4.3.

To determine the state of oxygenation in the tissues during CO exposure and various treatments the following calculations were made: (i) during a CO exposure, the duration for which the tissue PO₂'s are below the threshold PO₂ (P_{TH}O₂) for unconsciousness and other functional impairments to occur (referred as t<P_{TH}O₂), (ii) during a treatment, time taken for the tissue PO₂'s in brain, heart and muscle to reach a value above P_{TH}O₂ (referred as t_bP_{TH}O₂, t_cP_{TH}O₂, t_mP_{TH}O₂, respectively), and (iii) during a treatment, time taken for the tissue PO₂'s in brain, heart and muscle to reach a value above or equal to the pre-CO exposure tissue PO₂, P_rO₂ (referred as t_bP_rO₂, t_cP_rO₂, t_mP_rO₂ respectively). The time taken to reach P_rO₂'s is computed to determine the suggested duration of each administered treatment. Among the simulated therapies to treat otherwise-healthy CO poisoned patients, the treatment strategy in which time taken to

attain tissue PO_2 's above $P_{TH}O_2$ is fastest, will be considered as a therapy ensuring faster O_2 delivery to the tissues. If the time taken to reach tissue PO_2 's above $P_{TH}O_2$ is the same for two or more treatments, then the treatment taking less time to remove CO from the body will be considered to be the best treatment ensuring faster O_2 delivery to the tissues and CO removal.

To determine the rate of CO removal from the body during various treatments the following calculations were made: (i) the time taken by a treatment to remove 50% of the total CO body burden (CO_{body}) at the time of exposure ($CO_{body} T_{1/2}$), and (ii) the time taken by a treatment to reach %HbCO levels <10 ($T_{\%HbCO<10}$). A 10% HbCO level was chosen as no adverse effects of CO have been reported at these levels. $CO_{body} T_{1/2}$ is calculated to determine the treatment ensuring fastest CO removal from the body. $T_{\%HbCO<10}$ is computed to determine the minimum duration of each administered treatment. Also, the CO washout curves (CO_{body}) were fit to exponential functions to determine the time constants of these curves. The early (τ_e) and late (τ_l) time constants of these CO washout curves after short and long CO exposures were determined to compare the washout times during different treatments and CO exposures. To calculate the early and late time constants of CO washout curves, these curves were fit to an exponential function of the form $Ae^{bt}+De^{ct}$ using least squares method in Matlab, version 6.5. In the exponential functions, $1/b$ (τ_e) and $1/c$ (τ_l) are the early and late time constants. A and D are the magnitudes of the early (G_e) and the late (G_l) exponential decay functions. Early and late time constants of CO washout curves were determined only for the treatments, where the CO washout curves followed an exponential function.

RESULTS

The main goal of my study is to compare NBO_2 , HBO_2 and normocapnic NBO_2 to determine the best treatment strategy ensuring fastest CO removal and O_2 delivery after CO poisoning in healthy subjects. The validated mathematical model was used to perform simulation sets 1-4 to achieve this goal. Unconsciousness is reported to occur in CO poisoned subjects at a %HbCO levels ≥ 40 (Parkinson et al., 2002; Stewart, 1975). Prior to analyzing the results of the simulation sets 1-4, a CO exposure resulting in

HbCO's $\geq 40\%$ was simulated. Thus to determine the tissue oxygen threshold at which unconsciousness may possibly occur, a 20 min *CO* exposure of 6400 ppm of *CO* resulting in $\geq 40\%$ HbCO was simulated in six Benignus's subjects (S108, S112, S115, S118, S119 and S120). The PO_2 's in the second tissue subcompartments of brain, heart and skeletal muscle at 40% HbCO levels were assumed as the tissue oxygen threshold (P_{THO_2}) at which unconsciousness and functional impairments may possibly occur. From the results of these simulations in six subjects, P_{THO_2} was determined as 15 Torr. A tissue PO_2 below P_{THO_2} in the brain tissue is assumed to cause unconsciousness and tissue PO_2 below P_{THO_2} in the heart and skeletal muscle tissue is assumed to cause functional impairments. Unconsciousness is reported at a cerebral venous PO_2 of 16-20 Torr (Purves, 1972). Thus, a value of 15 Torr for P_{THO_2} in the brain is a reasonable assumption for unconsciousness to occur in a *CO* poisoned victim.

Results of simulation set 1: In this simulation set, 6 subjects were exposed to a concentration of 6400 ppm of *CO* for a duration of 20 min followed by a treatment on NBO_2 for 6 hr (${}^6\text{hr}NBO_2$). For the same inspired *CO* concentrations, the %HbCO levels in the subjects at the end of exposure ranged from 34%- 45% (Table 4.4). The durations for which the PO_2 's were below the threshold PO_2 (P_{THO_2}) were calculated for the brain ($t_b < P_{THO_2}$), heart ($t_c < P_{THO_2}$) and muscle ($t_m < P_{THO_2}$) tissues. Also the time taken to reach PO_2 's above the threshold values and the pre-*CO* exposure tissue PO_2 's (P_rO_2) were calculated for the brain ($t_b P_{THO_2}$, $t_b P_rO_2$), heart ($t_c P_{THO_2}$, $t_c P_rO_2$) and muscle ($t_m P_{THO_2}$, $t_m P_rO_2$) tissues. In 3 (S108, S112, S120) of the 6 subjects $t_b < P_{THO_2}$ was ~ 3 min, suggesting a possibility of occurrence of unconsciousness at the end of *CO* exposure in these subjects. The mean \pm SD values for $t_c < P_{THO_2}$ and $t_m < P_{THO_2}$ in 5 of the 6 subjects were 4.3 ± 2.7 and 4.5 ± 2.5 min, respectively. These values suggest that except in S119 ($t < P_{THO_2} = 0$, i.e., during *CO* exposure, PO_2 in the brain was never below 15 Torr), there is a possibility of occurrence of functional impairment in the heart and muscle tissues. The mean \pm SD values for $t_b P_{THO_2}$, $t_c P_{THO_2}$, and $t_m P_{THO_2}$ are 1.2 ± 0.5 , 3.7 ± 2.4 , and 4 ± 1.2 min, respectively. Thus during treatment with ${}^6\text{hr}NBO_2$, the PO_2 's in all the vital tissues are above P_{THO_2} in ~ 4 min for an otherwise-healthy *CO* poisoned subject with an average %HbCO level of 40. It should be noted that at ~ 4 min, though the PO_2 's in all the vital

tissues are above $P_{TH}O_2$, the body burden of CO (CO_{body}) is still greater than 50% (Table 4.5). Also, the PO_2 's in the brain, heart and muscle tissues reach P_rO_2 's within 4.8 ± 0.4 , 4.2 ± 0.3 , and 2.8 ± 0.1 hr respectively (Table 4.5). The %HbCO levels after 4.8 hr of treatment on NBO_2 immediately after end of CO exposure is $\sim 4.5\%$. The CO_{body} $T_{1/2}$ and $T_{\%HbCO < 10}$ values are 1.4 ± 0.2 and 2.8 ± 0.1 hr, respectively (Table 4.5). Also after short CO exposures resulting in higher %HbCO values followed by a treatment on ${}^6 \text{hr} NBO_2$, the PO_2 's in the brain, heart and muscle tissues are above $P_{TH}O_2$ and P_rO_2 levels and the %HbCO levels are less than 10 at the end of the treatment (Table 4.5). These results (Table 4.5-4.6A-C) suggest that in healthy subjects poisoned by short CO exposures, the O_2 levels and CO levels in the body are restored to control or pre- CO exposure values within 6 hr of treatment on NBO_2 .

Results of simulation set 2: In this simulation set, 6 subjects were exposed to a concentration of 450 ppm of CO for duration of 480 min (8 hr) followed by ${}^6 \text{hr} NBO_2$ treatment. The mean %HbCO level at the end of exposure is $\sim 42\%$ (Table 4.4). In five of the 6 subjects $t < P_{TH}O_2$ at the end of exposure was greater than 0 in all the tissues, suggesting a possible occurrence of unconsciousness and functional tissue impairments in these subjects. In one subject S 119, $t_b < P_{TH}O_2$ at the end of exposure was equal to 0. In the same subject, $t_c < P_{TH}O_2$ and $t_m < P_{TH}O_2$ at the end of exposure was greater than 0, suggesting a possible occurrence of functional impairments in the tissues. The mean \pm SD values for $t_b < P_{TH}O_2$, $t_c < P_{TH}O_2$ and $t_m < P_{TH}O_2$ in these subjects were 84 ± 38 min (5 subjects), 168 ± 69 min (6 subjects) and 209 ± 98 min (6 subjects), respectively. The mean \pm SD values for $t_b P_{TH}O_2$, $t_c P_{TH}O_2$, and $t_m P_{TH}O_2$ are 1.6 ± 0.75 , 10.5 ± 9 , and 4.7 ± 1.4 min, respectively. When compared to short CO exposures, though the tissue PO_2 's are below $P_{TH}O_2$ for a longer duration in long CO exposures, during treatment with ${}^6 \text{hr} NBO_2$, the PO_2 's in all the vital tissues are above $P_{TH}O_2$ in ~ 11 min for the otherwise-healthy CO poisoned subjects with an average %HbCO level of 42. It should be noted that at ~ 11 min, though the PO_2 's in all the vital tissues are above $P_{TH}O_2$, the body burden of CO (CO_{body}) is still greater than 50% (Table 4.5). Also, the PO_2 's in the brain, heart and muscle tissues reach P_rO_2 's within 5 ± 0.3 , 4.4 ± 0.4 , and 3 ± 0.3 hr respectively (Table 4.5). The %HbCO levels after 5 hr of treatment on NBO_2 immediately after end of CO

exposure is ~3.5%. The $CO_{\text{body}} T_{1/2}$ and $T_{\%HbCO < 10}$ values are 1.4 ± 0.2 and 3.0 ± 0.2 hr respectively (Table 4.5). These results (Table 4.5) suggest that in a healthy subject poisoned by long CO exposures, the O_2 levels and CO levels in the body are restored to control or pre- CO exposure values within 6 hr of treatment on NBO_2 .

Analysis of results from simulation sets 1 and 2, suggests that administering HBO_2 after ${}^6 \text{hr} NBO_2$ will have no additional benefits of improving O_2 delivery and CO removal in healthy subjects exposed to long or short durations of varying CO concentrations. Thus, for HBO_2 to have merit in treating a CO poisoned victim, this treatment may have to be applied within ${}^6 \text{hr} NBO_2$. To determine the maximum duration of NBO_2 after which administered HBO_2 therapy may still have a favorable effect in improving O_2 delivery to the tissues and speeding removal of CO from the body, simulation set 3 was performed.

Results of simulation set 3: In this simulation set, three subjects were exposed to CO levels of three different concentrations (6400, 8000, and 10000 ppm) for a duration of 20 min (See Table 4.6A-C for $\%HbCO$ levels). At the end of CO exposure, the subject was treated with one of the three different treatment protocols: (i) 2 hr NBO_2 followed by 1.5 hr HBO_2 at 3 ATA (${}^2 \text{hr} NBO_2 - {}^{1.5} \text{hr} HBO_2$), (ii) 3 hr NBO_2 followed by 1.5 hr HBO_2 at 3 ATA (${}^3 \text{hr} NBO_2 - {}^{1.5} \text{hr} HBO_2$) or (iii) 4 hr NBO_2 followed by 1.5 hr HBO_2 at 3 ATA (${}^4 \text{hr} NBO_2 - {}^{1.5} \text{hr} HBO_2$). The variables useful in assessing the state of O_2 delivery in the tissues and CO removal from the body during the treatments (${}^6 \text{hr} NBO_2$, ${}^2 \text{hr} NBO_2 - {}^{1.5} \text{hr} HBO_2$, and ${}^3 \text{hr} NBO_2 - {}^{1.5} \text{hr} HBO_2$) after different severities of CO poisoning are listed in Table 4.6A-C. In all the simulations of set 3, the treatment for the initial two hours after end of CO exposure was on NBO_2 and hence the $t_b P_{THO_2}$, $t_c P_{THO_2}$, and $t_m P_{THO_2}$ were not calculated for this simulation set (as they would be similar to that of ${}^6 \text{hr} NBO_2$). Thus in this simulation set, the criterion for determining the best treatment is based on $CO_{\text{body}} T_{1/2}$ and $T_{\%HbCO < 10}$ (as values for $t_b P_{THO_2}$, $t_c P_{THO_2}$, and $t_m P_{THO_2}$ are the same). The $CO_{\text{body}} T_{1/2}$ and $T_{\%HbCO < 10}$ values for treatment with ${}^4 \text{hr} NBO_2 - {}^{1.5} \text{hr} HBO_2$ were not different from the values with treatment on ${}^6 \text{hr} NBO_2$ (Table 4.6A-C). Also, the goodness of fit for the CO washout curves (CO_{body}) to fit the exponential functions ($Ae^{bt} + De^{ct}$) was statistically

poor. Thus, the early and late time constants were not calculated for this simulation set. On analysis of the results from this simulation set, the maximum duration of NBO₂ after which administering HBO₂ therapy may still have a favorable effect in improving O₂ delivery to the tissues and speeding removal of CO from the body is suggested as 3 hr for %HbCO levels <50. For CO poisonings resulting in %HbCO levels >50, the maximum duration of NBO₂ can be suggested as 3 hr. Thus for any severity of poisoning when compared to ^{6hr}NBO₂, treatments on ^{2hr}NBO₂-^{1.5 hr}HBO₂ suggests faster removal of CO from the tissues and the maximum duration of NBO₂ after which administering HBO₂ therapy may still have a favorable effect in speeding removal of CO from the body is suggested as 3 hr.

Results of simulation set 4: This simulation set was performed to test my hypothesis that “irrespective of the poisoning severity treating an otherwise-healthy CO poisoned victim with isocapnic (normocapnic) NBO₂ will always have a favorable effect in improving O₂ delivery and enhancing CO removal, when compared to treating the victim with poikilocapnic NBO₂”. Three subjects were exposed to three different concentrations of CO levels (6400, 8000, and 10000 ppm) for a duration of 20 min and the end of CO exposure was followed by a treatment with NBO₂ for 6 hr while maintaining isocapnia at the normocapnic level of the subject (^{6 hr}INBO₂). The durations for which the PO₂'s in the tissues are less than P_{TH}O₂ (t_c<P_{TH}O₂) is greater for the higher %HbCO levels and the values for t_bP_{TH}O₂ are similar for all the treatments for any severity of poisoning (Table 4.6A-C). For %HbCO levels <50, the values for t_cP_{TH}O₂ are smaller in ^{6 hr}INBO₂ than all other treatments, suggesting faster O₂ delivery to cardiac tissues during ^{6 hr}INBO₂. It is to be noted that t_bP_rO₂ in ^{2 hr}NBO₂-^{1.5 hr}HBO₂ is always less than t_bP_rO₂ in ^{6 hr}INBO₂, indicating a smaller suggested treatment duration in ^{2 hr}NBO₂-^{1.5 hr}HBO₂. Simulation results (Table 4.6A-C) suggests that for an otherwise-healthy CO poisoned subject with any degree of poisoning severity, ^{6 hr}INBO₂ is the best treatment strategy to ensure faster CO removal from the body when compared to treatments on ^{6 hr}NBO₂, ^{3 hr}NBO₂-^{1.5 hr}HBO₂ or ^{4 hr}NBO₂-^{1.5 hr}HBO₂. Thus, treating an otherwise-healthy CO poisoned victim with ^{6hr}INBO₂ is the best treatment to be administered.

Overall analysis of results from simulation sets 1-4 suggests that treating an otherwise-healthy human subject with hyperbaric oxygen immediately after a treatment on normobaric oxygen for 6 hr, may not have any benefits of improving oxygen delivery to the tissues or removal of *CO* from the body. Also, normocapnic normobaric oxygen (INBO₂) treatment seems to be a promising therapy to allow fast removal of *CO* from the body and thereby improve oxygen delivery to the tissues. In cases of high *CO* exposures (%HbCO >50%), treating an otherwise-healthy subject with HBO₂ (followed by <4 hr of treatment on NBO₂) or normocapnic NBO₂ is suggested. In cases of *CO* exposures of %HbCO <50, treating an otherwise-healthy subject with INBO₂ is suggested.

DISCUSSION

In this study, a validated mathematical model was used to compare O₂ delivery and *CO* removal during three treatments namely NBO₂, HBO₂ and INBO₂ administered after varying severities of *CO* poisoning in healthy subjects. The time varying tissue PO₂'s in the second compartments of the brain, heart and skeletal muscle were assumed as correlates of state of oxygenation during *CO* exposure and treatments. The time taken by the treatment to remove 50% of the *CO* from the body and to reach %HbCO levels <10% were the criterion to determine the efficacy of a treatment to remove *CO* during the course of the treatment.

Treatment for short vs. long CO exposures: A 6 hr, NBO₂ treatment was simulated immediately after short or long *CO* exposures in 6 healthy subjects. The inhaled concentrations of *CO* were intended to achieve similar %HbCO levels in a given subject at the end of exposure irrespective of the duration of the exposure. In 3 (S108, S112, S120) of the 6 subjects, similar %HbCO levels were reached at the end of short and long *CO* exposures. At the end of short *CO* exposures, the model predicted that 3 of the 6 subjects may be unconscious and 5 of the 6 subjects may have mild functional impairments. At the end of long *CO* exposures, 5 out of 6 subjects are predicted to be unconscious and 6 subjects may have severe functional impairments (as the tissue PO₂'s < 15 Torr for a longer duration). Despite similar %HbCO levels compared to a long duration *CO* exposure, less *CO* diffuses into the tissues and the increases in cardiac

output and blood flow to other tissues is faster (due to rapidly increasing %HbCO) during a short CO exposure (Bruce et al, 2008; Erupaka et al., 2010). Thus, the values for $t_b < P_{TH}O_2$, $t_c < P_{TH}O_2$ and $t_r < P_{TH}O_2$ were larger during long CO exposures compared to short CO exposures. During treatment on ${}^6 \text{ hr NBO}_2$, time taken to reach tissue PO_2 's above $P_{TH}O_2$ were greater in a treatment following long CO exposure compared to the short CO exposure (especially heart tissue). Prior to treatment, the tissue was hypoxic for a longer duration in long CO exposure. During CO exposure, the model predicted PCO_2 's in the cardiac and muscle tissue compartments are increasing. Greater extent of accumulation of metabolites like CO_2 in the tissues and decreases in pH as a consequence of prolonged tissue hypoxia may be a contributing factor for larger values of $tP_{TH}O_2$ in long CO exposures. Irrespective of the duration of exposure, the times taken to reach PrO_2 's in the tissues were similar during treatment on ${}^6 \text{ hr NBO}_2$ for a short or a long CO exposure. During treatment on ${}^6 \text{ hr NBO}_2$, removal of CO from the body followed by long and short CO exposures was not different (Table 4.5). As the O_2 delivery to tissues and CO removal from the body was similar during treatment on ${}^6 \text{ hr NBO}_2$ followed by short or long CO exposure, other treatments (${}^6 \text{ hr INBO}_2$, ${}^2 \text{ hr NBO}_2$ - ${}^{1.5} \text{ hr HBO}_2$, etc), were not simulated for a long CO exposure.

Suggested tissue specific treatments: In this study, oxygen delivery to the brain, heart and muscle tissues during various treatments after varying levels of poisoning severity (Table 4.6A-C) were assessed. For an otherwise- healthy CO poisoned subject, irrespective of the poisoning severity, the time to reach $P_{TH}O_2$ are similar in all treatments. However, treatment on ${}^2 \text{ hr NBO}_2$ - ${}^{1.5} \text{ hr HBO}_2$ has the advantage of availability of larger concentrations of dissolved O_2 when compared to treatments with ${}^6 \text{ hr NBO}_2$ or ${}^6 \text{ hr INBO}_2$. The advantage of enhanced O_2 delivery with treatment on ${}^6 \text{ hr INBO}_2$ over treatment with ${}^6 \text{ hr NBO}_2$ or other treatments (${}^2 \text{ hr NBO}_2$ - ${}^{1.5} \text{ hr HBO}_2$, ${}^3 \text{ hr NBO}_2$ - ${}^{1.5} \text{ hr HBO}_2$, ${}^4 \text{ hr NBO}_2$ - ${}^{1.5} \text{ hr HBO}_2$) are due to greater blood flows to the tissues and hyperventilation during isocapnia (Figure 4.1). Poikilocapnic hyperoxic treatments are accompanied with decreases in blood flow due hypocapnia and hyperoxia induced vasoconstriction. Maintaining isocapnia at the normoxic levels eliminates the effects of hypocapnia induced decreases in blood flow, thereby improving O_2 delivery to the tissues. Considering the difficulty and cost of administering any HBO₂ treatment (especially

within 2 hr of NBO₂), ^{6 hr}INBO₂ seems to be the suggested treatment of choice. At the end of treatment, when compared to ^{6 hr}NBO₂, treatment with ^{4hr}NBO₂-^{1.5 hr}HBO₂ seems to improve O₂ delivery to the brain tissues but not the heart or skeletal muscle tissues, thereby suggesting advantages of using HBO₂ to treat unconscious subjects or subjects showing symptoms of neurological impairments on admission (Table 4.6A-C). For the same level of CO poisoning severity administering ^{6 hr}INBO₂ allows faster O₂ delivery to the heart and muscle tissues when compared to treatment with ^{6 hr}NBO₂ ^{3hr}NBO₂-^{1.5 hr}HBO₂, or ^{4 hr}NBO₂-^{1.5 hr}HBO₂ (Table 4.6A-C). This could be due to faster removal of CO₂ and CO from the tissues containing myoglobin due to increased blood flows and increased ventilation in isocapnia compared to poikilocapnia. Thus, subjects showing cardiovascular abnormalities on admission should be treated with ^{6 hr}INBO₂ to ensure faster O₂ delivery to the heart tissues.

Suggested treatments for fast CO removal: The goal of any treatment administered after CO poisoning is to improve tissue oxygenation and enhance elimination of CO. Except for treatment on room air, administering NBO₂, INBO₂ or HBO₂ rapidly increases the tissue PO₂'s during treatment. Irrespective of the duration and severity of poisoning, the maximum time taken by the tissues to reach PO₂'s above P_{TH}O₂ is ~30 min (Table 4.5, 4.6A-C). But the half time elimination of CO on breathing room air, NBO₂ and HBO₂ at 3 ATA are ~ 320 min, 80 min and 23 min, respectively (Myers et al., 1985). Considering the difficulty of administering HBO₂ immediately after CO poisoning, emphasis of determining an efficient treatment should be based on its capability to quickly remove CO. In this study among the treatments compared (Table 4.5, 4.6A-C) for any level of poisoning severity in a healthy subject, the treatment with the fastest CO_{body} T_{1/2} and T_{%HbCO<10} was found to be for ^{6 hr}INBO₂. A %HbCO of 10 was chosen as the adverse effects of exposure at these levels are reported to be minimal in humans (Rucker et al., 2002; Stewart, 1975). This treatment allows faster elimination of CO due to hyperventilation and increases in blood flow, when compared to other treatments analyzed in this study.

Suggested treatments for otherwise healthy CO poisoned subjects: Analysis of simulation sets 1-4, suggests that INBO₂ is the best treatment available to ensure fast O₂ delivery and

removal of CO from the body. For high %HbCO levels, my study confirms the findings of Fisher et al. (1999) and Rucker et al. (2002) for otherwise-healthy CO poisoned male subjects. Treatment with $2\text{ hr NBO}_2\text{-}1.5\text{hr HBO}_2$ also improves O_2 delivery and enhances removal of CO from the body. But the superiority of INBO₂ is established over HBO₂ considering the limited availability of hyperbaric chambers in hospitals, cost of administering HBO₂, complications like barotrauma, claustrophobia arising from hyperbaric treatment (Juurlink et al., 2005) and faster removal of CO in INBO₂ when compared to HBO₂. It may also be hypothesized that maintaining isocapnia at levels 2-3 Torr greater than normocapnia (i.e., hypercapnic NBO₂) will prove to be more beneficial in ensuring fast O_2 delivery and removal of CO from the body as the increase in blood flow and ventilation will be greater in hypercapnic NBO₂ when compared to normocapnic NBO₂. I also hypothesize that hypercapnic HBO₂ or normocapnic HBO₂ will be highly beneficial in CO poisoning cases with high %HbCO levels as it would have the advantage of availability of high concentrations of dissolved O_2 in addition to increases in blood flow and ventilation. However, in CO poisoned patients with depressed ventilation or cardiovascular impairments at the time of hospital admission, INBO₂ may not be the suggested treatment (reasons discussed below).

Anticipated suggestions for treating high risk CO poisoned populations: Groups especially susceptible to the hypoxic stress of CO exposure would potentially be individuals with anemia (decreased hemoglobin content) (Penney, 1988; Weaver et al., 2002) and individuals with cardiovascular or coronary artery diseases (Penney, 1988; Raub et al., 2000; Satran et al., 2005; Stewart et al., 1973). These groups are assumed to be at increased risk because of the anticipated reduced (O_2 delivering) capacity to accommodate hypoxic stress caused due to CO . In these patients, the regulatory mechanisms are already activated in basal conditions to compensate the dysfunction and depending on the severity additional compensation during CO exposure may be difficult. Based on the simulation results, it is suggested that the anemic patient populations should be treated with INBO₂. Compared to NBO₂, the increases in blood flow to vital organs (like brain and heart) and ventilation are greater in INBO₂. Despite decreased O_2 delivering capacity due to low hemoglobin levels, treating anemic populations with INBO₂ compared to NBO₂ will increase O_2 delivery and CO removal (Figure 4.1).

However, treatment with INBO₂ is not suggested for CO poisoned patients with cardiovascular or coronary artery diseases. This is because during INBO₂ treatment, there is an increased work load on heart as the cardiac output and myocardial blood flow is increased (Figure 4.1). This increased workload may lead to myocardial injury in these patient populations during treatment. Thus it is anticipated that NBO₂ or HBO₂ may be a better treatment than INBO₂.

Also, there is evidence that healthy humans who are chronically or acutely exposed to CO under high work loads or physical stress (like exercise) have an increased risk for morbidity and mortality (Koskela, 1994; Stern et al., 1981). Groups exposed to CO during exercise are at increased risk of tissue injury, because the hypoxic stress on tissues due to increased O₂ demands (increased O₂ consumption) will increase. Also in conditions of exercise, there is increased uptake of CO due to increases in blood flow to the tissues and ventilation. In these populations, if the patients do not exhibit cardiovascular abnormalities or depressed ventilation at the time of hospital admission, then INBO₂ may be the preferred treatment over NBO₂ or HBO₂.

Other populations susceptible to hypoxic stress of CO exposure are the fetus, pregnant women (Penney, 1988; Weaver et al., 2002), and patients with obstructive lung diseases, cerebrovascular and peripheral vascular diseases. For patient populations with cerebrovascular and peripheral vascular diseases, INBO₂ may be the preferred treatment over NBO₂ due to the advantage of increased cerebral oxygenation (Figure 4.1). Patients with obstructive lung diseases should be treated with either NBO₂ or HBO₂, as INBO₂ is accompanied with increases in ventilation. In these patient populations flow of air in and out of the lungs is either impaired or limited and additional increases in ventilation during treatment on INBO₂ may have deleterious effects. The effects of INBO₂ on the human fetus and pregnant women are not known. Thus it would be difficult to suggest a treatment for these patient populations.

Limitations of the study: The foremost limitation of this study is lack of availability of experimental data to compare tissue O₂ levels in various tissues during high CO exposures and various treatments. Model predictions of possibility of occurrence of

unconsciousness or functional impairments are based on P_{THO_2} estimated by the model for tissues representing an average brain, heart or skeletal muscle. The model estimated times for $t < P_{THO_2}$, tP_{THO_2} or tP_{rO_2} during different *CO* exposures and treatments may either be an overestimate or underestimate in certain regions of the brain, heart or muscle tissues (cortex, gray matter, endocardium, epicardium, lower limb muscles, etc) with statistically significant differences in blood flow, oxygen consumption, capillary density, etc. Considering this limitation, I interpret my results with acknowledging the fact that the values for P_{THO_2} , $t < P_{THO_2}$, tP_{THO_2} or tP_{rO_2} may be poor approximations of the actual values.

During *CO* exposures, cardiac output and blood flow to tissues (brain, heart and muscle) increases as a function of %HbCO (Equations 3.18-3.17 of Chapter 3). These increases in blood flow are attributed to the vasodilatory effects of *CO*. Also, during treatment it is not known if the hyperoxia and hypocapnia induced vasoconstriction, compensates the vasodilatory effects of *CO*. The regression equations were developed from animal and human data during or at the end of *CO* exposure (Chapter 3). Contribution of *CO* to increases in blood flow during various treatments is not known. Rucker et al. (2002) compared brain blood flow during NBO_2 and $INBO_2$ in humans after a *CO* exposure resulting in ~10 %HbCO. The blood flow in this study decreased during the normocapnic treatment but the fall was not rapid, indirectly suggesting the possibility of the presence of vasodilatory effect of *CO* during treatment. However the contribution of *CO* to increases in blood flow at 10% HbCO may be smaller compared to a high %HbCO level (>25). For very high %HbCO levels (>50), the estimates of blood flows from the regression equations may be overestimating the increases in blood flow. Thus the uptake and removal of *CO* during *CO* exposure and treatment for the highest exposure level in this study may be underestimating the values for $CO_{body} T_{1/2}$, $T_{\%HbCO < 10}$, $t < P_{THO_2}$, tP_{THO_2} or tP_{rO_2} .

In this study O_2 delivery and *CO* removal was compared in healthy, adult, male subjects exposed to different concentrations and durations of *CO*. Treatments to ensure fast O_2 delivery and *CO* removal were suggested for otherwise-healthy *CO* poisoned, adult, male subjects. I hypothesize that the suggested treatments in this study will be

applicable to (i) otherwise-healthy *CO* poisoned, adult, nonpregnant, female subjects, (ii) anemic subjects, (iii) otherwise-healthy, elderly *CO* poisoned subjects, and (iv) subjects with coronary artery disease, cerebrovascular or peripheral vascular diseases. Applicability of the suggested treatments to enhance O_2 delivery or *CO* removal in other populations like the fetus, infants, children, pregnant women and patients with obstructive lung diseases is not predictable due to the complexity involved in the adaptation mechanisms in these groups. Also variations in treatments like administering $<100\%$ O_2 (in ambulance), room air (removing victim from site of *CO* exposure) or HBO_2 at lower atmospheric pressures have not been simulated in this study. Even if these variations were simulated, the treatments suggested in this study will still be the best therapies to treat otherwise-healthy *CO* poisoned subjects.

CONCLUSIONS

The main goal of my study was to compare NBO_2 , HBO_2 and normocapnic NBO_2 to determine the best treatment strategy ensuring fastest *CO* removal and O_2 delivery after *CO* poisoning in healthy subjects. A validated mathematical model was used to compare these treatments after exposure to *CO* of different durations and concentrations. Among the treatments compared, analysis of my simulation results suggests that normocapnic normobaric oxygen ($INBO_2$) is the best treatment available to ensure fast O_2 delivery and removal of *CO* from the body. Physicians and care givers should consider treating otherwise-healthy *CO* poisoned victims with normocapnic normobaric oxygen instead of poikilocapnic normobaric oxygen. Also, clinical trails should be conducted comparing the merits of treating *CO* poisoned victims with NBO_2 and $INBO_2$.

SUMMARY

Carbon Monoxide (*CO*) is responsible for a large number of accidental and intentional poisonings reported throughout the world. *CO* produces tissue toxicity by impairing oxygen (O_2) delivery to the tissues. Treatments for *CO* poisoned victims involve administering supplemental O_2 at normal (NBO_2) or high pressures (HBO_2). The merits of NBO_2 or HBO_2 with regards to improving O_2 delivery to the tissues and removing *CO* from the body during the treatments are not known. In this study, I use a

validated mathematical model to compare O_2 delivery and CO removal during three different treatments (NBO_2 , HBO_2 and isocapnic NBO_2). In my simulations, these treatments are administered immediately after exposure to long or short durations of varying CO concentrations. Analysis of the results of various simulations of treatments followed after varying severities in CO poisoning suggests that among the treatments compared, isocapnic NBO_2 is the most efficient therapy to ensure faster O_2 delivery to the tissues and CO removal from the body.

Table 4.1: Questions related to CO poisoning treatments

1. Are there any merits of treating otherwise-healthy *CO* poisoned subjects with HBO₂ after a 6 hr treatment of NBO₂?
2. For otherwise-healthy *CO* poisoned subjects, what is the maximum duration of NBO₂ after which administered HBO₂ therapy may still have a favorable effect in improving O₂ delivery to the tissues and speeding removal of *CO* from blood and tissues?
3. For otherwise-healthy *CO* poisoned subjects, are there any benefits of treating with normocapnic NBO₂ over poikilocapnic NBO₂?
4. Among the therapies available (NBO₂, HBO₂, normocapnic NBO₂) to treat otherwise-healthy *CO* poisoned subjects, which is the best treatment strategy that will ensure fastest *CO* removal and O₂ delivery during treatment?

Subject	*MRO ₂ , ml/min/Kg	Cardiac output (\dot{Q}), L/min	Blood volume (V _B), L	Muscle mass (V _M), Kg	⁺ DMCO, ml/min/Torr
115	240	6.6	5.1	31.8	7.19
108	194	7.5	4.0	28.0	6.34
112	320	6.7	5.3	38.8	8.80
118	167	5.1	3.5	25.6	5.81
119	285	6.9	6.9	36.2	8.20
120	231	5.8	4.4	31.3	7.08

* Total body oxygen consumption; ⁺ Muscle diffusion coefficient of *CO*

Table 4.3: Symbols and Definitions	
Symbol	Definition
P_{THO_2}	Threshold PO_2 , the PO_2 below which unconsciousness or other functional impairments in the tissues may occur.
$t < P_{THO_2}$	Before treatment, duration for which PO_2 is below P_{THO_2} in the brain tissue
$t < P_{THO_2}$	Before treatment, duration for which PO_2 is below P_{THO_2} in the heart tissue
$t < P_{THO_2}$	Before treatment, duration for which PO_2 is below P_{THO_2} in the muscle tissue
$t_b P_{THO_2}$	Time taken by a treatment to reach a PO_2 above P_{THO_2} in the brain tissue
$t_c P_{THO_2}$	Time taken by a treatment to reach a PO_2 above P_{THO_2} in the heart tissue
$t_m P_{THO_2}$	Time taken by a treatment to reach a PO_2 above P_{THO_2} in the muscle tissue
$P_r O_2$	Control or pre-CO exposure tissue PO_2 .
$t_b P_r O_2$	Time taken by a treatment to reach a PO_2 above $P_r O_2$ in the brain tissue
$t_c P_r O_2$	Time taken by a treatment to reach a PO_2 above $P_r O_2$ in the heart tissue
$t_m P_r O_2$	Time taken by a treatment to reach a PO_2 above $P_r O_2$ in the muscle tissue
CO_{blood}	Total CO blood burden (CO in all vascular compartments of the model)
CO_{tissue}	Total CO tissue burden (CO in all the tissue compartments of the model)
CO_{body}	Total CO body burden (CO in the blood and tissue compartments and the lungs)
$CO_{body} T_{1/2}$	Time taken by a treatment to remove 50% of the total CO body burden
$T_{\%HbCO < 10}$	Time taken by a treatment to reach %HbCO levels <10

Table 4.4: %HbCO levels at the end of CO exposure		
Subject	*Short, %HbCO	+Long, %HbCO
115	37.48	40.72
108	42.01	42.97
112	44.79	44.21
118	39.40	41.66
119	34.04	38.61
120	43.74	43.67

* Short CO exposure = 6400 ppm, 20 min; + Long CO exposure = 450 ppm, 480 min

Variable (Mean ±SD)	*Short exposure	+Long exposure
%HbCO	40.2±4.1	41.9±2.1
t _b P _r O ₂ , min	286±23	303±19
t _c P _r O ₂ , min	250±18	265±23
t _m P _r O ₂ , min	166±7.1	180±16
CO _{body} T _{1/2} , min	84.1±11	83.9±11
T %HbCO<10, min	167±7.9	179±14
τ _e , min	40.2±6.5	43.9±6
G _e	80.9±18	97.6±22
τ _l , min	149±17	151±18
G _l	417±81	459±101

* Short CO exposure = 6400 ppm, 20 min; + Long CO exposure = 450 ppm, 480 min

Variable	#%HbCO=37.5				%HbCO=46.7				&%HbCO=56.8			
	T ₁	T ₂	T ₃	T ₄	T ₁	T ₂	T ₃	T ₄	T ₁	T ₂	T ₃	T ₄
Treatment*	T ₁	T ₂	T ₃	T ₄	T ₁	T ₂	T ₃	T ₄	T ₁	T ₂	T ₃	T ₄
t _b P _r O ₂ , min	312	127	184	139	340	135	185	159	360	139	186	182
t _c P _r O ₂ , min	272	200	245	165	296	210	253	190	320	210	260	210
t _m P _r O ₂ , min	176	128	168	111	199	131	186	135	225	133	187	157
t _b <P _{TH} O ₂ , min	0	0	0	0	4	4	4	4	7	7	7	7
t _c <P _{TH} O ₂ , min	1.4	1.4	1.4	1.4	8	8	8	8	10	10	10	10
t _m <P _{TH} O ₂ , min	1.3	1.3	1.3	1.3	9	9	9	9	10	10	10	10
t _b P _{TH} O ₂ , min	0	0	0	0	3	3	3	4	16	16	16	18
t _c P _{TH} O ₂ , min	1.5	1.5	1.5	1	15	15	15	5	35	35	35	35
t _m P _{TH} O ₂ , min	1.5	1.5	1.5	3	6.5	6.5	6.5	22	15	15	15	3
CO _{body} T _{1/2} , min	91.	92.	92.	66.	85.	85.	85.	67.	78.	78.	78.5	69.4
T %HbCO<10, min	175	143	175	120	202	152	191	142	222	158	198	163

*T₁= CO exposure followed by treatment on NBO₂ for 6 hr (⁶hrNBO₂)

*T₂= CO exposure followed by treatment on NBO₂ for 2 hr followed by 1.5 hr (90 min) treatment on HBO₂ at 3ATA (²hrNBO₂-^{1.5}hrHBO₂).

*T₃= CO exposure followed by treatment on NBO₂ for 3 hr followed by 1.5 hr (90 min) treatment on HBO₂ at 3ATA (³hrNBO₂-^{1.5}hrHBO₂).

*T₄= CO exposure followed by treatment on isocapnic NBO₂ for 6 hr (⁶hrINBO₂)

Exposure to 6400 ppm of CO for 20 min

§ Exposure to 8000 ppm of CO for 20 min

& Exposure to 10000 ppm of CO for 20 min

Variable	#%HbCO=39.4				%HbCO=48.9				&%HbCO=59			
Treatment*	T ₁	T ₂	T ₃	T ₄	T ₁	T ₂	T ₃	T ₄	T ₁	T ₂	T ₃	T ₄
t _b P _r O ₂ , min	272	126	184	135	300	132	185	154	315	134	186	163
t _c P _r O ₂ , min	254	197	244	145	280	205	247	198	300	208	257	209
t _m P _r O ₂ , min	164	129	186	99	187	128	185	115	200	127	184	130
t _b <P _{TH} O ₂ , min	0	0	0	0	4.5	4.5	4.5	4.5	7.5	7.5	7.5	7.5
t _c <P _{TH} O ₂ , min	6	6	6	6	9	9	9	9	11	11	11	11
t _m <P _{TH} O ₂ , min	4	4	4	4	9.5	.5	9.5	9.5	10.5	10.5	10.5	10.5
t _b P _{TH} O ₂ , min	0	0	0	0	4	4	4	4	15	15	15	17
t _c P _{TH} O ₂ , min	6	6	6	4	10	10	10	6	15	15	15	13
t _m P _{TH} O ₂ , min	4	4	4	4	9.5	9.5	9.5	9	10.5	10.5	10.5	11
CO _{body} T _{1/2} , min	80.	80.	80.	52.	74.	74.	74.	53.	68	67.	67.8	54.5
T %HbCO<10, min	159	137	160	94	182	144	182	141	199	149	190	153

*T₁= CO exposure followed by treatment on NBO₂ for 6 hr (⁶hrNBO₂)

*T₂= CO exposure followed by treatment on NBO₂ for 2 hr followed by 1.5 hr (90 min) treatment on HBO₂ at 3ATA (²hrNBO₂-^{1.5}hrHBO₂).

*T₃= CO exposure followed by treatment on NBO₂ for 3 hr followed by 1.5 hr (90 min) treatment on HBO₂ at 3ATA (³hrNBO₂-^{1.5}hrHBO₂).

*T₄= CO exposure followed by treatment on isocapnic NBO₂ for 6 hr (⁶hrINBO₂)

Exposure to 6400 ppm of CO for 20 min

§ Exposure to 8000 ppm of CO for 20 min

& Exposure to 10000 ppm of CO for 20 min

Variable	#%HbCO=34				%HbCO=42.3				&%HbCO=51.4			
Treatment*	T ₁	T ₂	T ₃	T ₄	T ₁	T ₂	T ₃	T ₄	T ₁	T ₂	T ₃	T ₄
t _b P _r O ₂ , min	309	126	184	140	340	135	185	160	350	137	186	180
t _c P _r O ₂ , min	261	193	236	160	295	203	241	182	315	207	249	205
t _m P _r O ₂ , min	170	128	185	170	200	131	186	130	225	135	187	153
t _b <P _{TH} O ₂ , min	0	0	0	0	1.5	1.5	1.5	1.5	5	5	5	5
t _c <P _{TH} O ₂ , min	0	0	0	0	4	4	4	4	7	7	7	7
t _m <P _{TH} O ₂ , min	3.5	3.5	3.5	3.5	7	7	7	7	9.5	9.5	9.5	9.5
t _b P _{TH} O ₂ , min	0	0	0	0	1	1	1	1	7	7	7	8
t _c P _{TH} O ₂ , min	0	0	0	0	2.5	2.5	2.5	2	10	10	10	9
t _m P _{TH} O ₂ , min	2	2	2	2	3.5	3.5	3.5	3.5	10	10	10	11
CO _{body} T _{1/2} , min	103	103	103	73	97	97	97	73.5	90	89.8	89.8	74.2
T %HbCO<10, min	179	145	180	122	209	155	195	145	232	163	203	167

*T₁= CO exposure followed by treatment on NBO₂ for 6 hr (⁶hrNBO₂)

*T₂= CO exposure followed by treatment on NBO₂ for 2 hr followed by 1.5 hr (90 min) treatment on HBO₂ at 3ATA (²hrNBO₂-^{1.5}hrHBO₂).

*T₃= CO exposure followed by treatment on NBO₂ for 3 hr followed by 1.5 hr (90 min) treatment on HBO₂ at 3ATA (³hrNBO₂-^{1.5}hrHBO₂).

*T₄= CO exposure followed by treatment on isocapnic NBO₂ for 6 hr (⁶hrINBO₂)

Exposure to 6400 ppm of CO for 20 min

§ Exposure to 8000 ppm of CO for 20 min

& Exposure to 10000 ppm of CO for 20 min

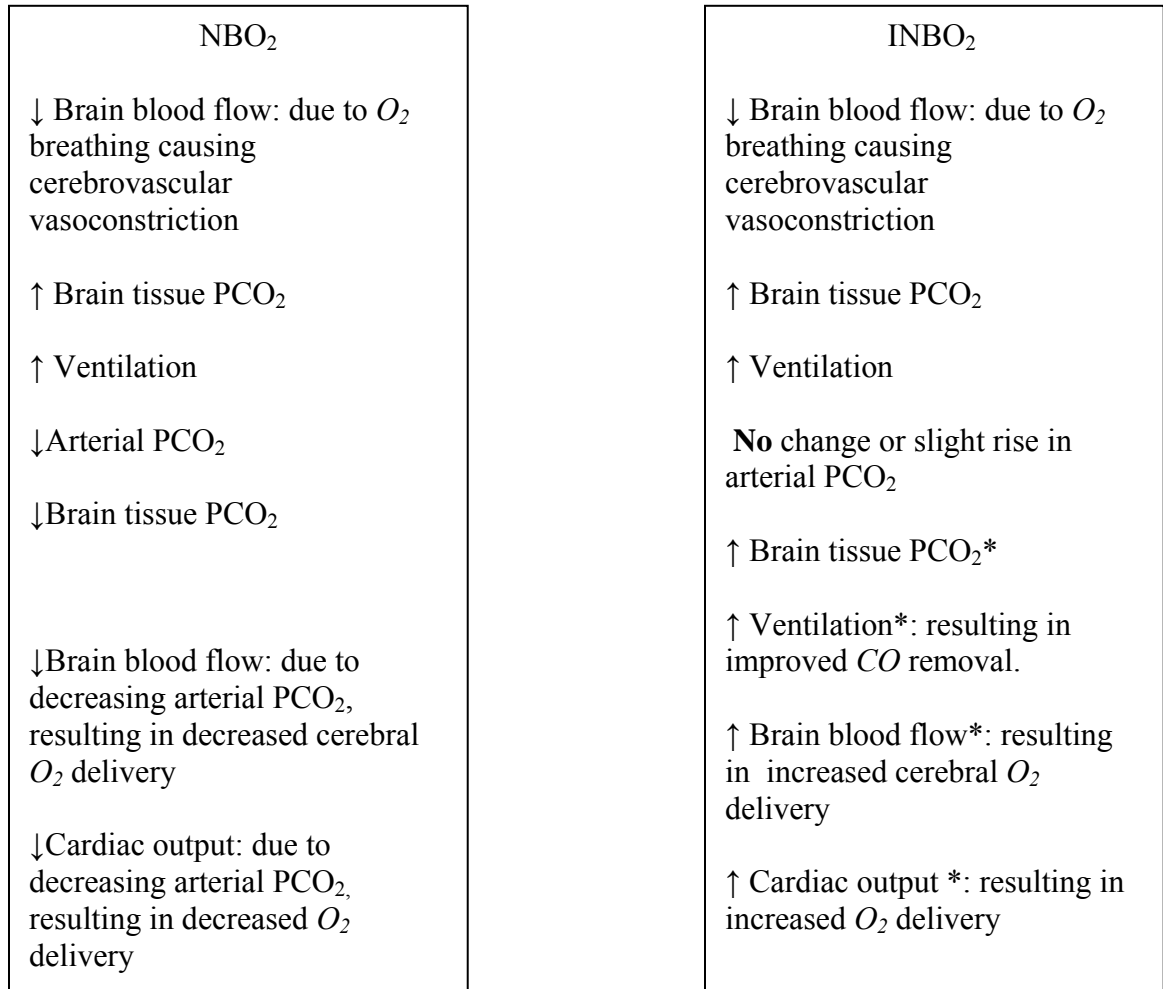


Figure 4.1: Poikilocapnic normobaric oxygen (NBO₂) vs. Isocapnic normobaric oxygen (INBO₂). * INBO₂ is administered using a mixture of 98% O₂ + 2% CO₂ and inspiration of CO₂ is accompanied with increases in brain blood flow, brain tissue PCO₂'s, and ventilation.

Chapter 5: Conclusions and Future work

CONCLUSIONS

In my dissertation, I have applied validated mathematical models (Erupaka et al., 2010, second specific aim) of human systems to understand and analyze physiological mechanisms in situations where experiments either provide limited information about the physiological process (first specific aim) or are unethical (third specific aim). I hypothesized that “accurately estimating the amount of *CO* bound to myoglobin during and after *CO* inhalation will (i) allow improving the accuracy of *CO*-rebreathing methods to determine hemoglobin mass and (ii) aid in suggesting treatments ensuring fast *CO* removal from the body.” As determination of amount of *CO* bound to myoglobin is difficult because non-invasive measurements of *MbCO* are not possible, a mathematical model was enhanced to address knowledge gaps in the literature. My dissertation has given me the opportunity to (i) analyze *CO*-rebreathing techniques used to estimate total hemoglobin mass, (ii) develop and validate a multicompartment model to compare *O*₂ delivery and *CO* removal during different treatments administered after *CO* poisoning and (iii) analyze treatment protocols for otherwise-healthy *CO*-poisoned subjects.

My project 1 (first specific aim) is the first study to determine the sources of errors in the existing *CO* rebreathing methods to estimate hemoglobin mass, M_{Hb} . Inaccuracies in estimation of volume of *CO* bound to myoglobin were determined as the major source of error. The existing *CO* rebreathing methods are used to estimate M_{Hb} to determine the effects of adaptation to exercise training, environmental stresses, illness or trauma. Also, reference ranges of M_{Hb} are developed for athletic and clinical purposes. The errors in estimation of hemoglobin mass from the current *CO* rebreathing methods were in the range of 2%-6% depending on the blood site sampled, *CO* rebreathing method applied, and intersubject variability. These errors suggest that in order to compare the mean M_{Hb} values among different studies and to develop accurate reference ranges for M_{Hb} , information about the source of error and the approximate magnitude of errors associated with each *CO* rebreathing method and sampling site should be considered. Thus, determining the magnitude and sources of errors in the existing *CO* rebreathing methods to estimate M_{Hb} is vital in interpreting and comparing the results of different

studies done in clinical and sports medicine. Also, if the errors in estimation of M_{Hb} are small then significant changes in M_{Hb} can be easily detected with a smaller population size, whereas a larger population is needed to detect significant changes with a method which has larger errors. Using a validated mathematical model to estimate the amount of CO bound to myoglobin during and after CO inhalation aided in improving the accuracy of CO -rebreathing methods to determine hemoglobin mass. Based on the simulation results, I have suggested modifications to the existing CO rebreathing methods to estimate total hemoglobin mass with low errors (Protocols $B_{modified}$ and $P_{modified}$). The proposed modifications to these methods were to use the suggested (i) regression equations to estimate volume of CO bound to myoglobin, (ii) T_{sample} 's, and (iii) blood sites. I have also proposed a new CO rebreathing method to estimate hemoglobin mass with low errors (Protocol N). In this study, I have made an attempt to understand the reasons for variability in the values reported in the literature for hemoglobin mass (M_{Hb}) estimates and mixing times from CO rebreathing studies differing in methods, durations of CO rebreathing, initial dose of CO administered and recruited subjects. I have also suggested optimal blood sites and sampling times to estimate hemoglobin mass with low errors. Making use of the optimal sampling time and blood site to obtain estimates of hemoglobin mass will make the CO rebreathing methods less inconvenient to the subject, and inexpensive. Following suggestions for shorter CO rebreathing durations will make these procedures easy to perform. In conclusion, estimating hemoglobin mass with modified versions of the existing CO rebreathing methods or the proposed new method will be less inconvenient to the subject, inexpensive, reliable, accurate, easy to perform and will make comparison of hemoglobin mass among different studies possible.

The mathematical model developed in my project 2 (second specific aim) is a significant contribution to the database of mathematical models. Significant enhancements made to my previous upgraded model (Erupaka et al., 2010) are addition of: (i) brain compartment (Figure 3.1), (ii) mass balance equations for CO_2 , (iii) control of ventilation, (iv) regulation of blood flow: cardiac output, cerebral blood flow, myocardial blood flow, skeletal muscle tissue and non-muscle tissue blood flow with changes in arterial O_2 saturation (S_{O_2}), PO_2 , PCO_2 , %HbCO and (v) Bohr effect on O_2

dissociation curve and Haldane effect on CO_2 dissociation curve. Regression relations to predict cardiac output and cerebral blood flow during high CO exposure levels ($\%HbCO > 30$) were developed. Regression relationships to predict cardiac output and brain blood flow during hyperoxic and hyperbaric conditions were developed as a function of arterial PO_2 and PCO_2 's. This developed multicompartiment model has the capability to estimate O_2 , CO and CO_2 tensions, bicarbonate levels, pH levels, blood $HbCO$ levels, and $MbCO$ levels (in myoglobin containing tissues) in all the vascular and tissue compartments in normoxia, hypoxia, CO hypoxia, hyperoxia, isocapnic hyperoxia and hyperbaric oxygen. Furthermore, reliable measurements of tissue oxygenation, P_tO_2 , in healthy human tissues (brain, heart and skeletal muscle) are difficult to make. To assess the quality of treatment (NBO_2 or HBO_2) administered to CO -poisoning patients, it is difficult to conduct large, controlled, randomized treatment clinical studies on CO poisoned victims. Thus, a better approach would be to use a validated mathematical model to estimate CO burden in different tissues (brain, heart, skeletal muscle) for various CO exposures and treatment sessions. Determination of P_tO_2 in the human brain, heart, and skeletal muscle tissues by the model, during CO exposure and treatment will provide valuable information on tissue oxygenation as noninvasive measurement of these values is difficult.

In project 3 of my dissertation, the most important issues (like comparison of merits of hyperbaric O_2 , normobaric O_2 and isocapnic normobaric O_2) pertaining to treatments of otherwise-healthy CO poisoned victims were addressed. Long and short CO exposures followed by treatment on normobaric O_2 (NBO_2) were simulated in healthy adult subjects. Also simulations of varying levels ($\%HbCO = 37.5, 47, 57$) of short CO exposures followed by 6 hr on NBO_2 , 2 hr on NBO_2 followed by 1.5 hr on HBO_2 , 3 hr on NBO_2 followed by 1.5 hr on HBO_2 , 4 hr on NBO_2 followed by 1.5 hr on HBO_2 , or 6 hr on NBO_2 with maintaining isocapnia at normocapnic levels were administered. Administering HBO_2 after 6 hr on NBO_2 did not have any merit in improving O_2 delivery or CO removal after long and short CO exposures in healthy, adult subjects. The maximum interval of NBO_2 after which administering HBO_2 had the benefit of improving O_2 delivery to the tissues and CO removal from the body was 4 hr.

A treatment protocol is optimal only if it can provide sustained high tissue PO_2 's, together with rapid clearance of CO and other metabolites. The time taken to reach a PO_2 above the threshold PO_2 was similar in all the treatments. However, the time taken to reach the resting PO_2 was shorter in normocapnic normobaric O_2 (INBO₂) treatments. Also the time taken to reach %HbCO levels <10, was shorter for INBO₂ treatment. For any severity of poisoning, administering normocapnic normobaric oxygen was beneficial in improving CO removal and oxygen delivery, when compared to poikilocapnic normobaric oxygen. In all the simulations for HbCO levels <50%, during treatment with INBO₂, the HbCO levels are <10% and the tissue PO_2 's also reach the control values (PO_2 's prior to CO exposure) within 3 hrs of treatment. Thus for %HbCO's less than 50, the normocapnic normobaric O_2 treatment duration can be reduced to 3 hrs for otherwise healthy CO poisoned subjects. Approximately normocapnic normobaric oxygen therapy can be administered by using a gas mixture of 2-3% of CO_2 in O_2 . The other best alternative to INBO₂ treatment is treating the otherwise healthy CO poisoned subjects with NBO₂ for 2 hr followed by 1.5 hr on HBO₂ (based on its availability). Also compared to poikilocapnic normobaric O_2 , hyperbaric O_2 treatment will always be beneficial in improving tissue O_2 delivery and CO removal to the otherwise-healthy CO poisoned subjects, provided it is administered within 6 hrs of administration of NBO₂. Based on the analysis of my simulations, I have proposed a treatment protocol (normocapnic normobaric oxygen) which enhances CO removal from the body and improves oxygen delivery after any severity of CO poisoning in healthy adults. This treatment was reported to improve O_2 delivery and enhance CO removal in humans for %HbCO levels <15. During normocapnic NBO₂ treatment, my simulation results confirm improved O_2 delivery and enhanced CO removal in humans for HbCO levels up to 50%. Physicians should consider the benefits of administering normocapnic NBO₂ over poikilocapnic NBO₂. However it should be noted that this therapy cannot be expected to reverse cell injury or prevent sequelae (neurological or myocardial) that may have occurred before the end of CO exposure. I have also suggested anticipated optimal treatments for "high risk" populations, but these suggestions were based on understanding of physiology and may have to be tested through simulations. Comparison of isocapnic treatments with poikilocapnic treatments have helped me in understanding

the role of CO_2 during treatments and suggest new treatment strategies (hypercapnic normobaric oxygen, normocapnic or hypercapnic hyperbaric oxygen) for treating CO poisoned victims. Irrespective of the poisoning severity, the suggested normocapnic normobaric oxygen therapy ensures fast removal of CO from the body, improves O_2 delivery to the tissues, and is easy and affordable to administer.

In this dissertation suggestions made for improving (i) CO rebreathing methods to estimate hemoglobin mass and (ii) treatments for fast CO removal in otherwise healthy CO poisoned populations are based on analysis of predictions from validated mathematical models. However, the findings from this study should be confirmed by conducting experiments. Experiments should be conducted to estimate hemoglobin mass using the suggested CO rebreathing methods and the estimated hemoglobin mass from these studies should be compared with the measurements made from the gold standard radioactive techniques. Also, physicians should conduct trials comparing normocapnic normobaric oxygen treatments with poikilocapnic normobaric oxygen and hyperbaric oxygen treatments in CO poisoned subjects.

FUTURE WORK

1. Conduct experiments in human subjects to estimate hemoglobin mass using the three *CO* rebreathing protocols suggested in this dissertation. These experiments should be conducted to ensure the validity of the conclusions made in my dissertation that using the modified versions of the existing *CO* rebreathing methods (Protocols B_{modified} and P_{modified}) or the newly proposed *CO* rebreathing method (Protocol N) to determine hemoglobin mass, the variability in the estimated values of hemoglobin mass will be negligible for a given subject. Also, the hemoglobin mass estimated from protocols B_{modified} , P_{modified} , and N can be compared to a known hemoglobin mass of a subject determined from any other method (except from a *CO* dilution technique), to verify the results of my model simulations that determination of hemoglobin mass from the *CO* rebreathing methods proposed (protocols B_{modified} and P_{modified} and N) in this study result in low errors.
2. Conduct clinical trials on patients with similar poisoning severities and symptoms randomized to receive poikilocapnic normobaric oxygen and normocapnic normobaric oxygen. In the literature, clinical trials comparing poikilocapnic normobaric oxygen and normocapnic normobaric oxygen have not been conducted. Prior to conducting clinical trials in humans, experiments to determine a better treatment for *CO* poisoned victims can be done in human like species e.g., monkeys. In these species, different treatments can be compared after a short (20 min) and long (8 hr) duration *CO* exposures resulting in HbCO levels upto 40%. My simulation results suggest that compared to poikilocapnic normobaric oxygen, normocapnic normobaric oxygen improves O_2 delivery and *CO* removal during treatment. Based on my simulation results, I suggest that these experiments should be conducted to compare the merits of poikilocapnic normobaric oxygen and normocapnic normobaric oxygen after *CO* poisoning occurs. Data concerning to (i) time taken for %HbCO levels to reach < 10% after treatment is administered, (ii) occurrence of myocardial abnormalities (ECG abnormalities, arrythimias etc.) during treatment, (iii) blood flow during treatments, (iv) blood gases and O_2

content during the treatments (v) neuropsychological tests after treatments and (vi) volume of CO exhaled during treatments should be recorded. The information from determining the time taken for %HbCO levels to reach $< 10\%$ and volume of CO exhaled during treatments will allow comparison of a treatment's efficiency to remove CO . The product of blood flow and oxygen content can be used as measure of O_2 delivery during the treatments. Also, the results from neuropsychological tests and myocardial performance tests may further assist in determining the state of oxygenation during treatments. In these clinical trials, continual statistical assessment of collected data should be done. If the statistical assessments favour a particular type of treatment, then the trial should be stopped and the physicians should be encouraged to administer the favoured treatment.

3. Apply mathematical model to compare NBO_2 , HBO_2 , normocapnic NBO_2 , hypercapnic NBO_2 and hypercapnic HBO_2 therapies to determine the best treatment strategy ensuring fastest CO removal and O_2 delivery after CO poisoning of varying severities in healthy populations consisting of young, middle aged, and elderly male and nonpregnant female subjects. Determine the sensitivity of these different treatments to intersubject variability in specific parameters like blood volume, cardiac output, muscle mass, ventilation, and fitness level.
4. Enhance and validate the model by implementing compensatory mechanisms accompanied with high altitude living, anemia, and by implementing disease states associated with impaired oxygen delivery, e.g., coronary artery diseases, cerebrovascular diseases or peripheral vascular diseases. Generally in patients with coronary artery diseases, there is decreased blood flow to the heart due to narrowed or blocked arteries. In my model, the blood flow to the myocardium can be reduced depending on the degree of blockage and myocardial oxygen tensions and body CO burden can be predicted during CO exposure and treatments. Then I can use the enhanced and validated mathematical model (suitable for simulating the disease state) to compare NBO_2 , HBO_2 , normocapnic NBO_2 , hypercapnic NBO_2 and hypercapnic HBO_2 therapies to determine the best treatment strategy ensuring

fastest CO removal and O_2 delivery after CO poisoning of varying severities in these populations consisting of young, middle aged, and elderly male and nonpregnant female subjects.

5. Compare CO dose to myocardium with occurrence of abnormal features in ECG (ElectroCardioGram). Myocardial hypoxia during CO exposures has been reported to produce changes in ECG (S-T segment elevation, QT dispersion, T wave changes). The extent to which the CO load ($HbCO$ and $MbCO$ levels) contributes to ECG alterations seen in CO poisoning victims is unknown. Assessing the correlations between the occurrence of predicted peak $MbCO$ and $HbCO$ levels with occurrence of abnormalities in ECG will aid in understanding the CO poisoning related increased risk of cardiac injury during treatments.
6. Develop and validate a multicompartment brain model representing different regions of the brain (cortex, white matter, gray matter, basal ganglia, and hippocampus) and assess the state of oxygenation in these regions during CO exposures and treatments.
7. Enhance the model further by implementing anaerobic metabolic pathways to understand energy production and utilization during CO induced hypoxic stress. Introduce interactions of cytochrome c oxidase with CO . Cytochrome c oxidase is also known to bind reversibly with CO . Understanding the contribution of this protein will further enhance the knowledge database for CO toxicity. Improve control of ventilation in the model by implementing effects of changes in H^+ ions on ventilation. Also implement lactate dynamics to determine lactate threshold for anaerobic metabolism to occur.

REFERENCES

1. Armin Ernst, and Joseph D. Zibrak, Carbon Monoxide Poisoning, Volume 339:1603-1608, 1998.
2. Hampson NB, Little CE., Hyperbaric treatment of patients with carbon monoxide poisoning in the United States, 2005 Jan-Feb;32(1):21-6.
3. Alonso JR, Cardellach F, Lopez S, Casademont J, Miro O. (2003). "Carbon monoxide specifically inhibits cytochrome c oxidase of human mitochondrial respiratory chain". *Pharmacol Toxicol* 93 (3): 142–6.
4. Andersen P, Henriksson J. Capillary supply of the quadriceps femoris muscle of man: adaptive response to exercise. *J Physiol.* 1977 Sep;270(3):677-90.
5. Anderson, R. F., D. C. Allensworth, and W. J. DeGroot. Myocardial toxicity from carbon monoxide poisoning. *Ann. Intern. Med.* 67(6):1172-1182, 1967.
6. Armin Ernst, and Joseph D. Zibrak, Carbon Monoxide Poisoning, Volume 339:1603-1608, 1998.
7. Atkins EH, Baker EL. Exacerbation of coronary artery disease by occupational carbon monoxide exposure: a report to two fatalities and a review of the literature. *Am J Ind Med.* 1985;7(1):73-9.
8. Bascom DA, Pandit JJ, Clement ID, Robbins PA..Effects of different levels of end-tidal PO₂ on ventilation during isocapnia in humans. *Respir Physiol.* 1992 Jun;88(3):299-311.
9. Becker HF, Polo O, McNamara SG, Berthon-Jones M, Sullivan CE. Effect of different levels of hyperoxia on breathing in healthy subjects.*J Appl Physiol.* 1996 Oct;81(4):1683-90.
10. BeganyTimothy, Volume6, No:2, 2001, <www.pulmonaryreviews.com/feb01/pr_feb01_hyperbaric.html>
11. Benignus VA, Hazucha MJ, Smith MV, Bromberg PA. Prediction of carboxyhemoglobin formation due to transient exposure to carbon monoxide.*J Appl Physiol.* 1994 Apr;76(4):1739-45.
12. Benignus VA, Petrovick MK, Newlin-Clapp L, Prah JD. Carboxyhemoglobin and brain blood flow in humans. *Neurotoxicol Teratol.* 1992 Jul-Aug;14(4):285-90.
13. Brodal P, Ingjer F, Hermansen L. Capillary supply of skeletal muscle fibers in untrained and endurance-trained men. *Am J Physiol.* 1977 Jun;232(6):H705-12.
14. Brown SD, Piantadosi CA., Reversal of carbon monoxide-cytochrome c oxidase binding by hyperbaric oxygen in vivo. *Adv Exp Med Biol.* 1989;248:747-54.
15. Bruce EN, Bruce MC, Erupaka K. Prediction of the rate of uptake of carbon monoxide from blood by extravascular tissues..*Respir Physiol Neurobiol.* 2008 Apr 30;161(2):142-59.
16. Bruce EN, Bruce MC, Erupaka KC. A mathematical modeling approach to risk assessment for normal and anemic women chronically exposed to carbon monoxide from biomass-fueled cookstoves, (Under Review).
17. Bruce EN, Bruce MC. A multicompartment model of carboxyhemoglobin and carboxymyoglobin responses to inhalation of carbon monoxide.*J Appl Physiol.* 2003 Sep;95(3):1235-47. Epub 2003
18. Burge CM, Skinner SL. Determination of hemoglobin mass and blood volume with CO: evaluation and application of a method. *J Appl Physiol.* 1995 Aug;79(2):623-31.

19. Charbel FT, Hoffman WE, Misra M, Hannigan K, Ausman JI. Cerebral interstitial tissue oxygen tension, pH, HCO₃, CO₂. *Surg Neurol.* 1997 Oct;48(4):414-7.
20. Chiari L, Avanzolini G, Ursino M. A comprehensive simulator of the human respiratory system: validation with experimental and simulated data. *Ann Biomed Eng.* 1997 Nov-Dec;25(6):985-99.
21. Chiodi H, D. B. Dill, F. Consolazio, and S. M. Horvath . Respiratory and circulatory responses to acute carbon monoxide poisoning. *Am J Physiol* 134: 683-693, 1941.
22. Choi, I. S. Delayed neurologic sequelae in carbon monoxide intoxication. *Arch. Neurol.* 40:433-435, 1983.
23. Collier CR. Oxygen affinity of human blood in presence of carbon monoxide. *J Appl Physiol.* 1976 Mar;40(3):487-90.
24. Cosby, R., and M. Bergeron. Electrocardiographic changes in carbon monoxide. *Am. J. Cardiol.* 11:93-96, 1963.
25. Daniel Mathieu, *Handbook on Hyperbaric Medicine*, part 1, Springer Netherlands, 2006, pp 49-101
26. Darling RC, Cournand A, Mansfield JS, Richards DW. Studies in the intrapulmonary mixture of gases. I Nitrogen elimination from blood and body tissues during high oxygen breathing. *J Clin Invest.* 1940 Jul;19(4):591-7.
27. Demchenko IT, Luchakov YI, Moskvina AN, Gutsaeva DR, Allen BW, Thalmann ED, Piantadosi CA. Cerebral blood flow and brain oxygenation in rats breathing oxygen under pressure. *J Cereb Blood Flow Metab.* 2005 Oct;25(10):1288-300.
28. Doblzar DD, Santiago TV, Edelman NH. Correlation between ventilatory and cerebrovascular responses to inhalation of CO. *J Appl Physiol.* 1977 Sep;43(3):455-62.
29. Ducasse JL, Celsis P, Marc-Vergnes JP. (1995). "Non-comatose patients with acute carbon monoxide poisoning: hyperbaric or normobaric oxygenation?". *Undersea Hyperb Med* 22 (1): 9-15.
30. Duffin J, Mohan RM, Vasiliou P, Stephenson R, Mahamed S. A model of the chemoreflex control of breathing in humans: model parameters measurement. *Respir Physiol.* 2000 Mar;120(1):13-26.
31. Eintrei C, Lund N. Effects of increases in the inspired oxygen fraction on brain surface oxygen pressure fields in pig and man. *Acta Anaesthesiol Scand.* 1986 Apr;30(3):194-8.
32. Einzig S, Nicoloff DM, Lucas RV Jr. Myocardial perfusion abnormalities in carbon monoxide poisoned dogs. *Can J Physiol Pharmacol.* 1980 Apr;58(4):396-405.
33. Environmental Health Criteria For Carbon Monoxide, Environmental Health Criteria 13, Carbon Monoxide, World Health Organization, 1979.
34. Erecińska M, Silver IA. Tissue oxygen tension and brain sensitivity to hypoxia. *Respir Physiol.* 2001 Nov 15;128(3):263-76.
35. Erupaka K, Bruce EN, Bruce MC. Prediction of extravascular burden of carbon monoxide (CO) in the human heart. *Ann Biomed Eng.* 2010 Feb;38(2):403-38.
36. Fatemian M, Robbins PA. Human ventilatory response to CO₂ after 8 h of isocapnic or poikilocapnic hypoxia. *J Appl Physiol.* 1998 Nov;85(5):1922-8.
37. Fisher AB, Dodia C. Lung as a model for evaluation of critical intracellular PO₂ and PCO. *Am J Physiol.* 1981 Jul;241(1):E47-50.

38. Fisher JA, Rucker J, Sommer LZ, Vesely A, Lavine E, Greenwald Y, Volgyesi G, Fedorko L, Iscoe S., Isocapnic hyperpnea accelerates carbon monoxide elimination. *Am J Respir Crit Care Med.* 1999 Apr;159(4 Pt 1):1289-92.
39. Fisher JA, Rucker J, Sommer LZ, Vesely A, Lavine E, Greenwald Y, Volgyesi G,
40. Floyd TF, Clark JM, Gelfand R, Detre JA, Ratcliffe S, Guvakov D, Lambertsen CJ, Eckenhoff RG. Independent cerebral vasoconstrictive effects of hyperoxia and accompanying arterial hypocapnia at 1 ATA. *J Appl Physiol.* 2003 Dec;95(6):2453-61.
41. Folbergrová J, Minamisawa H, Ekholm A, Siesjö BK. Phosphorylase alpha and labile metabolites during anoxia: correlation to membrane fluxes of K⁺ and Ca²⁺. *J Neurochem.* 1990 Nov;55(5):1690-6.
42. Gandini, C., A. F. Castoldi, S. M. Candura, C. Locatelli, R. Butera, S. Priori, and L. Manzo. Carbon monoxide cardiotoxicity. *J. Toxicol. Clin. Toxicol.* 39(1):35-44, 2001.
43. Garvican LA, Burge CM, Cox AJ, Clark SA, Martin DT, Gore CJ. CO uptake kinetics of arterial, venous and capillary blood during CO-rebreathing. *Exp Physiol.* 2010 Sep 3.
44. Gore CJ, Bourdon PC, Woolford SM, Ostler LM, Eastwood A, Scroop GC. Time and sample site dependency of the optimized co-rebreathing method. *Med Sci Sports Exerc.* 2006 Jun;38(6):1187-93.
45. Gore CJ, Hopkins WG, Burge CM. Errors of measurement for blood volume parameters: a meta-analysis. *J Appl Physiol.* 2005 Nov;99(5):1745-58
46. Gorelov V. Theoretical value of Hüfner's constant. *Anaesthesia.* 2004 Jan;59(1):97.
47. Gorman DF. (1999). "Hyperbaric or normobaric oxygen for acute carbon monoxide poisoning: a randomised controlled clinical trial. Unfortunate methodological flaws". *Med J Aust* 170 (11): 563.
48. Grodins FS, Buell J, Bart AJ. Mathematical analysis and digital simulation of the respiratory control system. *J Appl Physiol.* 1967 Feb;22(2):260-76.
49. Hampson NB, Little CE., Hyperbaric treatment of patients with carbon monoxide poisoning in the United States, 2005 Jan-Feb;32(1):21-6.
50. Hart GB, Strauss MB., Gender differences in human skeletal muscle and subcutaneous tissue gases under ambient and hyperbaric oxygen conditions. *Undersea Hyperb Med.* 2007 May-Jun;34(3):147-61.
51. Hart GB., Wells, CH., Strauss MB. Human skeletal muscle and subcutaneous tissue carbon dioxide, nitrogen and oxygen gas tension measurements under ambient and hyperbaric conditions. *J. Appl. Research,* Issue 2, 2003.
52. Hara S, Mizukami H, Kurosaki K, Kuriwa F, Mukai T. Existence of a threshold for hydroxyl radical generation independent of hypoxia in rat striatum during carbon monoxide poisoning. *Arch Toxicol.* 2011.
53. Heinicke K, Wolfarth B, Winchenbach P, Biermann B, Schmid A, Huber G, Friedmann B, Schmidt W. Blood volume and hemoglobin mass in elite athletes of different disciplines. *Int J Sports Med.* 2001 Oct;22 (7):504-12
54. Henry, C. R., D. Satran, B. Lindgren, C. Adkinson, C. I. Nicholson, and T. D. Henry. Myocardial injury and long-term mortality following moderate to severe carbon monoxide poisoning. *J.A.M.A.* 295:398–402, 2006.
55. Hoffman WE, Albrecht RF 2nd, Ripper R, Jonjev ZS. Brain compared to heart tissue oxygen pressure during changes in arterial carbon dioxide in the dog. *J Neurosurg Anesthesiol.* 2001 Oct;13(4):303-9.

56. Honda Y, Hayashi F, Yoshida A, Ohyabu Y, Nishibayashi Y, Kimura H. Overall "gain" of the respiratory control system in normoxic humans awake and asleep. *J Appl Physiol*. 1983 Nov;55(5):1530-5.
57. Horrigan DJ, Wells CH, Guest MM, Hart GB, Goodpasture JE., Tissue gas and blood analyses of human subjects breathing 80% argon and 20% oxygen. *Aviat Space Environ Med*. 1979 Apr;50(4):357-62.
58. Hütler M, Beneke R, Böning D. Determination of circulating hemoglobin mass and related quantities by using capillary blood. *Med Sci Sports Exerc*. 2000 May;32(5):1024-.
59. Iheagwara KN, Thom SR, Deutschman CS, Levy RJ., Myocardial cytochrome oxidase activity is decreased following carbon monoxide exposure. *Biochim Biophys Acta*. 2007 Sep;1772(9):1112-6.
60. Ingjer F. Effects of endurance training on muscle fibre ATP-ase activity, capillary supply and mitochondrial content in man. *J Physiol*. 1979 Sep;294:419-32.
61. Isbister GK, McGettigan P, Harris I. (2003). "Hyperbaric oxygen for acute carbon monoxide poisoning". *N Engl J Med* 348 (6): 557–60.
62. Ishida S, Takeuchi A, Azami T, Sobue K, Sasano H, Katsuya H, Fisher JA., Cardiac output increases the rate of carbon monoxide elimination in hyperpneic but not normally ventilated dogs. *J Anesth*. 2007;21(2):181-6.
63. Jafri, M. S., S. J. Dudycha, and B. O'Rourke. Cardiac energy metabolism: models of cellular respiration. *Annu. Rev. Biomed. Eng*. 3:57-81, 2001.
64. Jamieson D, Vandenbrenk HA. Measurement of oxygen tensions in cerebral tissues of rats exposed to high pressures of oxygen. *J Appl Physiol*. 1963 Sep;18:869-76.
65. Juurlink DN, Stanbrook MB, McGuigan MA. Hyperbaric oxygen for carbon monoxide poisoning. *Cochrane Database Syst Rev*. 2000;(2):CD002041.
66. Kalay, N., I. Ozdogru, Y. Cetinkaya, N. K. Eryol, A. Dogan, I. Gul, T. Inanc, I. Ikizceli, A. Oguzhan, and A. Abaci. Cardiovascular effects of carbon monoxide poisoning. *Am. J. Cardiol*. 99(3):322-324, 2007.
67. Kalliokoski KK, Oikonen V, Takala TO, Sipilä H, Knuuti J, Nuutila P. Enhanced oxygen extraction and reduced flow heterogeneity in exercising muscle in endurance-trained men. *Am J Physiol Endocrinol Metab*. 2001 Jun;280(6):E1015-21.
68. Kizakevich, P. N., M. L. McCartney, M. J. Hazucha, and L. H. Sleet. Noninvasive ambulatory assessment of cardiac function and myocardial ischemia in healthy subjects exposed to carbon monoxide during upper and lower body exercise. *Am. J. Appl. Physiol*. 83:7-16, 2000.
69. Kleinert HD, Scales JL, Weiss HR. Effects of carbon monoxide or low oxygen gas mixture inhalation on regional oxygenation, blood flow, and small vessel blood content of the rabbit heart. *Pflugers Arch*. 1980 Jan;383(2):105-11.
70. Koehler RC, Traystman RJ, Zeger S, Rogers MC, Jones MD Jr. Comparison of cerebrovascular response to hypoxic and carbon monoxide hypoxia in newborn and adult sheep. *J Cereb Blood Flow Metab*. 1984 Mar;4(1):115-22.
71. Kolbitsch C, Lorenz IH, Hörmann C, Hinteregger M, Löckinger A, Moser PL, Kremser C, Schocke M, Felber S, Pfeiffer KP, Benzer A. The influence of hyperoxia on regional cerebral blood flow (rCBF), regional cerebral blood volume (rCBV) and cerebral blood flow velocity in the middle cerebral artery (CBFV/MCA) in human volunteers. *Magn Reson Imaging*. 2002 Sep;20(7):535-41.

72. Korhonen K, Kuttala K, Niinikoski J., Tissue gas tensions in patients with necrotising fasciitis and healthy controls during treatment with hyperbaric oxygen: a clinical study. *Eur J Surg.* 2000 Jul;166(7):530-4.
73. Koskela, R. S. Cardiovascular diseases among foundry workers exposed to carbon monoxide. *Scand. J. Work. Environ. Health.* 20:286–293, 1994.
74. Kreck TC, Shade ED, Lamm WJ, McKinney SE, Hlastala MP., Isocapnic hyperventilation increases carbon monoxide elimination and oxygen delivery. *Am J Respir Crit Care Med.* 2001 Feb;163(2):458-62.
75. Lahiri S, Mulligan E, Nishino T, Mokashi A, Davies RO. Relative responses of aortic body and carotid body chemoreceptors to carboxyhemoglobinemia. *J Appl Physiol.* 1981 Mar;50(3):580-6.
76. Lambertsen CJ, Bunce PL, Drabkin DL, Schmidt CF. Relationship of oxygen tension to hemoglobin oxygen saturation in the arterial blood of normal men. *J Appl Physiol.* 1952 Jun;4(12):873-85.
77. Lambertsen CJ, Dough RH, Cooper DY, Emmel GL, Loeschcke HH, Schmidt CF. Oxygen toxicity; effects in man of oxygen inhalation at 1 and 3.5 atmospheres upon blood gas transport, cerebral circulation and cerebral metabolism. *J Appl Physiol.* 1953 Mar;5(9):471-86.
78. Lambertsen CJ, Ewing JH, Kough RH, Gould R, Stoud MW. Oxygen toxicity. Arterial and internal jugular blood gas composition in man during inhalation of air, 100% O₂ and 2% CO₂ in O₂ at 3.5 atmospheres ambient pressure. *J Appl Physiol.* 1955 Nov;8(3):255-63.
79. Lambertsen CJ, Stroud MW, Gould RA, Kough RH, Ewing JH, Schmidt CF. Oxygen toxicity; respiratory responses of normal men to inhalation of 6 and 100 per cent oxygen under 3.5 atmospheres pressure. *J Appl Physiol.* 1953 Mar;5(9):487-93.
80. Lambertsen, C.J., R.H. Kough, D.Y. Cooper, G.L. Emmel, H.H. Loeschcke and C.F. Schmidt. Comparison of relationship of respiratory minute volume to PCO₂ and pH of arterial and internal jugular blood in normal man during hyperventilation produced by low concentrations of CO₂ at 1 atmosphere and by O₂ at 3.0 atmospheres. *J. Appl. Physiol.* 5(12): 803-813, 1953.
81. Langston P, Gorman D, Runciman W, Upton R. The effect of carbon monoxide on oxygen metabolism in the brains of awake sheep. *Toxicology.* 1996 Dec 18;114(3):223-32.
82. Leenders KL, Perani D, Lammertsma AA, Heather JD, Buckingham P, Healy MJ, Gibbs JM, Wise RJ, Hatazawa J, Herold S, et al. Cerebral blood flow, blood volume and oxygen utilization. Normal values and effect of age. *Brain.* 1990 Feb;113 (Pt 1):27-47.
83. Lindell K. Weaver, Ramona O. Hopkins, Karen J. Chan, Susan Churchill, N.P., C. Gregory Elliott, Terry P. Clemmer, James F. Orme, Jr., Frank O. Thomas, M.D., and Alan H. Morris, Hyperbaric Oxygen for Acute Carbon Monoxide Poisoning., *New England Journal of Medicine*, October, 2002.
84. Lobdell DD. An invertible simple equation for computation of blood O₂ dissociation relations. *J Appl Physiol.* 1981 May;50(5):971-3.
85. Longobardo G, Evangelisti CJ, Cherniack NS. Effects of neural drives on breathing in the awake state in humans. *Respir Physiol.* 2002 Jan;129(3):317-33.
86. Lumb AB, Nair S. Effects of increased inspired oxygen concentration on tissue oxygenation: theoretical considerations. *Eur J Anaesthesiol.* 2010 Mar;27(3):275-9.

87. Martinez-Tica JF, Berbarie R, Davenport P, Zornow MH. Monitoring brain PO₂, PCO₂, and pH during graded levels of hypoxemia in rabbits. *J Neurosurg Anesthesiol.* 1999 Oct;11(4):260-3.
88. Mathieu D, Mathieu-Nolf M, Durak C, Wattel F, Tempe JP, Bouachour G, Sainty JM. (1996). "Randomized prospective study comparing the effect of HBO vs 12 hours NBO in non-comatose CO-poisoned patients: results of the preliminary analysis". *Undersea Hyperb Med abstract* 23: 7.
89. McMahon TJ, Moon RE, Luschinger BP, Carraway MS, Stone AE, Stolp BW, Gow AJ, Pawloski JR, Watke P, Singel DJ, Piantadosi CA, Stamler JS. Nitric oxide in the human respiratory cycle. *Nat Med.* 2002 Jul;8(7):711-7. Epub 2002 Jun 3.
90. Middleton, G., D. Ashby, and F. Clark. Delayed and long-lasting electrocardiographic changes in carbonmonoxide poisoning. *Lancet* 1:12-14, 1961
91. Mintun MA, Lundstrom BN, Snyder AZ, Vlassenko AG, Shulman GL, Raichle ME. Blood flow and oxygen delivery to human brain during functional activity: theoretical modeling and experimental data. *Proc Natl Acad Sci U S A.* 2001 Jun 5;98(12):6859-64. Epub 2001 May 29.
92. Nishimura N, Iwasaki K, Ogawa Y, Shibata S. Oxygen administration, cerebral blood flow velocity, and dynamic cerebral autoregulation. *Aviat Space Environ Med.* 2007 Dec;78(12):1121-7.
93. Ohta H. No To Shinkei. 1986 Oct;38(10):949-59. The effect of hyperoxemia on cerebral blood flow in normal humans.
94. Oscar M Jordi C, Barrientos, Antoni; Urbano-Marquez, Alvaro; Cardellach, Francesc, Mitochondrial Cytochrome c Oxidase Inhibition during Acute Carbon Monoxide Poisoning. *Pharmacology & Toxicology.* 82(4):199-202, April 1998.
95. Parkinson RB, Hopkins RO, Cleavinger HB, Weaver LK, Victoroff J, Foley JF, Bigler ED. White matter hyperintensities and neuropsychological outcome following carbon monoxide poisoning. *Neurology.* 2002 May 28;58(10):1525-32.
96. Paulson OB, Parving HH, Olesen J, Skinhoj E. Influence of carbon monoxide and of hemodilution on cerebral blood flow and blood gases in man. *J Appl Physiol.* 1973 Jul;35(1):111-6.
97. Penney, D. G. A review: Hemodynamic response to carbon monoxide. *Environ. Health Perspect.* 77:121-130, 1988.
98. Petersen MR, Lapp NL, Amandus HE. The relationship of several ventilatory capacities and lung volumes to age, height, and weight. *J Occup Med.* 1975 Jun;17(6):355-6.
99. Piantadosi CA. Carbon monoxide poisoning. *Undersea Hyperb Med.* 2004 Spring;31(1):167-77.
100. Poulin MJ, Cunningham DA, Paterson DH, Kowalchuk JM, Smith WD. *J Appl Physiol.* Ventilatory sensitivity to CO₂ in hyperoxia and hypoxia in older aged humans. 1993 Nov;75(5):2209-16.
101. Prommer N, Schmidt W. Loss of CO from the intravascular bed and its impact on the optimised CO-rebreathing method. *Eur J Appl Physiol.* 2007 Jul;100(4):383-91.
102. Purves MJ, *Physiology of the cerebral circulation.* Monographs of the Physiological Society. Cambridge University Press; 1 edition (May 31, 1972)

103. Raphael JC, Elkharrat D, Jars-Guinestre MC, Chastang C, Chasles V, Vercken JB, Gajdos P. (1989). "Trial of normobaric and hyperbaric oxygen for acute carbon monoxide intoxication". *Lancet* 2 (8660): 414–9.
104. Rasanen J, Downs JB, Malec DJ, Oates K. Oxygen tensions and oxyhemoglobin saturations in the assessment of pulmonary gas exchange. *Crit Care Med* 15:1058 –1061, 1987.
105. Raub JA, Mathieu-Nolf M, Hampson NB, Thom SR. Carbon monoxide poisoning--a public health perspective. *Toxicology*. 2000 Apr 7;145(1):1-14.
106. Raub JA., Chapman RS., Air Quality Criteria for Carbon Monoxide., National Center for Environmental Assessment., US Environmental Protection Agency, October 1999.
107. Ren X, Fatemian M, Robbins PA. Changes in respiratory control in humans induced by 8 h of hyperoxia. *J Appl Physiol*. 2000 Aug;89(2):655-62.
108. Rolett EL, Azzawi A, Liu KJ, Yongbi MN, Swartz HM, Dunn JF. Critical oxygen tension in rat brain: a combined (31)P-NMR and EPR oximetry study. *Am J Physiol Regul Integr Comp Physiol*. 2000 Jul;279(1):R9-R16.
109. Roughton FJW, Darling RC. The effect of carbon monoxide on the oxyhemoglobin dissociation curve. *Am J Physiol* 141 (1) 17-31.
110. Rucker J, Tesler J, Fedorko L, Takeuchi A, Mascia L, Vesely A, Kobrossi S, Slutsky AS, Volgyesi G, Iscoe S, Fisher JA. Normocapnia improves cerebral oxygen delivery during conventional oxygen therapy in carbon monoxide-exposed research subjects. *Ann Emerg Med*. 2002 Dec;40(6):611-8.
111. Sagiv M, Goldhammer E, Ben-Sira D, Amir R. What maintains energy supply at peak aerobic exercise in trained and untrained older men? *Gerontology*. 2007;53(6):357-61.
112. Santiago TV, Edelman NH. Mechanism of the ventilatory response to carbon monoxide. *J Clin Invest*. 1976 Apr;57(4):977-86.
113. Santiago TV, Neubauer JA, Edelman NH. Correlation between ventilation and brain blood flow during hypoxic sleep. *J Appl Physiol*. 1986 Jan;60(1):295-8.
114. Satran, D., C. R. Henry, C. Adkinson, C. I. Nicholson, Y. Bracha, and T. D. Henry. Cardiovascular manifestations of moderate to severe carbon monoxide poisoning. *J. Am. Coll. Cardiol*. 45:1513–1516, 2005.
115. Scheinkestel CD, Bailey M, Myles PS, Jones K, Cooper DJ, Millar IL, et al. Hyperbaric or normobaric oxygen for acute carbon monoxide poisoning: a randomized controlled clinical trial. *Med J Australia* 1999; 170: 203-210
116. Scheinkestel CD, Jones K, Myles PS, Cooper DJ, Millar IL, Tuxen DV. (2004). "Where to now with carbon monoxide poisoning?". *Emerg Med Australas* 16 (2): 151–4.
117. Schmidt W, Prommer N. Impact of alterations in total hemoglobin mass on VO₂max. *Exerc Sport Sci Rev*. 2010 Apr;38(2):68-75
118. Schmidt W, Prommer N. The optimised CO-rebreathing method: a new tool to determine total haemoglobin mass routinely. *Eur J Appl Physiol*. 2005 Dec;95(5-6):486-95.
119. Severinghaus JW. Blood gas calculator. *J Appl Physiol*. 1966 May;21(3):1108-16.
120. Severinghaus JW. Proposed standard determination of ventilatory responses to hypoxia and hypercapnia in man. *Chest*. 1976 Jul;70(1 Suppl):129-31.

121. Severinghaus JW. Simple, accurate equations for human blood O₂ dissociation computations. *J Appl Physiol*. 1979 Mar;46(3):599-602.
122. Sharan M, Jones MD Jr, Koehler RC, Traystman RJ, Popel AS. A compartmental model for oxygen transport in brain microcirculation. *Ann Biomed Eng*. 1989;17(1):13-38.
123. Sharan M, Singh MP, Aminataei A. A mathematical model for the computation of the oxygen dissociation curve in human blood. *Biosystems*. 1989;22(3):249-60.
124. Smith ML, Counelis GJ, Maloney-Wilensky E, Stiefel MF, Donley K, LeRoux PD. Brain tissue oxygen tension in clinical brain death: a case series. *Neurol Res*. 2007 Oct;29(7):755-9
125. Smith ML, Counelis GJ, Maloney-Wilensky E, Stiefel MF, Donley K, LeRoux PD. Brain tissue oxygen tension in clinical brain death: a case series. *Neurol Res*. 2007 Oct;29(7):755-9
126. Sokhanvar S, Dargahi J, Packirisamy M, Esmailzadeh E. Modeling of chemical control of human respiratory system. *Biomed Mater Eng*. 2005;15(6):467-81.
127. Steiner T, Wehrin JP. Comparability of haemoglobin mass measured with different carbon monoxide-based rebreathing procedures and calculations. *Scand J Clin Lab Invest*. 2010 Nov 23.
128. Stern, F. B., R.A. Lemen, and R.A. Curtis. Exposure of motor vehicle examiners to carbon monoxide: a historical prospective mortality study. *Arch. Environ. Health* 36:59-65, 1981.
129. Steven B Heymsfield, Timothy G Lohman, Zimian Wang. *Human Body Composition*. Second Edition, May 2005, Human Kinetics Publishers, ISBN-13: 9780736046558, Chapter 15, Pg: 221.
130. Stewart RD. The effect of carbon monoxide on humans. *Annu Rev Pharmacol*. 1975;15:409-23.
131. Stewart, R. D., J. E. Peterson, T. N. Fisher, M. J. Hosko, E. D. Baretta, H. C. Dodd, and A. A. Herrmann. Experimental human exposure to high concentrations of carbon monoxide. *Arch. Environ. Health*. 26(1):1-7, 1973.
132. Stuhmiller JH, Stuhmiller LM. A mathematical model of ventilation response to inhaled carbon monoxide. *J Appl Physiol*. 2005 Jun;98(6):2033-44.
133. Takeuchi A, Vesely A, Rucker J, Sommer LZ, Tesler J, Lavine E, Slutsky AS, Maleck WH, Volgyesi G, Fedorko L, Iscoe S, Fisher JA. A simple "new" method to accelerate clearance of carbon monoxide. *Am J Respir Crit Care Med*. 2000 Jun;161(6):1816-9.
134. Thom SR, Taber RL, Mendiguren II, Clark JM, Hardy KR, Fisher AB. (1995). "Delayed neuropsychologic sequelae after carbon monoxide poisoning: prevention by treatment with hyperbaric oxygen". *Ann Emerg Med* 25 (4): 474-80.
135. Tibbles PM, Perrotta PL. Treatment of carbon monoxide poisoning: a critical review of human outcome studies comparing normobaric oxygen with hyperbaric oxygen. *Ann Emerg Med* 1994; 24: 269-276.
136. Tibes U, Hemmer B, Böning D. Heart rate and ventilation in relation to venous [K⁺], osmolality, pH, PCO₂, PO₂, [orthophosphate], and [lactate] at transition from rest to exercise in athletes and non-athletes. *Eur J Appl Physiol Occup Physiol*. 1977 Jan 14;36(2):127-40.

137. Topor ZL, Pawlicki M, Remmers JE. A computational model of the human respiratory control system: responses to hypoxia and hypercapnia. *Ann Biomed Eng.* 2004 Nov;32(11):1530-45.
138. Tucker M, Eichold B, Carbon Monoxide Poisonings After Two Major Hurricanes, Alabama and Texas, August-October 2005.
139. Ursino M, Magosso E, Avanzolini G. An integrated model of the human ventilatory control system: the response to hypoxia. *Clin Physiol.* 2001 Jul;21(4):465-77.
140. Vander, Sherman, Luciano's Human Physiology, The Mechanisms of Body Function, Mc Graw Hill Higher Education, 2004.
141. Weaver LK, Hopkins RO, Chan KJ, Churchill S, Elliott CG, Clemmer TP, Orme JF Jr, Thomas FO, Morris AH. Hyperbaric oxygen for acute carbon monoxide poisoning. *N Engl J Med.* 2002 Oct 3;347(14):1057-67.
142. Weaver LK, Hopkins RO, Elliott G. Carbon monoxide poisoning. *N Engl J Med.* 1999 Apr 22;340(16):1290
143. Weaver LK, Howe S, Hopkins R, Chan KJ., Carboxyhemoglobin half-life in carbon monoxide-poisoned patients treated with 100% oxygen at atmospheric pressure. *Chest.* 2000 Mar;117(3):801-8.
144. Weaver LK, Howe S, Snow GL, Deru K. Arterial and pulmonary arterial hemodynamics and oxygen delivery/extraction in normal humans exposed to hyperbaric air and oxygen. *J Appl Physiol.* 2009 Jul;107(1):336-45.
145. Weaver LK, Howe S., Normobaric measurement of arterial oxygen tension in subjects exposed to hyperbaric oxygen. *Chest.* 1992 Oct;102(4):1175-81.
146. Weaver LK, Larson-Lohr V, Hein S, Howe S, Kristo D, Habestock D (1995) Hemodynamic and oxygen delivery/extraction in normal humans exposed to hyperbaric oxygen and O₂. *Undersea Hyper Med* 1995; 22 (Suppl.): 77.
147. Weaver LK. Carbon monoxide poisoning. *Crit Care Clin.* 1999 Apr;15(2):297-317, viii.
148. Weaver LK. Clinical practice. Carbon monoxide poisoning. *N Engl J Med.* 2009 Mar 19;360(12):1217-25.
149. Weaver LK. Hyperbaric oxygen in carbon monoxide poisoning. *BMJ.* 1999 Oct 23;319(7217):1083-4.
150. Weaver, L. K. Carbon monoxide poisoning. *Crit. Care Clin.* 15:297-317, 1999.
151. Whalen RE, Saltzman HA, Holloway DH Jr, McIntosh HD, Sieker HO, Brown IW. Cardiovascular and blood gas responses to hyperbaric oxygenation. *Am J Cardiol.* 1965 May;15:638-46.
152. Wolf MB, Garner RP. A mathematical model of human respiration at altitude. *Ann Biomed Eng.* 2007 Nov;35(11):2003-22.
153. Yanir, Y., A. Shupak, A. Abramovich, S. A. Reisner, and A. Lorber. Cardiogenic shock complicating acute carbon monoxide poisoning despite neurologic and metabolic recovery. *Ann. Emerg. Med.* 40:420-424, 2002.
154. Ye GF, Moore TW, Buerk DG, Jaron D. A compartmental model for oxygen-carbon dioxide coupled transport in the microcirculation. *Ann Biomed Eng.* 1994 Sep-Oct;22(5):464-79.
155. Zauner A, Bullock R, Di X, Young HF. Brain oxygen, CO₂, pH, and temperature monitoring: evaluation in the feline brain. *Neurosurgery.* 1995 Dec;37(6):1168-76; discussion 1176-7.

156. Zauner A, Daugherty WP, Bullock MR, Warner DS. Brain oxygenation and energy metabolism: part I-biological function and pathophysiology. *Neurosurgery*. 2002 Aug;51(2):289-301
157. Zhou H, Saidel GM, Cabrera ME. Multi-organ system model of O₂ and CO₂ transport during isocapnic and poikilocapnic hypoxia. *Respir Physiol Neurobiol*. 2007 Jun 15;156(3):320-30.
158. Zhu N, Weiss HR. Myocardial venous O₂ saturation becomes more heterogeneous during hypoxic and carbon monoxide hypoxia. *Microvasc Res*. 1995 May;49(3):253-67.
159. Zoladz JA, Semik D, Zawadowska B, Majerczak J, Karasinski J, Kolodziejcki L, Duda K, Kilarski WM. Capillary density and capillary-to-fibre ratio in vastus lateralis muscle of untrained and trained men. *Folia Histochem Cytobiol*. 2005;43(1):11-7.

VITA

Date and place of birth:

- 02-09-1982, Hyderabad, INDIA

Educational institutions attended and degrees already awarded:

- B. E., Bachelors in Biomedical Engineering, Jawaharlal Nehru Technological University, AP, INDIA
- Post Graduate Diploma in Information Technology, AP, INDIA

Professional positions held:

- Biomedical Engineer , Apollo Hospitals, Hyderabad, AP, India
- Research Assistant, Computational Physiology Laboratory, University of Kentucky, Kentucky, USA

Professional publications:

- Chada K, Bruce E.N., Bruce M. C., Mathematical model aided analysis of carbon monoxide (CO) rebreathing methods to estimate hemoglobin mass. (Under Review)
- Chada K, Bruce E.N., Bruce M. C., Mathematical model aided analysis of treatments administered to treat CO poisoned victims. (In preparation)
- Bruce E. N., Bruce M. C., Erupaka-Chada K. A mathematical modeling approach to risk assessment for normal and anemic women chronically exposed to carbon monoxide from biomass-fueled cookstoves. J Appl Physiol. 2011 May 19. (In print).
- Erupaka K, Bruce E.N., Bruce M. C., Prediction of extravascular burden of carbon monoxide (CO) in the Human Heart. Ann Biomed Eng. 2010 Feb; 38(2):403-38.
- Bruce, E. N., Bruce M. C., and Erupaka K. Prediction of the rate of uptake of carbon monoxide from blood by extravascular tissues. Respir. Physiol. Neurobiol. 161(2):142-159, 2008.

Professional honors:

- Graduate Assistantship, 2005–2007, 2010–2011, University of Kentucky
- Max Steckler Fellowship, 2007, 2010, University of Kentucky
- Kentucky Opportunity Fellowship, 2008–2010, University of Kentucky
- Outstanding Project of the Year, 2003, Biomedical Engineering Department, Jawaharlal Nehru Technological University

- Vision2k Telemedicine Award Winner, 2003, Jawaharlal Nehru Technological University
- Meditech student innovator, 2002, Osmania University

Professional memberships:

- American Association for the Advancement of Science (AAAS)
- Society of Industrial and Applied Mathematics (SIAM)
- Biomedical Engineering Society (BMES)

Typed name of student on final copy

- Kinnera Chada